ISSN 1173-5996

# THE COMBUSTION BEHAVIOUR OF UPHOLSTERED FURNITURE MATERIALS IN NEW ZEALAND

**BY**

**Hamish R Denize**

**Supervised by**
**Dr Charley Fleischmann**

**Fire Engineering Research Report 00/4**

**March 2000**

This report was presented as a project report
as part of the M.E. (Fire) degree at the University of Canterbury

School of Engineering
University of Canterbury
Private Bag 4800
Christchurch, New Zealand

Phone 643 364-2250
Fax 643 364-2758

# Abstract:

This Research Project evaluates the combustion severity of New Zealand upholstered furniture materials. Experimental combustion tests on typical upholstered furniture fabric and polyurethane foam combinations form the basis for all conclusions reached.

63 bench-scale Cone Calorimeter and 10 full-scale armchair Furniture Calorimeter combustion tests were conducted in the Fire Engineering Laboratory at the University of Canterbury. 7 different polyurethane foams, including 2 fire-retardant, are tested along with 100% polypropylene and 95% woollen fabrics. These tests demonstrate that the variation of foam and fabric covering play a substantial role in influencing the combustion characteristics.

Between the wool and polypropylene fabric types, there were several combustion behavioural differences identified. Most significantly was the ability of the woollen fabric to remain in place under intense heat exposure for a longer time than the polypropylene. This had the effect of prolonging the ignition times in the Cone Calorimeter tests and increasing the time to peak heat release rates (HRRs) for both the Cone and Furniture Calorimeter tests.

The effects of the various types of polyurethane foam were generally less significant than the effects caused by varying the fabric type. However, one type of fire retardant foam showed combustion characteristics that were significantly out of pattern from the others, by having prolonged ignition times and longer times to peak HRRs in the Cone and Furniture Calorimeter tests respectively. Thus the effects of the fire retardant foam was clearly shown to interfere with the combustion behaviour.

All experimental methods in this Research Project follow the methods developed by the European fire research programme CBUF - Combustion Behaviour of Upholstered Furniture. Thus, the results in this Research Project are meaningful on an international level.

Model I, a method for predicting full-scale burning combustion characteristics from bench-scale test data, as developed by the European CBUF research, is applied to the New Zealand

materials. The full-scale furniture combustion Model is compared in three areas, which are the value of peak HRR (kW), time to peak HRR (s) and the total amount of heat released (MJ), from burning full-scale armchairs. The Model does not accurately predict the full-scale burning characteristics, especially for the predicted time to peak HRR and total heat released. Instead the Model is conservative from a design perspective, predicting the time to peak HRR in a shorter time and a higher total heat release. For the peak HRR prediction, the Model achieves a level of confidence comparable with the European data that was used to validate the Model. Therefore it is considered accurate enough to be used to predict the peak HRR for the selected full-scale armchair style, without doing full-scale tests.

# Acknowledgments:

I would like to sincerely thank the following people for their advice and assistance during the production of this Research Project.

My project supervisor Dr Charley Fleischmann, for his assistance and advice at all stages throughout this Research Project. He was the driving force behind the topic ensuring that it was both demanding and educational.

Professor Andy Buchanan for his time management and reporting advice.

Tony Parkes, Frank Greenslade and Grant Dunlop for their assistance while conducting the experimental combustion tests in the Fire Engineering Laboratory.

Terry O'Loughlin of *Dunlop Flexible Foams New Zealand* and Martin Kiddey of *Vita New Zealand* for their professional advice and information on polyurethane foams.

Murray Hill of *Murray's Furniture Ltd* for the efficient manufacture of the full-scale upholstered armchairs.

1999-2000 Fire Engineering classmates, for the good comradeship and fun times we had throughout these Research Projects.

Genevieve Haszard for her grammar and proofreading corrections to my report write-up.

Lastly my family, for the support throughout the year which made this all possible.

Thank you.

# Table of Contents:

# List of Figures:

# List of Tables:

# Nomenclature:

| Symbol | Description | Units |
|---|---|---|
| E | heat release per unit mass of oxygen consumed | kJ/g |
| k | $t^2$ fire growth constant | $s/MW^{1/2}$ |
| m | mass of the cone calorimeter sample | kg |
| $m_{comb.\ total}$ | entire combustible mass of full-scale sample (all except steel) | kg |
| $m_{soft}$ | mass of upholstery (fabric, filling, interliner, etc) of full scale item | kg |
| $\dot{m}_a$ | mass flow rate of ambient air | kg/s |
| $\dot{m}_e$ | mass flow rate of exhaust combustion products | kg/s |
| $\dot{q}$ | Energy/heat release rate | kW |
| $\dot{q}''_{35\text{-}pk}$ | peak HRR of cone calorimeter | $kW\ m^{-2}$ |
| $\dot{q}''_{pk\#1}$ | first peak of cone calorimeter HRR curve | $kW\ m^{-2}$ |
| $\dot{q}''_{trough}$ | trough of cone calorimeter HRR curve | $kW\ m^{-2}$ |
| $\dot{q}''_{pk\#2}$ | second peak of cone calorimeter HRR curve | $kW\ m^{-2}$ |
| $\dot{q}''_{35\text{-}60}$ | 60 second average HRR value from the cone calorimeter | $kW\ m^{-2}$ |
| $\dot{q}''_{35\text{-}180}$ | 180 second average HRR value from the cone calorimeter | $kW\ m^{-2}$ |
| $\dot{q}''_{35\text{-}300}$ | 300 second average HRR value from of cone calorimeter | $kW\ m^{-2}$ |
| $q''_{35\text{-}tot}$ | total heat release of cone calorimeter | $MJ\ m^{-2}$ |
| $\dot{q}''_{35\text{-}180}\%diff$ | 180 second average HRR percentage difference | % |
| Q | $t^2$ fire heat release rate | MW |
| $\dot{Q}$ | prediction of the full-scale peak heat release rate | MW |
| $Q_{tot}$ | prediction of the full-scale total heat release | MJ |
| t'' | time | s |
| $t_{ig\text{-}35}$ | cone calorimeter ignition time | s |
| $t_{pk}$ | time to peak HRR, from start of sustained burning | s |
| $t_{pk\#1,ignition}$ | time to first peak of cone calorimeter HRR curve, from ignition | s |
| $t_{pk\#1,start\ of\ test}$ | time to first peak of cone calorimeter HRR curve, from start of test | s |
| $Y^a_{O2}$ | mass fraction of oxygen in the combustion air | g/g |

| | | |
|---|---|---|
| $Y^{e}_{O2}$ | mass fraction of oxygen in the combustion products | g/g |
| $\Delta h_c$ | net heat of combustion | MJ $kg^{-1}$ |
| $\Delta h_{c,eff}$ | effective heat of combustion | MJ $kg^{-1}$ |

# 1.0 Introduction:

## *1.1 Impetus for this Research:*

Domestic fires across the world dominate annual fire death statistics. Typically in houses, upholstered furniture is the largest contributor to the internal fuel loading. The rapid growth rate and high amount of organic stored energy contained within upholstered furniture make them frequently predominant contributors to hazardous conditions and uncontrollable fires.

Unlike various overseas countries (such as the United Kingdom and the State of California USA[10]), there are no flammability regulations that upholstered furniture in New Zealand (NZ) must adhere to. Thus, the manufacturers of upholstery fabrics, foams and the furniture makers themselves are free to use any composition and combinations of materials when making furniture for consumers.

This Research Project continues with ongoing University of Canterbury (UC) research, assessing the combustion characteristics and severity of NZ upholstered furniture materials. Particular emphasis in this project is focused on predicting the hazard of NZ upholstered furniture by applying an existing predictive furniture fire model developed by the European Communities. This model functions by using bench-scale test data to predict full-scale furniture combustion characteristics.

This Research Project is of relevance to determine whether NZ upholstered furniture materials behave in a similar manner to European materials. Also combustion differences between fabric coverings and polyurethane foams will be compared, to determine their impact on combustion behaviour. The European Model is applied to NZ materials to determine if it is accurate enough to make predictions on NZ furniture materials. A successful predictive model would reduce the cost of surveying full-scale combustion characteristics of NZ furniture materials, by only requiring bench-scale tests on various upholstered furniture material combinations.

Experimental combustion tests of NZ furniture materials will form the bulk of the data on which conclusions are based upon. The same processes and procedures, as used in European research, are used in this Research Project so that all data is directly transferable. This makes the data from this research reusable on an international study level.

## *1.2 General Introduction:*

Most of today's upholstered furniture relies on polyurethane foam as the primary cushioning material, which is covered by various fabrics. This is because foams provide the desired long-lasting comfort, while the exterior fabrics provide the style, colour and surface durability of the furniture item. Components of typical upholstered furniture include:

- Frame (wood, plastic, steel)
- Springs
- Webbing
- Padding (most commonly polyurethane foam)
- Fabric (leather, vinyl, wool or synthetic weaves, etc)

The University of Canterbury (UC) has the most advanced combustion research laboratory facilities in NZ for conducting tests on upholstered furniture. In this Research Project, combustion tests of full-scale furniture items are carried out using the *Furniture Calorimeter* and bench-scale tests are carried out using the *Cone Calorimeter*. Both of these apparatuses are described fully in following sections.

Predicting how full-scale furniture will burn from bench-scale test data is advantageous for several reasons. The most important is that an assessment of the full-scale furniture fire hazard can be made from much cheaper bench-scale tests. The Commission of the European Communities is the main contributor to this type of research. This work was carried out within the European fire research programme CBUF - Combustion Behaviour of Upholstered Furniture. The prediction models attempt to estimate the peak Heat Release Rate (HRR),

time to peak HRR and the total heat released for full-scale furniture, as well as several other characteristics that are not relevant to this Research Project.

This Research Project uses the European CBUF Final Report[4] as a basis for all Cone and Furniture Calorimeter testing and a comprehensive model is applied to NZ materials to determine whether NZ furniture is compatible with this study.

## *1.3 Direction of this Work:*

Given that there are no regulations controlling polyurethane foam flammability and the moderately large range available for furniture in NZ, it was first necessary to conduct an investigation into which foams are commonly used for this purpose. This technique was also applied to fabric coverings, in an attempt to make the research as relevant as possible to today's actual practice, by selecting current materials.

The first experimental step was bench-scale combustion tests on various fabric/foam combinations to determine general combustion characteristics. Secondly a selection of these material combinations, depending on the results, were manufactured into full-scale furniture and burned in the Furniture Calorimeter.

Using the first of three models presented in the CBUF Final Report[4], full-scale predictions made from Cone Calorimeter test data are compared to the measured full-scale tests results from the Furniture Calorimeter. Unfortunately because there is no listed combustion data in the CBUF Final Report[4] which is identical in method and style to the full-scale furniture tests conducted in this Research Project, there is no way of directly comparing full-scale combustion characteristics. This means that the severity of the NZ upholstered furniture materials cannot be assessed against the European research, instead only the accuracy of the predictive model used can be evaluated.

The advantage of successfully predicting full-scale furniture burning behaviour will be that only bench-scale tests will then be necessary, at a fraction of the cost of full-scale tests, for

determining the fire hazard of various upholstered furniture material combinations. However perfect modelling is only in an ideal situation, and because the materials and styles are continually changing with fashion, an attempt to accomplish a close relationship would be an aim of this type of research.

It is common practice to model furniture HRRs as behaving in a time-squared manner having growth rates of slow, medium, fast or ultra fast. Successfully being able to predict such characteristics as the peak HRR and time to peak HRR, will allow various composite combinations of fabrics and foams to be appropriately categorized. This could lead to more realistic design-fires[1] being used by Fire Protection Engineers.

## *1.4 Outline of this Report:*

This Research Project is split up into the following four main parts:

*Part 1:* An investigation into NZ upholstered furniture materials is conducted to make sure that this research uses materials that are common practice in NZ. This includes Section 5, 'Selection of Materials' for determining the upholstered materials to be used in the bench-scale tests. Also Section 7, 'Full Scale Furniture Details' for refining the selection of materials to be used in the more expensive full-scale tests.

*Parts 2 and 3:* Experimental combustion tests are conducted using the selected materials on both bench-scale and full-scale levels using the UC Cone and Furniture Calorimeters respectively. The Cone Calorimeter apparatus and testing procedures are outlined in Sections 3, 'Experimental Facilities' and Section 4, 'Experimental Procedures' respectively. The combustion test results and discussions are detailed in Section 6, 'Cone Calorimeter Results and Discussion'. The Furniture Calorimeter apparatus and testing procedures are similarly outlined in Sections 3, 'Experimental Facilities' and Section 4, 'Experimental Procedures'

[1] A design-fire is a chosen realistic and possible fire that a Fire Engineer designs safety measures around to protect people and (or) property. It is commonly the case that the combustion of upholstered furniture is used for design-fires, as generally these are a main component of internal fuel loading.

respectively. The combustion test results and discussions are detailed in Section 8, 'Furniture Calorimeter Results and Discussion'.

*Part 4:* A Model for predicting full-scale combustion characteristics from bench-scale test data, as developed by the European CBUF research programme, is applied to the experimental data from the combustion tests to determine its validity when applied to NZ materials. A full description of the predictive Model is outlined in Section 9, 'Predicting Full-Scale Combustion Characteristics from Bench-Scale Test Data'. The Model's predictions and accuracy is assessed against the full-scale test data in Section 10, 'Model I Results and Discussion'.

# 2.0 Previous Research:

## *2.1 Introduction:*

This project is centered around the experimental practices and techniques presented in the European CBUF Final Report[4] programme, which is summarized below. There have been several other recent postgraduate studies conducted at UC, which have also in-part used the European CBUF research programme as their methodology basis. Most relevant to this Research Project is the works' carried out by Tony Enright[5] and James Firestone[6], which are discussed separately.

## *2.2 European CBUF Research Programme:*

The European CBUF research programme was established to develop methods for measuring and predicting the burning behaviour of upholstered furniture. This was in response to European statistics showing that the majority of deaths in fires were due to fires in upholstered furniture and for the possible implementation of European Union legislation and standardization.

The CBUF research programme developed fire testing procedures and mathematical models to predict full-scale furniture combustion characteristics from bench-scale test data, such as the peak HRR, time to peak HRR and total amount of heat released. The models' formulation and their validation were achieved by burning over 1500 items in Calorimeters.

Strict protocols were introduced so that eleven participating European countries were able to reproduce identical testing conditions between various laboratories. Furniture Calorimeters (NT FIRE 032)[11] were used as the full-scale furniture testing apparatuses, while the Cone Calorimeter (ISO 5660)[8] was used for bench-scale combustion tests. Reproducibility precision between laboratories was proven with inter-laboratory calibrations.

Test samples were selected to represent a large spectrum of burning behaviour from representative European upholstered furniture. Some items developed flames very rapidly, while others were found to show no burning at all. Fabric and foam combinations were identified which gave improved fire resistance.

The results from over 1500 Calorimeter tests are compiled in an FDMS standard data base, which includes such data as heat release rate, temperature, heat flux, smoke density and concentrations of various gas species.

Of particular importance to this Research Project is predictive Model I, which attempts to predict full-scale furniture combustion characteristics from bench-scale test data. This Model is described fully in Section 9, 'Predicting Full-scale Combustion Characteristics from Bench-scale Test Data'.

The UC combustion analyzing apparatuses, namely the Cone and Furniture Calorimeter, attempt to enable NZ-CBUF research to be able to reproduce the same testing conditions as used in the European CBUF research. For this reason, in all of the combustion tests conducted in this Research Project, the same test protocols, as were developed in the European CBUF work, are used.

## *2.3 Other CBUF Work at University of Canterbury:*

### 2.3.1 Enright's Research:

Enright's research[5] was conducted in the UC Fire Laboratory, and mainly focused on calorimetric techniques, calorimetric technique uncertainties and instrumentation and validation of furniture fire modelling. Of particular relevance, is the European CBUF predictive Model I that was applied to NZ furniture. A total of thirteen armchairs were burned in the UC Furniture Calorimeter to assess the model.

For the full-scale furniture combustion tests, the NZ furniture armchairs consistently exhibited significantly higher peak HRRs for relatively similar levels of total heat released. Unfortunately the times to peak HRR could not be compared, as they were not recorded in the CBUF Final Report[4].

Comparisons between the full-scale furniture combustion results and the model predictions showed that exemplary NZ furniture presents a significantly greater fire hazard than its European counterparts by reaching a higher peak HRR than predicted, also in a reduced time frame than predicted.

Fabric effects were identified in both the bench and full-scale combustion tests. For both tests, the fabric showed a trend to either (i) melt and peel, or (ii) split and remain in place – that is, to become chair forming. In the first phenomena typically a large single peak HRR was observed as both the fabric and foam contributed to the energy in a similar manner. For the second phenomena, a single sharp peak HRR was observed followed by a slower 'foam' peak.

It was concluded that Model I did not accurately predict the behaviour of the exemplary NZ furniture tested. A lack of goodness of fit of the measured data to the model was especially pronounced in prediction of the peak HRR. The European CBUF Testing Protocols were

followed strictly, so Enright's work is directly related and transferable to this Research Project.

### 2.3.2 Firestone's Research:

Firestone's research[6] was undertaken on experimental combustion data, which was in-part to test the European CBUF Model I for predicting full-scale combustion characteristics from bench-scale test data. Two fabrics were tested, which were a cotton/linen blend and the other 100% polypropylene, with two polyurethane foams. These were classified as standard and high resilience foams.

All of the full-scale (141) and most of the bench-scale (33) combustion test data were obtained from prior combustion tests from the Cone and Furniture Calorimeters at CSIRO in Melbourne. A further 22 Cone Calorimeter tests were conducted at UC. There was no conclusive evidence found that the prior tests, most of which were done in 1993, followed any specific testing protocols.

Firestone's work concluded that the fabric/foam interaction was crucial to the degree of combustion severity. The worst fabric/foam combination determined was the standard polyurethane foam with polypropylene fabric, which produced the highest HRRs across all seat ranges.

Model I was shown to accurately predict the full-scale furniture combustion characteristics of the peak HRR, time to peak HRR and total heat released for the standard polyurethane foam with both fabric coverings. For the high resilience foam however, the model significantly over-predicted the full-scale combustion characteristics.

# 3.0 Experimental Facilities:

## *3.1 Introduction:*

The bulk of this Research Project centres on experimental tests conducted in the UC Fire Engineering Laboratory. Bench-scale combustion tests are undertaken using the Cone Calorimeter apparatus, while full-scale furniture tests are conducted using the Furniture Calorimeter.

During the combustion of each burning article, parameters such as the combustion product concentrations of $O_2$, $CO_2$ and CO are recorded over time. The most important burning characteristic is the HRR, which is derived by applying the oxygen consumption calorimetry technique to the recorded test data.

## *3.2 Oxygen Consumption Calorimetry:*

During the combustion of most materials the heat of combustion released per unit mass of oxygen consumed E, is a nearly constant number. Huggett[7] examined a wide variety of fuels concluding that E = 13.1 kJ/g, represents a typical value for most combustibles, including gases, liquids and solids.

The basic requirement for using the oxygen consumption technique is to extract all the combustion products from a burning sample through an exhaust duct and at a point downstream where the gases have sufficiently mixed, measure the flow rate and composition. A sample of the exhaust flow is extracted allowing the oxygen concentration and other species to be measured. The exhaust oxygen concentration varies only a few percent from the ambient conditions, on the order of 18% - 21%. The oxygen concentration and the flow rate varying with time are recorded, so that the complete combustion history is recorded for a test.

The basic mathematical method to implement the oxygen consumption principle is that gas-sensing instruments measure the total mass flow of oxygen in the combustion products and compare that to an ambient flow. The energy released, $\dot{q}$, (in kW) is simply given by the following expression:

$$\dot{q} = E\,(\dot{m}_a Y^a_{O_2} - \dot{m}_e Y^e_{O_2}) \qquad \text{[Equation 1]}$$

Where:

E = heat release per unit mass of oxygen consumed (13.1 kJ/g)

$Y^a_{O_2}$ = mass fraction of oxygen in the combustion air (0.232 g/g in dry air)

$Y^e_{O_2}$ = mass fraction of oxygen in the combustion products (g/g).

$\dot{m}_a$ = mass flow rate of ambient air.

$\dot{m}_e$ = mass flow rate of exhaust combustion products.

There are several problems associated with the use of this formula for determining the HRR. Firstly, oxygen analyzers measure the mole fraction, not the mass fraction in the exhaust gas sample. Therefore the mole fractions need to be converted into mass fractions by multiplying the mole fraction by the ratio between the molecular mass of oxygen and molecular mass of the gas sample. The latter is usually close to that of air (29 g/mol). Secondly, water vapour is removed before the gas sample passes through the gas analyzers, so that the resulting mole fraction is on a dry basis. Thirdly, flow meters in the exhaust duct measure a volumetric flow rate, not the mass flow rate required for the above equation.

There are four ways in which the oxygen consumption calorimetry technique can be applied by measuring different combinations of various species concentrations in the exhaust flow. The more gas species measurements recorded, the better is the level of accuracy achieved. These are by:

- Measuring the $O_2$ concentration
- Measuring the $O_2$ and $CO_2$ concentrations
- Measuring the $O_2$, $CO_2$ and CO concentrations
- Measuring the $O_2$, $CO_2$, CO and $H_20$ concentrations

The specific equations for each of these methods have been formulated in great detail in many texts, and need not be repeated here. For further information on the ways in which each method is used, it is recommended to consult the works of Janssens[9] or Enright[5].

The UC sampling system has been modified over the past years and currently it is able to measure the concentrations of $O_2$, $CO_2$ and CO species. Through measuring the CO concentration, this caters for incomplete combustion, which is usually significant in diffusion flames. In all the combustion experiments undertaken in this Research Project, there will be a significant amount of CO production. This is because characteristically diffusion flames exhibit less than complete combustion and the geometry of the samples could be considered restrictive to creating an efficient flame.

## *3.3 Cone Calorimetry:*

The Cone Calorimeter is an apparatus that was developed to measure bench-scale combustion characteristics of various materials or combinations of materials. It operates by using radiation feedback from an electrical element to heat and cause test samples to practically burn completely away. It is presently the most common and preferred instrument for measuring HRRs for bench-scale combustion tests worldwide.

The name 'Cone Calorimeter' is derived from the shape of the electrical heating element, which is in a cone configuration. It was first developed by Dr. V. Babrauskas at NBS in the early 1980s. The apparatus and testing procedure has been standardized in the US and internationally[8]. The Cone Calorimeter can measure many combustion quantities and functions such as:

1. Heat release rate (HRR)
2. Effective heat of combustion
3. Mass loss rate
4. Ignitability
5. Smoke and soot production
6. Toxic gases production

The Cone Calorimeter uses oxygen consumption calorimetry as the basis for its measurement operation, which is outlined above. The general configuration and operation of the Cone Calorimeter is discussed briefly below in this report so as to outline its main features. For a more comprehensive description of the Cone Calorimeter, it is recommended to consult the works of Babrauskas[1, 2].

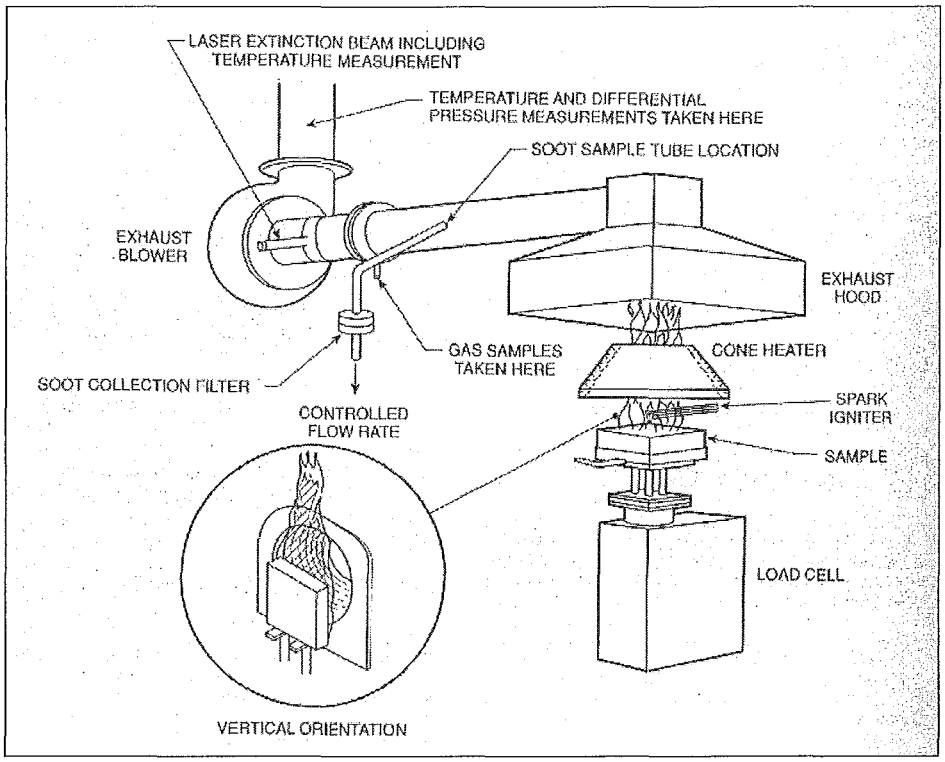


Figure 3.1: Schematic view of a Cone Calorimeter: (source[12])

The UC Cone Calorimeter is similar to the schematic representation shown in Figure 3.1. However, there are also many control devices, as well as the entire gas species sampling system, which are not shown here. It is not worth describing the UC Cone Calorimeter in great detail as it is typical of the current standard, therefore a summary outlining the most important features are discussed separately.

### 3.3.1 Element:

The heating element is in a truncated cone configuration, which delivers a near constant radiative heat flux across a specimen's surface. The temperature of the element is measured by three thermocouples in contact with the element, spaced regularly at equidistant points on the diameter of the cone. The temperature, which determines the heat flux level radiating from the coil, is taken as the average of these three values and is kept at a desired temperature by a digital temperature controller. The control temperature to deliver a desired heat flux ($kW/m^2$) is determined prior to all tests, by using a heat flux gauge as is illustrated in the Calibration Procedure[13].

### 3.3.2 Spark Igniter:

The location of the spark igniter is shown in Figure 3.1, which is positioned 25mm above the centre of the specimen. An electrical discharge creates an arc across a gap in the circuit, located over the centre of the sample, several times each second. The arc delivers enough energy to ignite combustible gases evaporating from a specimen's surface, which are caused from the heated element's incident radiation. Note: After ignition has occurred the spark igniter is shifted out of the flaming area.

### 3.3.3 Gas Analyzers:

The gas analyzers are the instruments that determine concentrations of $O_2$, $CO_2$ and CO from the sample extracted from the exhaust duct. The gas analyzing components of the gas sampling train includes a Servomex 540A paramagnetic oxygen analyzer for $O_2$ and a Siemens ULTRAMAT 6.0 NDIR gas analyzer (dual-cell, dual-beam with a flowing reference gas) for $CO_2$ and CO. The instrument panel and analyzers can be seen in the photograph in Figure 3.2. For these to operate correctly there must be a constant volumetric flow rate passing the inlet of the exhaust sample. A pump located downstream of the sample-port controls the flow, labelled 'exhaust blower' in Figure 3.1.

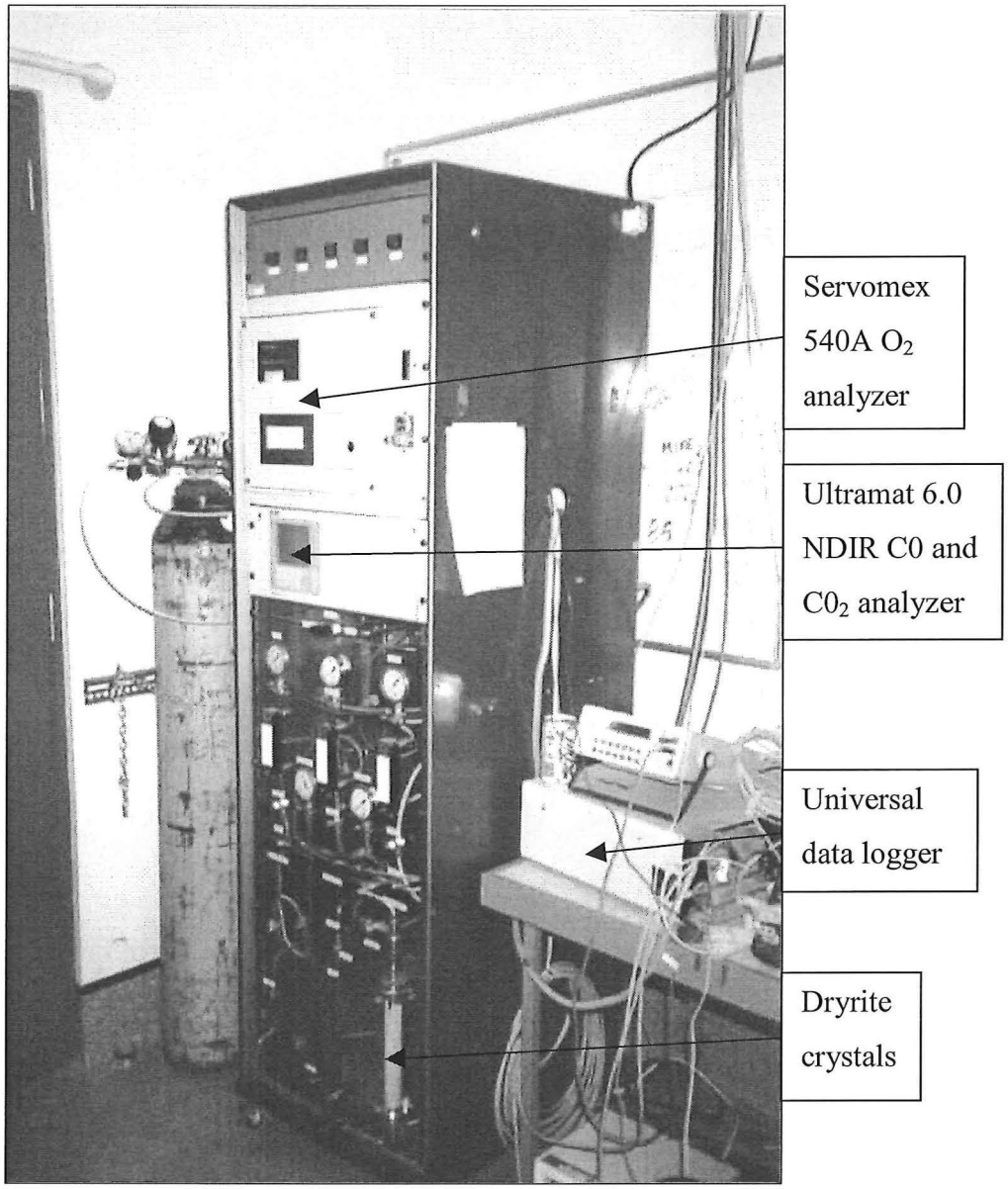


Figure 3.2: Gas Analyzer Instrumentation:

The configuration of the gas analyzer equipment includes various support components, some of which can be seen in the photograph in Figure 3.2. These include:

- A suction pump to provide the negative pressure within the system to draw the extract gases from the exhaust flue.
- A cold trap which condenses out water from the hot exhaust gas flow.

- A series of dryrite crystals, which absorb any remaining moisture that pass through the cold trap.
- Data Logger and Computer to store the information over time.

During a test run the recorded data is tabulated, with time, in a spreadsheet (*.csv format). To obtain useful HRR curves this raw data is modified in an Excel Spreadsheet Program developed specifically for the UC Cone Calorimeter. This modifies the raw data, using the oxygen consumption calorimetry principle outlined above and sets out the HRR, which can be usefully graphed.

## *3.4 Furniture Calorimetry:*

Furniture Calorimeters measure combustion characteristics from objects such as chairs, sofas, mattresses and other full-scale burning items. The specimen is burnt in much the same way as in Cone Calorimeter tests, but simply on a larger scale. One major difference between the calorimeter apparatuses is that the Cone Calorimeter uses a radiant heat flux from a heated element throughout an entire combustion test, which causes the sample to burn almost completely away. However, by contrast in Furniture Calorimetry, the ignition method is less standardized and it is a free burn that is investigated, once self sustained growth is reached. Commonly a gas burner is used for the initial stages of fire growth and then the item is allowed to burn under its own radiation feedback.

In a similar manner to the Cone Calorimeter, the specimen is placed on a load cell platform beneath a hood and extract system in order to collect all the combustion products. Instrumentation is provided in the exhaust duct to measure the flow rate and extract a gas flow sample for measuring the $O_2$, CO and $CO_2$ concentrations. The HRR as well as other functions and quantities are calculated in the same way as for Cone Calorimetry.

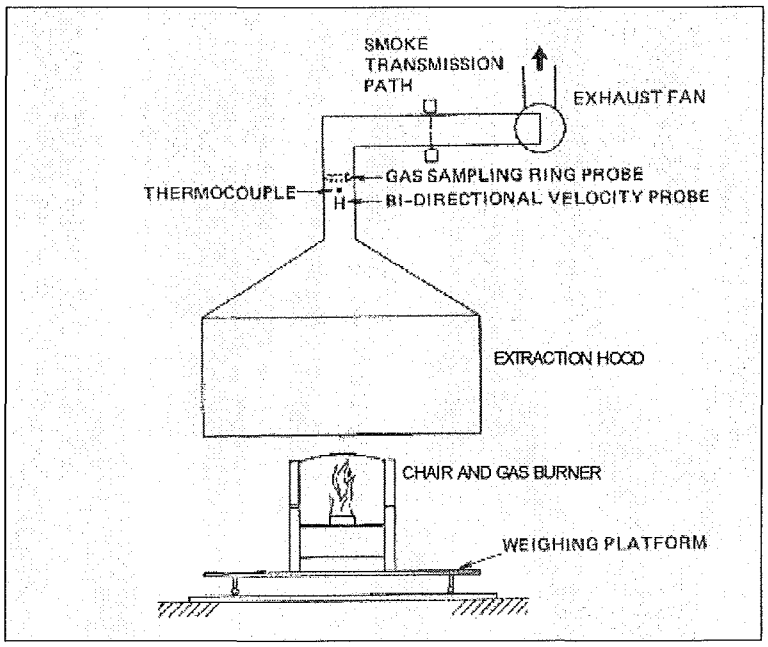


Figure 3.3: Schematic view of a Furniture Calorimeter:

Figure 3.3 shows the typical layout of the Furniture Calorimeter. The UC Furniture Calorimeter uses a square hood with 3m sides and is also 3m above the concrete floor of the laboratory. The extraction rate is designed to be $4m^3/s$, which from previous experience has shown to be more than sufficient for the size of furniture in this Research Project.

The UC Furniture Calorimeter uses the same gas analyzing equipment that is described for the Cone Calorimeter above. One major difference between the instruments apart from obvious scale differences, are the differences in the ignition source used in each. For details of this refer to the Furniture Calorimeter Procedures in Section 4. Below are listed the details of certain instrument components, to make the reader understand the specific set-up used for the full-scale tests.

### 3.4.1 Ignition:

For the furniture items, a square ring LPG gas burner, with a HRR of 30kW is used as an ignition source. This can be seen in the photograph in Figure 3.4, which shows the general testing configuration of the UC Furniture Calorimeter. The gas flames make contact the item, thus overcoming the uncertainty of ignition. The reason for making the tests relatively independent of ignition is for two reasons. Firstly by allowing enough LPG gas to burn, this essentially ensures that an item reaches a level of sustained burning, where it can burn under its own flaming radiation feedback once the burner is switched off. Secondly this ignition type allows the ease of ignition repeatability, where furniture of any description can be consistently ignited rapidly, after which its self-sustaining burning characteristics take over.

### 3.4.2 Mass Scale:

The mass scale has a large protective-tray fitted over it, as can be seen in the photograph in Figure 3.4, which shows the testing apparatus configuration. This is in-part to catch any materials, such as molten-flowing foam, which fall from the burning article and partly to protect the mass scale from being overheated. The mass of the burning item is recorded by having four legs pass through the catching table, which support an above catching tray that

the test item rests on. This method was developed specifically for the combustion tests in this Research Project.

### 3.4.3 Gas Analyzers:

The extraction duct is designed to achieve 4 $m^3/s$ of air at normal atmospheric pressure and 25°C. The gas sample is extracted, measured and recorded in the same manner as for the Cone Calorimeter tests, this being from a sample point in the exhaust duct. From this data the HRR curves are derived by a similar Excel Program to the Cone Calorimeter's, again using the oxygen consumption calorimetry principle. This program is developed specifically for the UC Furniture Calorimeter.

### 3.4.4 Other Instrument Features:

As well as the necessary exhaust properties that are measured to determine the HRR, additional measurements were recorded for further research, as can be seen in the photograph in Figure 3.4. These included:

- 3 heat flux gauges located at 1.5, 2.5 and 3.5m from the burning chair
- 9 Thermocouples located directly above the chair, at 200mm spacings
- Video recording of all the armchairs from two different angles.
- Still camera photographs taken at 15-second intervals.

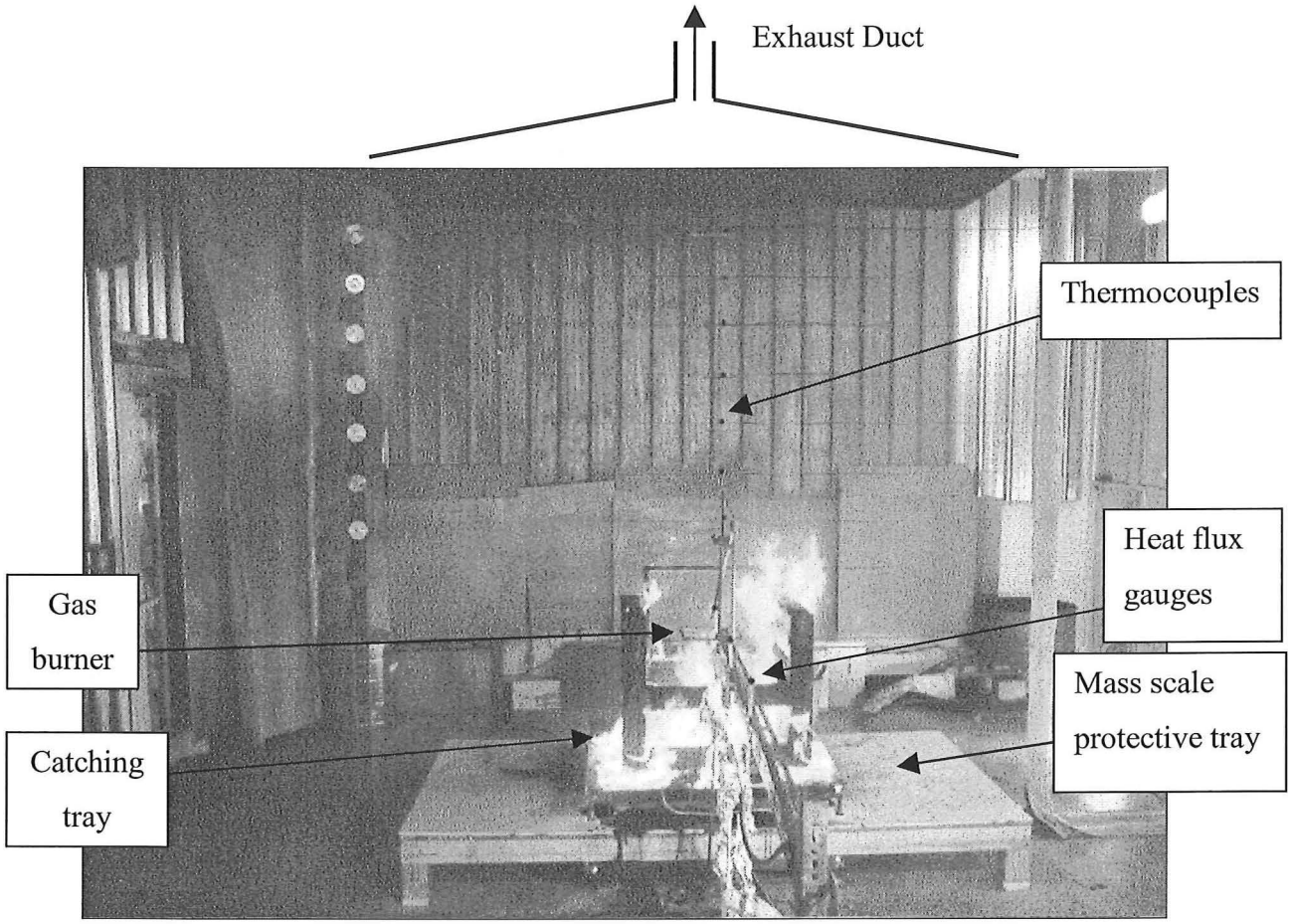


Figure 3.4: UC Furniture Calorimeter Testing Configuration, during the combustion of one of one of the Full-Scale Furniture Items:

# 4.0 Experimental Procedures:

## *4.1 Introduction:*

The bulk of this Research Project centers around experimental data obtained from bench-scale composite combustion tests on the Cone Calorimeter and full-scale tests on the Furniture Calorimeter. The Cone Calorimeter complies with the standard test method[8]as amended by Appendix A6 of the CBUF Final Report[4] "Cone Calorimeter Testing". The specimen preparation, test protocol and reporting are all performed according to the strict CBUF Protocol specification. Correspondingly the Furniture Calorimeter complies with the Standard[11] as amended by Appendix A7 of the CBUF Final Report[4] "Furniture Calorimeter Test Protocol". Likewise the specimen preparation, test protocol and reporting are all followed as per the CBUF Protocol specification.

## *4.2 Cone Calorimeter Testing Procedure:*

As mentioned above, the specimen preparation, test protocol and reporting are all performed according to the strict specification of the CBUF Protocol. It is not necessary to repeat the full specification in this section, instead only areas of emphasis and a broad overview are included. For the complete protocol method refer to the CBUF Final Report[4].

### 4.2.1 Test Set-up and Procedure:

An overview of what are the most important aspects of the Cone Calorimeter test set-up and procedure is included here to make the reader understand some of the necessary technical detail.

All foam samples were cut using the specified cutting blade on a band saw to within the tolerances specified as square faces of 102.5mm ±0.5mm × 50mm nominally thick. These were weighed in triplicate sets to ensure that masses did not differ by greater than ±5% from their arithmetic mean.

All completed foam/fabric specimens in their foil cups were conditioned at 23 ± 2°C and 50% relative humidity, for at least 24 hours prior to testing.

The specifically written UC Cone Calorimeter Test Procedure[14], which is based on the CBUF Protocol, was followed for each test run. Similarly, a specifically written UC Cone Calorimeter Calibration Procedure[13] was used to calibrate the apparatus with a 5kW methane flame at the beginning of each day on which tests were carried out. Both this and the Test Procedure were amended throughout testing, to make it user-friendlier for future tests.

A two-minute baseline was run before each Cone Calorimeter test. At approximately 1:50 minutes of baseline data, the cone shield was closed and the specimen holder, containing the test specimen was placed on the load cell. At as close to 2:00 minutes as possible, the shield was opened exposing the test specimen to the heat flux from the heated element and the spark igniter was moved into position directly above the specimen. The ignition time was recorded, after which the spark igniter was shifted from the flaming area. After all burning had finished, approximately 3:00 minutes of approaching-ambient test data was recorded.

In the extraction duct the volumetric flow rate is determined from the pressure difference across an orifice plate. Gas concentrations of $O_2$, $CO_2$ and CO are measured from a sample extracted from the exhaust duct. In the photograph in Figure 4.1, is composite G-21 burning in the Cone Calorimeter 20 seconds after ignition. The HRR is approximately 2kW. Note, for details of the composite coding method, refer to Section 5, 'Selection of Materials'.

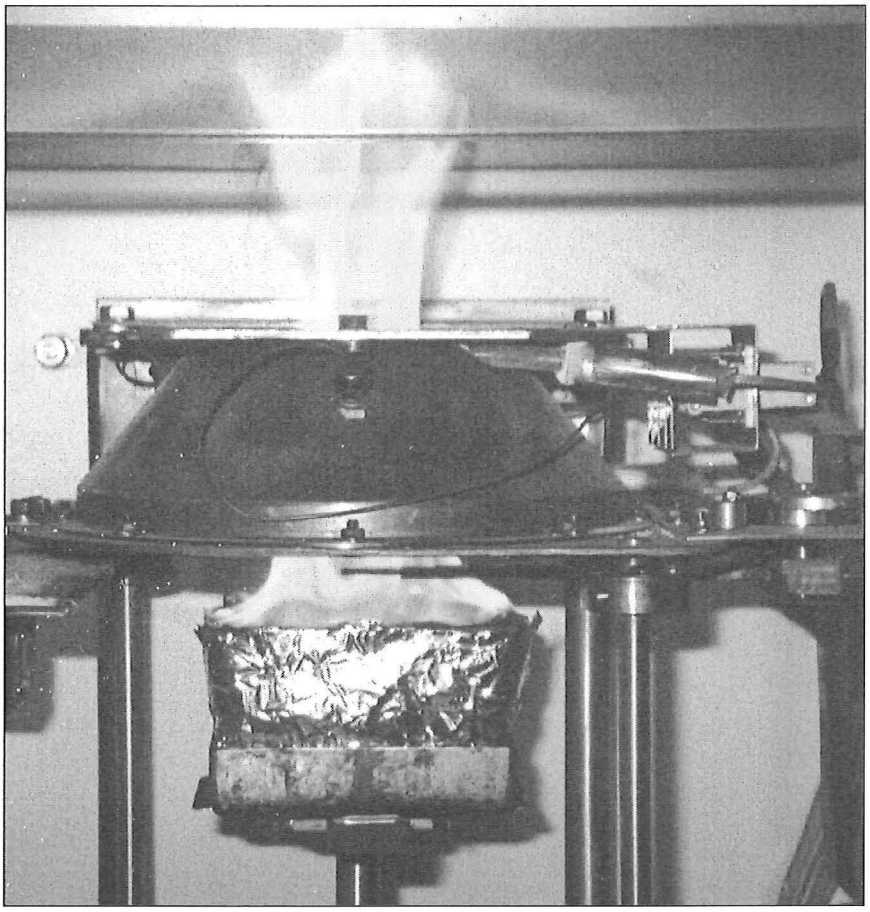

Figure 4.1: Cone Calorimeter Combustion test of Composite G-21:

All Cone Calorimeter tests were conduced under a uniform radiant flux of 35kW/m$^2$, in a horizontal orientation. Each set of triplicate tests was conducted on each testing material combination in quick succession, so that apparatus drifting calibration changes would be kept to a minimum. The triplicate test values of the $\dot{q}''_{180}$ (180-second average HRR) values were compared. If they differed by more than ±10% from their arithmetic mean, then a further three tests were required by the procedure. Note: This was not the case for any of the tests conducted, so each sample combination was only triplicated once. Refer to Section 6, 'Cone Calorimeter Results', for $\dot{q}''_{180}$ percentage differences.

## *4.3 Furniture Calorimeter Testing Procedure:*

As mentioned above, the specimen preparation, test protocol and reporting were all performed according to the strict specification of the CBUF Protocol. It is not necessary to repeat the full specification in this section, instead only areas of emphasis and a broad overview are included. For the complete protocol method, refer to the CBUF Final Report[4].

### 4.3.1 Test Set-up and Procedure:

As with the Cone Calorimeter, there are specific UC Furniture Calorimeter Testing[16] and Calibration Procedures[15] that have been developed over past years, which are specifically designed for the Furniture Calorimeter. These procedures were followed for all tests. The general requirements for the test set-up, as specified in the CBUF Final Report[4], were met to the best of the laboratory resource limitations.

Gas analyzer calibrations were conducted at the beginning of each day, and full LPG gas burner calibration runs were conducted several times throughout the tests to make sure that results were not drifting greater than ±10%.

All furniture items were conditioned at 23 ± 2°C and 50% relative humidity, for at least two weeks prior to testing.

The furniture items were ignited using a square ring LPG gas burner, with side dimensions of 250 mm and a HRR of 30kW. This burner was developed at FRS (Fire Research Station) and NIST (National Institute of Standards and Technology). It is the primary ignition source in the California TB 133 furniture test. The burner is placed 25mm above the middle of the seating cushion. The gas flames make contact the item, thus overcoming the uncertainty of ignition. Essentially ignition is practically guaranteed with the 30kW-flame source. This methodology is in contrast to the Cone Calorimeter tests where the ignition times, and hence ignitability of the test items are parameters that are under investigation. A mass flow controller having a set-point at the desired (30kW) flow rate controls the LPG flow to the burner.

A three-minute baseline was recorded before the LPG square burner was ignited. It was located 25mm above the center of the seating cushion and was allowed to burn for two minutes while the flames were spreading over the specimen, then the gas flow was shut off by means of the mass flow controller.

During the combustion, gas concentrations of $O_2$, $CO_2$ and CO are measured from a sample extracted from the exhaust duct by the same gas sampling and analyzing system as for the Cone Calorimeter. The photograph in Figure 4.2 shows Armchair J-21-S2-1 burning approximately 4 minutes after ignition. The HRR is approximately 550kW. Note, for details of the furniture coding, refer to Section 7, 'Full Scale Furniture Details'.

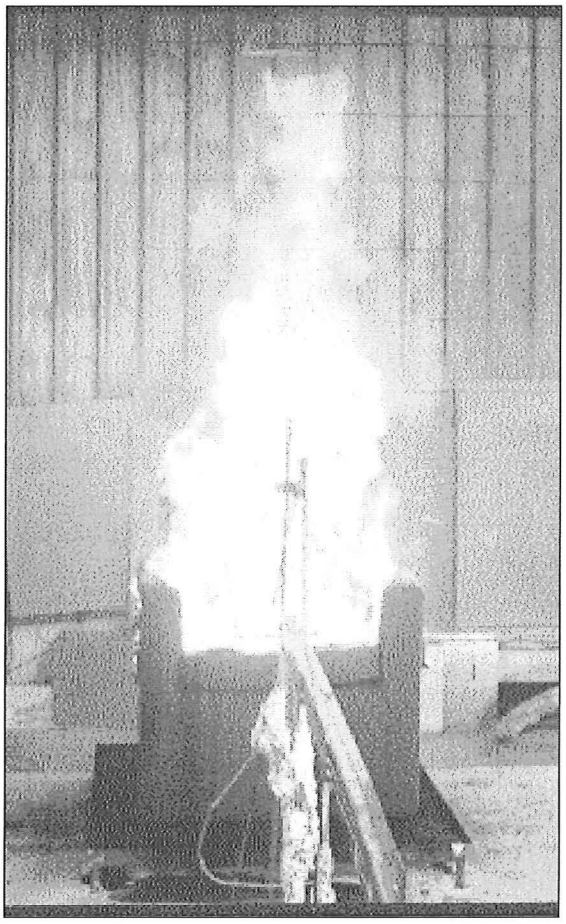

Figure 4.2: UC Furniture Calorimeter during the Combustion test of Armchair J-21-S2-1:

Note:

The general requirements for the test set-up, as specified in the CBUF test protocol, were met to the best of the resources' limitations. There were however a few discrepancies (mentioned below) where the Furniture Calorimeter did not enable all to be met, however these should have minimal impact on the results, or at least they will be consistent within all results.

The environment around the sample is required to be draught free with no more than two enclosing walls, defined as being within 2m from the smoke collection hood[4]. The UC Furniture Calorimeter has three enclosing walls. From the outer edge of the extraction hood, the north, south and east walls are 1.3m, 1.0m and 0.8m respectively from the building walls. During all tests the main door to the Laboratory was left open approximately 15cm. This was adopted as it was noticed in the larger flaming gas calibration runs, that the flames would straighten up more vertically if the door were propped open in this manner. Further, the measurement of toxic gas species other than CO concentrations, such as HCN and HCl, as well as soot production were not recorded.

## *4.4 Time Delays and Response Times:*

The calculated HRR is a function of many time-dependent variables. There are time delays between each property being produced and its value being recorded by the various measuring instruments. These time delays are not uniform from the time when each property is generated and when physically they reach the measuring devices. Therefore, when the data is recorded over time in the computer spreadsheet file, the property values correspond to different times, with respect to the combustion event and relative to each other.

An example of such a difference is between the measurement of the mass and gas species concentrations. The mass scale simply measures the instantaneous mass of the burning specimen. However, the gas species measurement is recorded only after the combustion products have physically travelled to the gas sampling collection point in the exhaust duct, then moved through the sample line and water extraction devices to the gas sensors. Thus,

both are out of time sequence from each other, due to two types of lags: transport lag and response lag.

The *transport lag* time refers to the time taken for the sample to physically reach the measuring instruments. The *response lag* time is a function of the instruments themselves, and is the time that it takes an instrument to read and register the measurement.

For the Cone and Furniture Calorimeter Apparatuses, Enright[5] studied the contributions of the time delays in detail, so for the specific characteristics of the apparatuses, it is recommended to consult his work.

The Excel Programs used in this Research Project to derive the HRRs' from the Cone and Furniture Calorimeter raw data, has these various time delays built into it. Thus as much as possible, errors are minimized for time lag contributions.

## *4.5 Choosing a Uniform starting time for the HRR Curves:*

When examining HRR curves from the Cone Calorimeter combustion tests, it was necessary to superimpose each triplicate set of test runs in order to determine the required average properties for the CBUF Model I prediction equations. This is necessary in order to remove any time dependence on ignition time, because the samples ignited at different times from each other. The method used was to position the leading edge of the HRR curves so that they coincide. Thus all samples will have ignited at approximately the same time relative to each other on the horizontal time scale. The triplicate-averaged values are then determined by reporting all the values from each individual run, and averaging the three identical test values. Refer to Appendix A, 'Cone Calorimeter Results' for details of this method.

It is also necessary to choose a starting HRR for the Furniture Calorimeter upon which the time to peak HRR criteria can be based. To be consistent with previous work by European CBUF[4], Enright[5] and Firestone[6], a zero time was taken as when a HRR of 50kW was first reached. This was essentially chosen because it signified the time when items began burning under their own growth rate and would not significantly have been altered if the ignition source had been removed. It should be kept in mind that the ignition source used in the Furniture Calorimeter is a gas burner, with a HRR of 30kW.

Note:

For many chairs tested in this Research Project, the HRR rose above 50kW for some time and then dropped below this value after the gas burner was removed. This shows that the chairs had not begun to develop self-sustained growth under their own burning intensity. This trend was particularly noticeable for the armchairs with Foam J and all of the woollen fabric covered armchairs. Refer to Section 8, 'Furniture Calorimeter Results and Discussion' for details.

# 5.0 Selection of Materials:

## *5.1 Introduction:*

The selection of the polyurethane foams and fabric coverings was of crucial importance to this Research Project. Essentially, every attempt was made to make sure that materials were as close to the compositions that are commonly used in real life situations in NZ furniture.

Polyurethane foam samples were chosen on the following basis:

- Common use as seating foam in upholstered furniture.
- Supplier. (use of the main foam supplying companies)
- Grade of foam and special applications.

Fabric sample were chosen on the following basis:

- Common use as a covering fabric for upholstered furniture.
- Composition.
- Price and availability.

## *5.2 Polyurethane Foam Selection:*

Polyurethane foam suppliers in Christchurch were consulted in person to determine from their range, which were the most suitable to use in the various furniture tests that were to be conducted. Their ranges included different quality foams for uses in commercial or domestic settings with variations in density and ranges of *fire retardant* foams.

The methodology used was firstly to select foams for doing bench-scale tests using the Cone Calorimeter and then refine the selection when testing the full-scale furniture. The types of foam were selected as common seating foams, which were generally nearer the heavier density end from each category. Initially seven foams were chosen to conduct the Cone Calorimeter tests, these are listed in summary below.

To distinguish the foams from one another, each foam type was coded with a letter beginning from "G" to be consistent with other UC research coding. The coding, colour, density and manufacturer's designed applications of the foams are listed in Table 5.1.

| Code | Colour | Density $kg/m^3$ | Applications |
|---|---|---|---|
| G | Lightgreen | 28 | Domestic furniture seats |
| H | Blue | 37 | Superior domestic furniture (fire retardant) |
| I | Pink | 35 | Superior domestic furniture, public seating |
| J | Yellow | 36 | Public auditorium seating (fire retardant) |
| K | Green | 27 | Domestic and commercial seat backs, cushions and arms |
| L | Grey | 36 | Public auditorium and transport seating |
| M | Darkgrey | 29 | Special applications, packaging |

Table 5.1: Foam Coding Identification and Specifications:

Note: The *fire retardant* foams meet different performance requirements. Foam J is combustion-modified, produced by the addition of inorganic compounds. It conforms to FAA/CAA flammability retardation requirements for seating foams. Correspondingly Foam H meets the flammability requirements of BS4735. The density shown here is the manufacturers quoted lowest-range density. Therefore the foams may not actually be in the rank order given in Table 5.1, weighing the foam types during tests will assess this.

## *5.3 Fabric Selection:*

Fabric stockists in Christchurch were consulted to determine which were their most commonly used fabrics for upholstered furniture covering. The final selection however was essentially decided on by fabric composition. Two common fabrics were selected having compositions of 100% polypropylene and 95% wool respectively. It was intended to use 100% constituent fabrics, however 100% wool is not commonly used as it tends to be fragile to weave and has reduced wear properties. A 5% polymer is thus added to the woollen fabric to make it more durable. The chosen fabrics are listed in Table 5.2 and are number-coded, using the same methodology as for the foams.

| **Composition** | **Basic Colour** | **Number Code** |
|---|---|---|
| 100% Polypropylene | Grey | 21 |
| 95% Wool 5% synthetic | Blue | 22 |

Table 5.2: Fabric Coding Identification:

Throughout this report the two different fabrics are simply referred to as "type 21" or "woollen fabric", and "type 22" or "polypropylene fabric". The differences in combustion characteristics, especially in ignition, between wool and polypropylene fabrics are well known. Generally wool has a tendency to prolong ignition when they are subjected to identical ignition tests. The experimental tests in this Research Project will test this generalization predominantly in the bench-scale tests.

Note: The fabric colour has the effect of changing the emissivity slightly, which is most significant to the radiant Cone Calorimeter tests. However, it is not an investigated parameter in this research, so most importantly the fabrics are kept identical throughout all tests.

## *5.4 Foam - Fabric Testing Combinations:*

For the Cone Calorimeter tests there were seven types of foam and two types of fabric as detailed above. This enabled fourteen possible composite combinations for conducting tests on. In addition to these, whilst using the same testing procedures, the seven types of foam were tested without any fabric covering. Thus a total of 21 different material tests were undertaken using the Cone Calorimeter. Furthermore, since each sample type was reproduced three times, or triplicated as per the Testing Procedures[14], this meant a total of 63 Cone Calorimeter tests in this Research Project.

Of main importance were the fabric-covered composite samples for two reasons. This is because the results from these tests determine which foams would be used in the full-scale furniture tests, as these are more expensive to conduct. Therefore careful thought was needed so as to justify the selection of the composition in the larger chairs. Also the bench-scale composite combustion data is used to predict the full-scale furniture combustion characteristics and hence assess the accuracy of the CBUF prediction model.

It should be noted that the tests conducted on the foams without fabric covering did not have any link to the European CBUF research. These experiments were conducted outside the main scope of this project so individual foam combustion characteristics, without any fabric influences, could be determined. This allows direct comparisons to be made between the foams with and without the fabric coverings, therefore showing how the types of fabric effect combustion behaviour.

For the Cone Calorimeter tests, the various composites were coded by listing the foam type, followed by the fabric type. Similarly for the tests on the foams without any fabric covering, only the foam type was used as the test code. An example is shown below for Composite G-21:

G – 21

- 'G' stands for the foam type.
- '21' stands for the fabric type (which is the polypropylene fabric).

## *5.5 Materials Effective Heats of Combustion:*

For reference, the net heat of combustion ($\Delta h_c$) for polyurethane, polypropylene and wool materials are listed in Table 5.3.

| **Material** | **Unit Composition** | **$\Delta h_c$ (MJ/kg) net** |
|---|---|---|
| Polyurethane | $C_{6.3}H_{7.1}NO_{2.1}$ | 22.70 |
| Polyurethane foam | - | 23.2 – 28.0 |
| Polyurethane foam FR | - | 24.0 – 25.0 gross |
| Polypropylene | $C_3H_6$ | 43.23 |
| Wool | - | 20.7 - 26.6 gross |

Table 5.3: Net Heat of Combustion and related properties of Selected Materials: (source[12])

Note: For the FR (fire retardant) foam and wool materials, a $\Delta h_c$ was not listed. Generally the gross heat of combustion is on the order of 10-20% higher than the $\Delta h_c$.

# 6.0 Cone Calorimeter Results and Discussion:

## *6.1 Introduction:*

The Cone Calorimeter tests on the 14 composites and 7 individual foam types were triplicated, as described in Section 4, 'Experimental Procedures', thus this meant a total of 63 bench-scale tests all up. The 63 HRRs from these tests are graphed individually in Appendix A, 'Cone Calorimeter Results', by grouping together each set of triplicate tests corresponding to the same material combination. Features from the individual HRR curves, (such as the peak HRR) are termed "*points of interest*". In this section, all results refer to values that are the average of each set of triplicated test runs. An example of how this calculation is made is illustrated in Appendix A for Composite J-22.

## *6.2 Cone Calorimeter Composite Test Results:*

In the following Tables 6.1 and 6.2 are shown the averaged triplicate values for the "points of interest" from the 21 test sample types. From these tables there are interesting trends that are discussed. In Table 6.1 are the results from the Cone Calorimeter tests on the fourteen composite types.

| | | Foam Type – Fabric Type | | | | | | | | | | | | | |
|---|---|---|---|---|---|---|---|---|---|---|---|---|---|---|---|
| **Parameter** | **Units** | **G-21** | **G-22** | **H-21** | **H-22** | **I-21** | **I-22** | **J-21** | **J-22** | **L-21** | **L-22** | **K-21** | **K-22** | **M-21** | **M-22** |
| m | kg | 0.0247 | 0.0280 | 0.0297 | 0.0324 | 0.0282 | 0.0311 | 0.0296 | 0.0322 | 0.0321 | 0.0355 | 0.0248 | 0.0284 | 0.0252 | 0.0290 |
| $\dot{q}''_{35\text{-}pk}$ | kW m$^{-2}$ | 435.0 | 350.8 | 440.9 | 347.9 | 470.3 | 373.8 | 379.8 | 354.1 | 450.4 | 405.3 | 429.4 | 321.1 | 424.0 | 355.3 |
| $\dot{q}''_{pk\#1}$ | kW m$^{-2}$ | 243.0 | 261.7 | 214.7 | 263.7 | 253.7 | 276.3 | 211.3 | 237.0 | 284.7 | 264.7 | 310.7 | 277.7 | 312.3 | 270.7 |
| $\dot{q}''_{trough}$ | kW m$^{-2}$ | 229.7 | 221.7 | 197.3 | 196.7 | 220.0 | 230.0 | 191.3 | 174.7 | 245.0 | 221.3 | 284.0 | 264.3 | 192.0 | 234.0 |
| $\dot{q}''_{pk\#2}$ | kW m$^{-2}$ | 435.0 | 350.8 | 440.9 | 347.9 | 470.3 | 373.8 | 379.8 | 354.1 | 450.4 | 405.3 | 429.4 | 321.1 | 424.0 | 355.3 |
| $\dot{q}''_{35\text{-}60}$ | kW m$^{-2}$ | 221.5 | 228.4 | 167.4 | 195.7 | 193.9 | 218.3 | 189.9 | 165.1 | 218.5 | 230.4 | 246.9 | 242.2 | 234.6 | 249.9 |
| $\dot{q}''_{35\text{-}180}$ | kW m$^{-2}$ | 321.2 | 254.3 | 312.5 | 262.3 | 343.2 | 278.0 | 289.6 | 239.5 | 338.3 | 296.9 | 337.8 | 261.4 | 313.5 | 271.4 |
| $\dot{q}''_{35\text{-}300}$ | kW m$^{-2}$ | 208.2 | 158.2 | 239.6 | 183.2 | 239.7 | 193.0 | 206.9 | 171.8 | 266.8 | 216.4 | 213.8 | 167.9 | 207.6 | 167.0 |
| $q''_{35\text{-}tot}$ | MJ m$^{-2}$ | 62.7 | 47.7 | 72.1 | 55.2 | 72.2 | 58.2 | 62.4 | 51.6 | 80.4 | 65.2 | 64.4 | 50.6 | 62.6 | 50.3 |
| $t_{ig\text{-}35}$ | s | 10.7 | 17.7 | 10.7 | 17.3 | 13.0 | 16.7 | 51.3 | 16.0 | 7.7 | 18.3 | 14.7 | 18.7 | 10.7 | 19.0 |
| $t_{pk}$ | s | 104.5 | 117.7 | 133.1 | 143.4 | 107.4 | 150.3 | 132.0 | 147.0 | 140.4 | 157.3 | 125.4 | 86.5 | 105.2 | 76.3 |
| $t_{pk\#1,ignition}$ | s | 26.8 | 12.5 | 32.6 | 15.0 | 29.7 | 15.8 | 26.0 | 16.9 | 34.8 | 12.8 | 27.9 | 16.1 | 35.6 | 12.8 |
| $t_{pk\#1,start\ of\ test}$ | s | 37.4 | 30.1 | 43.3 | 32.4 | 42.7 | 32.4 | 77.4 | 32.9 | 42.5 | 31.2 | 42.5 | 34.8 | 46.2 | 31.8 |
| $\Delta h_{c,eff}$ | MJ kg$^{-1}$ | 25.4 | 17.1 | 24.3 | 17.1 | 25.6 | 18.7 | 21.1 | 16.0 | 25.0 | 18.4 | 26.0 | 17.8 | 24.8 | 17.4 |
| $\dot{q}''_{35\text{-}180}$% diff (max) | % | 2.6 | 1.9 | 2.9 | 3.6 | 4.1 | 4.5 | 3.4 | 2.9 | 5.6 | 9.7 | 2.7 | 3.6 | 0.9 | 0.8 |

Table 6.1: Averaged HRR data for the Fourteen Composites:

In Table 6.2 are the results for the Cone Calorimeter tests on the seven types of foam, without any fabric covering.

| | | Foam Type | | | | | | |
|---|---|---|---|---|---|---|---|---|
| **Parameter** | **Units** | **G** | **H** | **I** | **J** | **L** | **K** | **M** |
| m | kg | 0.0148 | 0.0190 | 0.0185 | 0.0187 | 0.0218 | 0.0156 | 0.0156 |
| $\dot{q}''_{35\text{-}pk}$ | kW m$^{-2}$ | 362.6 | 402.9 | 348.2 | 317.6 | 389.8 | 368.8 | 353.2 |
| $\dot{q}''_{35\text{-}60}$ | kW m$^{-2}$ | 203.7 | 165.8 | 184.9 | 216.2 | 203.9 | 238.5 | 241.7 |
| $\dot{q}''_{35\text{-}180}$ | kW m$^{-2}$ | 171.8 | 214.7 | 210.5 | 164.7 | 251.4 | 187.7 | 183.5 |
| $\dot{q}''_{35\text{-}300}$ | kW m$^{-2}$ | 105.4 | 130.8 | 131.1 | 101.4 | 153.6 | 114.9 | 112.1 |
| $q''_{35\text{-}tot}$ | MJ m$^{-2}$ | 31.8 | 39.4 | 39.5 | 30.6 | 46.3 | 34.6 | 33.8 |
| $t_{ig\text{-}35}$ | s | 5.3 | 5.7 | 4.7 | 93.7 | 3.7 | 3.7 | 4.7 |
| $t_{pk}$ | s | 91.3 | 79.2 | 82.5 | 69.3 | 119.9 | 82.9 | 74.1 |
| $\Delta h_{c,eff}$ | MJ kg$^{-1}$ | 21.4 | 20.8 | 21.4 | 16.3 | 21.2 | 22.1 | 21.7 |
| $\dot{q}''_{35\text{-}180}$% diff (max) | N/A | 5.1 | 0.16 | 8.65 | 5.78 | 1.72 | 1.73 | 0.59 |

Table 6.2: Averaged HRR data for the seven types of foam without fabric covering:

Each set of triplicate combustion tests show a close average $\dot{q}''_{35\text{-}180}$%diff. If the difference of any one of these values of $\dot{q}''_{35\text{-}180}$%diff varied by greater than ±10% from the arithmetic mean of the triplicate runs, then a further three identical tests were required by the Testing Procedure[14]. For all tests, no values of $\dot{q}''_{35\text{-}180}$%diff greater than ±10% were calculated, so consequently no further tests were necessary for repeatability reasons.

## *6.3 Combustion Characteristics Caused by Fabric Type:*

For the Cone Calorimeter composite samples, the type of fabric covering has a noticeable influence on the combustion characteristics. Regular differences in all triplicate combustion tests were noticed between the wool and polypropylene fabric covered samples, for the same foam types in the following areas, as shown in Table 6.3.

- The peak HRR are highest for the samples with polypropylene fabric
- The total heat release are greater for the samples with polypropylene fabric
- The ignition time are shortest for the samples with polypropylene fabric
- The effective heat of combustion are highest for the samples with polypropylene fabric

| | **Polypropylene Fabric** | | **Wool Fabric** | |
|---|---|---|---|---|
| **Parameter** | **Range** | **Mean** | **Range** | **Mean** |
| m (kg) | 0.0321 - 0.0247 | 0.0278** | 0.03549 - 0.0280 | 0.0309** |
| $\dot{q}''_{35\text{-pk}}$ (kW/m$^2$) | 470.3 - 379.8 | 432.8 | 405.3 - 321.1 | 358.4 |
| $q''_{35\text{-tot}}$ (MJ/m$^2$) | 80.4 - 62.4 | 68.1 | 65.2 - 47.7 | 54.1 |
| $t_{ig\text{-}35}$ (s) * | 14.7 - 7.7 | 11.2 | 19.0 - 16.7 | 17.9 |
| $\Delta h_{c,eff}$ (MJ/kg) | 26.0 - 21.1 | 24.6 | 18.7 - 16.0 | 17.5 |

Table 6.3: Ranges and Mean Values of the "points of interest" for both the Different Fabric Covered Composite Samples:

Note:

* Composite J-21 behaved in an inconsistent manner for the ignition time. As can be seen in Table A1, (in Appendix A) the ignition times for the three J-21 Composites vary greatly, taking 32, 110 and 12 seconds (51.3 seconds on average as in Table 6.1) to ignite for each of the triplicate tests. Therefore, because of the high inconsistency and because these values are way out of pattern with the other ignition times, these values have been omitted from the average ignition times shown in Table 6.3. Furthermore, to be consistent, Composite J-22 is also omitted from the ignition times shown in Table 6.3. The reasons for Composite J-21 behaving differently are discussed in Section 6.5.

** The percentage difference in the fabric masses can be calculated from Table 6.3, as there are 42 samples to compare in the average mass values shown. This shows that the wool is approximately 11% heavier than the polypropylene fabric on an area coverage basis.

### 6.3.1 Peak HRR:

The peak HRR for the polypropylene covered samples are higher for all seven types of foam than their corresponding woollen covered composite samples. This result is caused because the polypropylene fabric burns more readily than the wool. This is for two reasons, firstly this is caused by the differences in *flammability* of the fabrics and secondly the differences in their effective heats of combustion.

Here the term flammability of the fabrics, is referring to the ease at which the samples ignite. It is evident from the ignition tests that the woollen fabric shows a greater resistance to ignite compared with polypropylene. This is shown by the woollen samples having longer ignition times than the corresponding polypropylene samples. This behaviour is easily noticed during observations of the tests, as the wool does not "*peel*" off the composites as quickly as the polypropylene does when they are exposed to the identical radiant heat. So therefore it is possible to say that the polypropylene has a higher flammability (in regard to the ignitability) than the woollen fabric in this context.

Wool has a lower effective heat of combustion than polypropylene, which are 20.7 – 26.6 and 43.23 MJ/kg respectively (refer to Section 5.5). Thus, even though the polypropylene samples are lighter, the large difference between the effective heats of combustion, combined with the higher flammability of the synthetic fabric, cause the polypropylene covered samples' to exhibit higher peak HRRs.

### 6.3.2 Total Heat Release:

The total heat released from the polypropylene covered samples are higher for all seven types of foam than their corresponding woollen covered samples. This is a result of more energy being stored inside the polypropylene composite samples than in the woollen samples.

There is approximately twice as much stored energy in the polypropylene fabric per unit mass, than the woollen fabric, as given above. Thus, even though the polypropylene is lighter by approximately 11% (refer to Table 6.3), there is still a total excess of energy available to be burnt in the polypropylene samples. Consequently, in the Cone Calorimeter tests where practically all the sample is burnt due to the high intensity incident radiation, more heat is released because the polypropylene samples simply have more stored energy available to be oxidized.

Note: For all tests in this Research Project, the total heat release is the calculated integrated area, with respect to time, under the HRR curves.

### 6.3.3 Ignition Time:

The ignition time for the polypropylene covered composites are lower for all types of foam, excluding composites with Foam J, than their corresponding woollen covered samples. The principle reason for this is because the woollen fabric resists peeling from the composites for a longer time than the polypropylene fabric. Samples with Foam J did not show this trend and are discussed separately in Section 6.5.

During the tests, characteristic observational differences between the two types of fabric were noticed when they were exposed to the radiant heat. The polypropylene fabric melted and peeled away almost immediately when it was exposed. The wool however, boiled, charred black and set hard before it began to spread. The difference in these circumstances is because of the different thermal properties of the fabrics. These two observations can be observed in the photographs taken during the pre-ignition stages of the tests as shown in Figures 6.1 and 6.2.

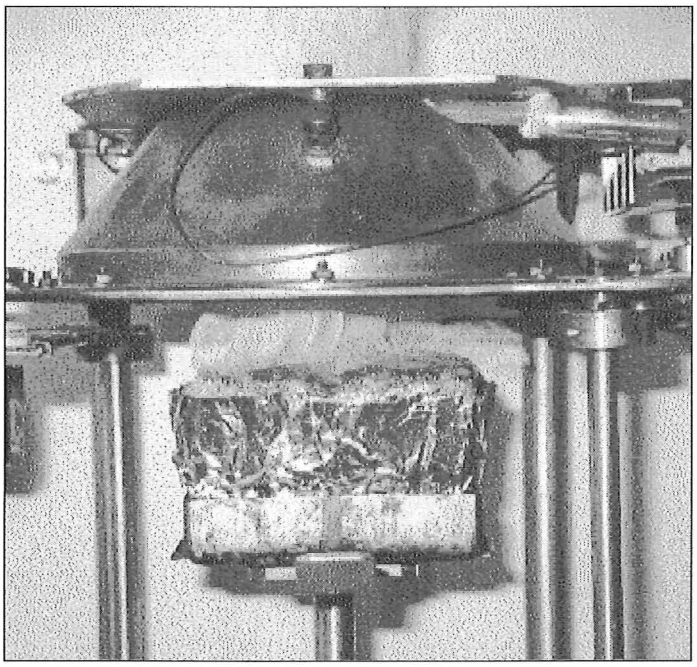

Figure 6.1: Test on Polypropylene Fabric Sample G-21: Note the melting and peeling fabric.

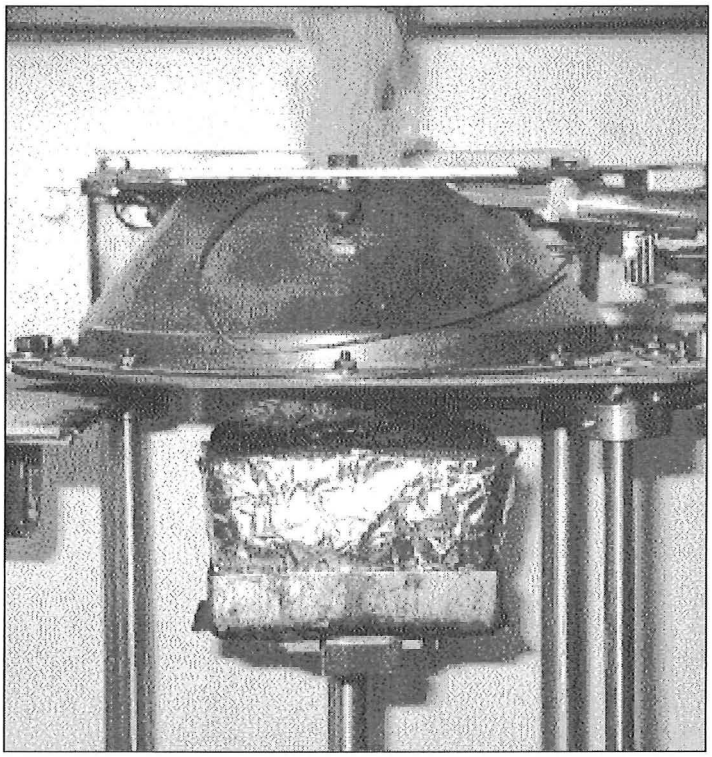

Figure 6.2: Test on Woollen Fabric Sample G-22: Note the charring fabric.

Polypropylene is synthetic and has a melting point of approximately 170°C. When the fabric reaches this temperature it rapidly peels off the surface to expose the foam. Wool however, has protein and is not synthetic. It does not appear to melt, but instead chars and then shrinks so that it peels in this way. In all tests conducted, it was observed that it was the flammable fumes from the polyurethane foam, rather than from the fabric, which appeared to expel the gases that ignited first. Therefore the wool covering simply prevents the foam being exposed to the radiation for a longer time, and hence this is the mechanism that accounts for the increased ignition times.

### 6.3.4 Effective Heat of Combustion:

The effective heat of combustion ($\Delta h_{c,eff}$) for the polypropylene covered samples are higher for all seven types of foam than their corresponding woollen covered samples. The $\Delta h_{c,eff}$, as given by Equation 10 (in Section 9), is simply the total heat released, divided by the mass of the combustibles.

Because the total heat release is highest for the polypropylene samples and their average mass is less, this combined effect raises the $\Delta h_{c,eff}$ to a markedly greater extent, over the woollen samples.

The calculated average $\Delta h_{c,eff}$ values of 17.5 MJ/kg and 24.6 MJ/kg (as in Table 6.3), for the woollen and polypropylene covered samples respectively, are lower than either of the composites' listed $\Delta h_c$. This discrepancy is mainly due to incomplete combustion of the total energy available to be oxidized in each sample.

## *6.4 Combustion Characteristics Caused by Excluding the Fabric:*

Regular differences in all triplicate combustion test samples were noticed between the fabric-covered composite samples and the non-covered samples, for all seven foam types in the following areas, as shown in Table 6.4.

- The non-covered foam samples produce lower total heat release values.
- The non-covered foam samples have the shortest ignition times.
- The non-covered foam samples produce an effective heat of combustion ($\Delta h_{c,eff}$) which are higher than the woollen covered samples' yet lower than the polypropylene samples'.

| | **Polypropylene** | | **No Fabric** | | **Wool** | |
|---|---|---|---|---|---|---|
| **Parameter** | **Range** | **Mean** | **Range** | **Mean** | **Range** | **Mean** |
| m (kg) | 0.0321 - 0.0247 | 0.0278 | 0.0218 - 0.0148 | 0.0177 | 0.03549 - 0.0280 | 0.0309 |
| $q''_{35\text{-}tot}$ ($MJ/m^2$) | 80.4 - 62.4 | 68.1 | 46.3 - 30.6 | 36.6 | 65.2 - 47.7 | 54.1 |
| $t_{ig\text{-}35}$ (s) * | 14.7 - 7.7 | 11.2 | 5.7 - 3.7 | 4.6 | 19.0 - 16.7 | 17.9 |
| $\Delta h_{c,eff}$ (MJ/kg) | 26.0 - 21.1 | 24.6 | 22.1 - 16.3 | 20.7 | 18.7 - 16.0 | 17.5 |

Table 6.4: Ranges and Mean Values of the "points of interest" for both the Fabric Composites and Non-Covered Samples:

Note:

* Foam J behaved in an inconsistent manner for the ignition time. As can be seen in Table A2 (in Appendix A), the ignition times for the J Foam samples vary greatly, taking 37, 108 and 136 seconds (93.7 seconds on average as in Table 6.2) for each of the triplicate runs. Therefore, because of the high inconsistency and because these values are way out of pattern with the other ignition times, these values have been omitted from the average ignition times shown in Table 6.4. Furthermore, to be consistent Composite J-21 and J-22 are also omitted from the ignition time values shown in Table 6.4.

### 6.4.1 Total Heat Release:

The total heat release values are lowest for the samples without any fabric covering for all seven types of foam. This is not surprising, as there is simply less energy available to be oxidized because there is no fabric contribution. The difference between the total heat release values in Table 6.4, thus represent the amount of energy stored within the fabrics.

### 6.4.2 Ignition Time:

The ignition times are lower for the samples without any fabric covering than both of their corresponding fabric covered samples for all types of foam, excluding Foam J samples. In all tests conducted, it was observed that it was the flammable fumes from the polyurethane foam, rather than from the fabric, which appeared to expel the gases that ignited first. Therefore because there was no delay in exposing the foam, the non-fabric covered samples allowed the radiant heat to begin to vaporize the foam sooner than for the fabric covered samples. Consequently the ignition times are less for the non-fabric covered samples. Samples with Foam J did not show this trend and are discussed separately in Section 6.5.

### 6.4.3 Effective Heat of Combustion:

The effective heat of combustion ($\Delta h_{c,eff}$) for the samples without any fabric covering, were in-between the $\Delta h_{c,eff}$ for the wool and polypropylene covered samples for all seven types of foam. The $\Delta h_{c,eff}$ were highest for the polypropylene covered samples and lowest for the woollen covered samples.

This result shows that the polypropylene fabric enhances the burning of the composite, whereas the woollen fabric retards the burning on a heat release basis per unit mass of sample. Thus, a real difference in the effects of the different fabric covering is revealed.

The average calculated $\Delta h_{c,eff}$ of the seven foam types is 20.7 MJ/kg, which is lower than the listed $\Delta h_c$ for polyurethane foam of 23.2 – 28.0 MJ/kg (refer to Section 5.5). This discrepancy is most likely due to incomplete combustion of the samples.

## *6.5 Combustion Characteristics Caused by Foam Type:*

### 6.5.1 Foam J, Fire Retardant Effects:

From the combustion of the samples with and without fabric coverings, there were profound noticeable differences in the combustion characteristics of Foam J, especially in the ignition times. The manufacturer lists this foam as having fire-retardant properties conforming to FAA/CAA flammability retardation requirements for seating foams.

Throughout all Cone Calorimeter tests, this foam had a lot of inconsistency associated with its combustion characteristics, which was especially pronounced in the ignition times. This is most likely due to the fire-retardant properties of the foam. The vapour expelling from the samples that was being drawn passed the spark igniter behaved as being on the borderline of being flammable. Thus on some occasions it has ignited like the other samples, although on three occasions it took a long time, in the order of 2:00 minutes. As such there was some doubt as to whether or not these samples would ignite each time they were tested. The other fire-retardant foam, Type H, did not behave significantly differently in any way from the rest of the foam types in these tests.

### 6.5.2 Other Foam Characteristics:

Foam L consistently released the highest amount of total heat release, regardless of the type or absence of fabric covering. This is simply because this foam has the greatest density, which is concluded because the average foam sample mass is greatest for this type, refer to Table A1, in Appendix A. Therefore, there is simply more stored energy available to be oxidized, as the combustible mass is greatest.

Note: As already suggested, the manufacturers listed foam densities, as in Table 5.1, were not entirely accurate for ranking the foams in order of mass. Table 5.1 suggests that Foam H is heaviest, when in fact it clearly was not, as the measurement of the samples' masses confirmed Foam L was considerably the heaviest.

# 7.0 Full-Scale Furniture Details:

## *7.1 Introduction:*

On the retail market there are essentially unlimited styles of upholstered furniture, forever changing with new fashion trends and manufacturing technology. The full-scale furniture items had to be selected as conforming to the European CBUF research and yet also be typical of designs currently in use in NZ.

The full-scale items had to be suitably sized for various reasons. Firstly to ensure that the smoke production and temperatures would not exceed the UC Furniture Calorimeter extraction system capabilities. Secondly, the cost per item was also an issue as this Research Project is linked to other UC research, which requires the same type of full-scale furniture. Thus this Research Project set a precedent in furniture style and also in the materials used for other UC research.

The furniture items had to be custom-made regardless of design, to ensure that the selected fabric and foams were used and traceable to each furniture item. The style selected was a simplified armchair design, made specifically for doing combustion tests in the European CBUF research. It is a fully padded single-seater armchair, the details of which are outlined below.

## *7.2 Description of the Custom Armchair:*

The custom armchair design is given in Appendix A2 of the CBUF Final Report[4]. Three series of armchairs are detailed, each of which enable different aspects of combustion to be investigated. The Series 2 armchair was selected for this Research Project, as this was most suited to the aspects that were being investigated.

The Series 2 armchair was designed with the intention of investigating differences in combustion behaviour caused by the use of different fabric/foam combinations. The

armchair is a fully upholstered style, where the arms, seats and backs are upholstered down to the ground. This "*control chair*" style was selected at the time of European CBUF research, as it was prolific throughout the European domestic sector and formed a major category in the commercial sector. The armchair technical specifications and drawings for this style are given in Figures 7.1 and 7.2.

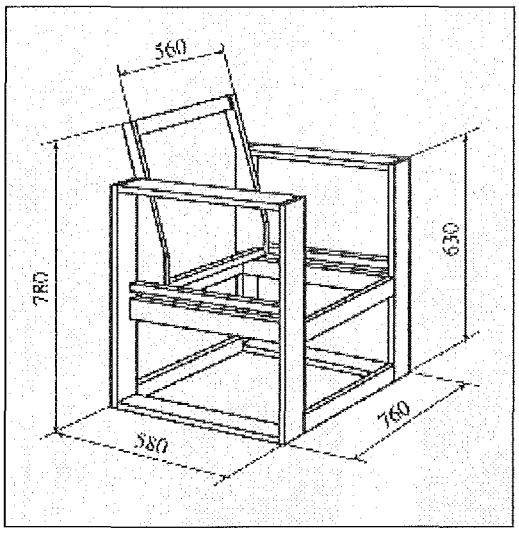


Figure 7.1: Frame Design for the Custom Armchair: (source[4])

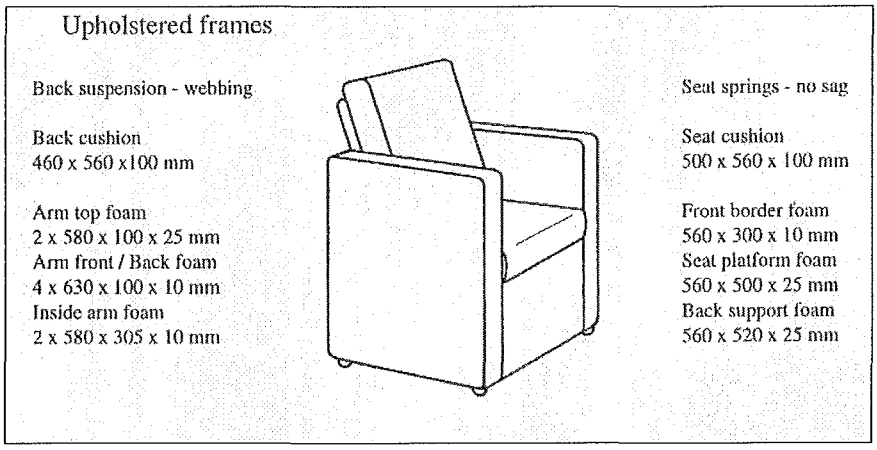


Figure 7.2: Foam Dimensions and Suspension Details for the Armchair: (source[4])

## *7.3 Selection of the Armchair Materials:*

From the Cone Calorimeter combustion results, the initial seven types of polyurethane foam selected had to be refined in order to use the most appropriate materials in the construction of the more expensive full-scale armchairs.

It was always an intention that both the wool and polypropylene fabrics were going to be tested, so it was only the foam selection that needed to be finalized. Through consultation with my Project Supervisor, the foams were assessed by taking into account the following concerns:

- The behaviour of each foam in the Cone Calorimeter tests.
- The most common use of each foam.
- Special features that were claimed by the manufacturers, such as fire retardant properties.

On this basis, it was decided to use all the same polyurethane foams, as for the Cone Calorimeter tests, except for Foam M. The reason for this is that this type of foam is not very commonly used as furniture padding. Foam M is listed as being purposely designed for special applications, such as packaging, giving clear justification why this type should be omitted from the full-scale materials. It was also decided to duplicate a mid-range performing foam, Foam G, so that combustion consistency and repeatability could be investigated.

Since in this Research Project only ten full-scale furniture combustion tests were planned, the duplicate armchairs with Foam G were not tested, as well as the Foam K armchairs, as this was another mid-range performing foam. Thus full-scale combustion consistency and repeatability could not be investigated. It is envisioned that these four armchairs will be burnt in future UC research and that the results will be compared to the results in Research Project. For a complete list of the ten selected armchairs, refer to Section 7.4.

## *7.4 Armchair Coding:*

To distinguish between the various different materials that were included in each armchair, and to be consistent with other UC research, the following coding method was adopted for the full-scale furniture items, as the example of Armchair # 2 shows:

**G – 21 – S2 – 1** (this is the coding for Armchair #2)

- 'G' stands the foam type.
- '21' stands the fabric type.
- 'S2' refers to the style, which in this research conforms to the European CBUF Series 2 armchair specification details, hence 'S2'.
- '1' is the number of persons that can sit on the furniture item.

Thus, for the ten full-scale furniture items, the chair numbers and individual material codes are as follows in Table 7.1:

| Armchair Number | Armchair Code |
|---|---|
| 2 | G-21-S2-1 |
| 5 | G-22-S2-1 |
| 6 | H-21-S2-1 |
| 8 | H-22-S2-1 |
| 9 | I-21-S2-1 |
| 11 | I-22-S2-1 |
| 12 | J-21-S2-1 |
| 14 | J-22-S2-1 |
| 18 | L-21-S2-1 |
| 20 | L-22-S2-1 |

Table 7.1: Armchair Numbers and Codes for the Full-Scale Furniture Items:

Note: The armchair numbers are not in consecutive order as various chairs were manufactured for other UC research projects. Throughout this Research Project, the armchairs are identified by their codes.

## *7.5 Armchair Manufacturing Details:*

### 7.5.1 Quality Control:

A local manufacturer was contracted to build twenty armchairs according to the custom specifications. Ten of these chairs were the full-scale items that were to be burned in this Research Project. The rest were manufactured for other UC research, and were made from the same materials. The local manufacturer was visited many times during fabrication of the armchairs to ensure that the exact components of each chair was correct, as ordered, and so the manufacturing methods were witnessed.

Ensuring that each armchair had the correct foam components, used in the appropriate location, was crucial for maintaining the credibility of this research. To guarantee that every foam piece was correctly sized, the dimensions of all the individual pieces were ordered directly from the foam manufacturers. These pieces were then grouped into piles that represented each individual chairs foam components. Each pile was weighed, bagged and labelled with a specific chair number, which corresponded each to a specific armchair frame and fabric type. Furthermore, each piece of foam was coded to represent the specific piece of foam that it was, as some pieces had very close dimensions. By doing this every effort was made to make it as easy as possible for the manufacturer to avoid making a mistake. The labels and numbering identification system can be seen in the photograph of Armchair I-22-S2-1 being manufactured in Figure 7.3. All the parts are coded and numbered ensuring that foam pieces were correctly located during manufacture.

The wooden frames, after being assembled, were weighed and numbered from 1 to 20. As each chair was made, the labelled foam pieces were used on the corresponding frames. The fabric was cut and fitted over the chairs, zips were included on the seating and back cushions, as per common practice.

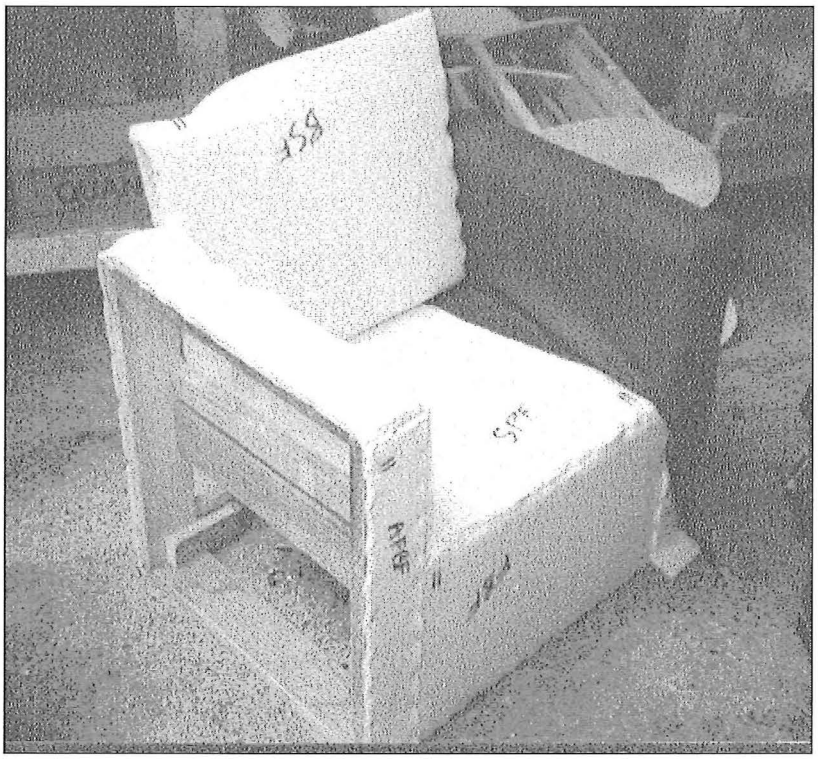

Figure 7.3: Armchair I-22-S2-1 being manufactured: Note the labels on each piece of foam corresponding to the frame.

### 7.5.2 General Construction:

The general construction used staples as the fixing mechanism. Staples hold the wooden frame components together, the foam pieces to the wood, as well as the fabric to the wood. Throughout the construction, regular visits ensured that correct foams and fabrics were being matched with the right frames. There were four areas in the manufacturing of the Series 2 armchairs that were either not fully described in the CBUF Final Report[4], or are not common practice, which led to slight deviations from the specified design. These were to do with the type of timber used, seat springing method, the covering under the seat cushion and the use of small feet under the armchair.

The wooden frame type is specified in the CBUF Final Report[4] as consisting of beech timber. By contrast, as is common practice in NZ, radiata pine timber was used for the frame, as this makes it more relevant to actual NZ furniture. However, in reality since the frame only plays

a small part in the 'fierce' stages of furniture combustion, this change is likely to have insignificant impacts on the results compared with effects caused by the variations in upholstery materials.

It is specified in Figure 7.2, which shows the suspension details for the armchair, that seat springs with no sag support the seat cushion and that the back cushion suspension uses webbing. However, it is current practice to use semi-elastic webbing for the seat suspension as well. For this reason, webbing was used as the seating suspension, which makes the armchairs relatively steel free as is the case with modern upholstered-wooden furniture of this nature. It is also unspecified what covers the seat suspension to protect the seat cushion from wearing on the springs. Therefore, to be consistent with the selection of seat webbing, durable fabric covering was used, which was common for this purpose. The placement of the seat webbing can be seen in the photograph of a typical armchair frame under construction in Figure 7.4.

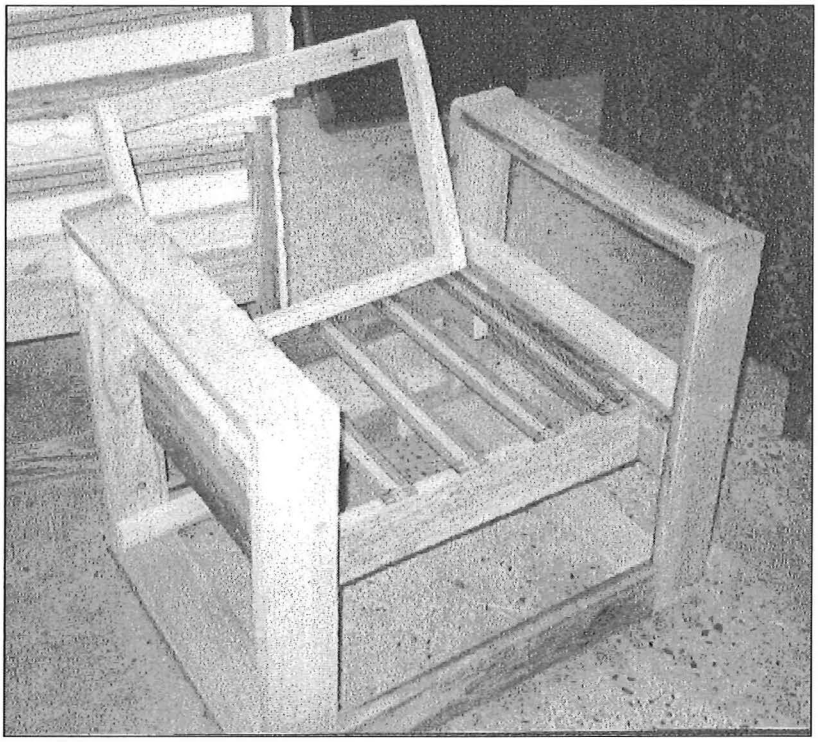

Figure 7.4: Typical Armchair Frame: Note the seat webbing suspension.

Another small variation was the inclusion of four plastic disc feet that were placed under each corner of the armchairs. In Figure 7.2, which shows a general layout of the armchair design, the feet can be seen under each corner of the armchair. No description or dimensions of these feet were given in the CBUF Final Report[4]. The inclusion of these feet was left up to the manufacturer, who used current techniques. Again this makes the armchair a more realistic example of current furniture in use in NZ. This has the effect of raising the base of the chair approximately 15mm off the floor. It should be noted that this could possibly change the combustion characteristics of the armchair. It is not the plastic burning itself that could modify the combustion, but the created air gap allowing extra *drawing*[2] under the base of the armchair, which may enable more air supply to the fire.

[2] Drawing is referring to a flow of air that is sucked up through a fire from underneath. It generally helps a fire receive oxygen and consequently helps to create more heat by increasing the combustion rate.

# 8.0 Furniture Calorimeter Results and Discussion:

## *8.1 Introduction:*

The ten full-scale armchair combustion tests are individually graphed in Appendix B, 'Furniture Calorimeter Results'. These show the HRR histories, CO, $CO_2$ and $O_2$ concentrations and the mass fraction of $CO/CO_2$ produced from each armchair test. Features from the individual HRR curves, such as the peak HRR and total heat release give an indication as to the severity of each chairs combustion. In this section, the armchairs general behaviour, and noticeable combustion differences between the two fabric types and the different types of foam are discussed.

## *8.2 General Burning Characteristics of the Armchairs:*

The armchairs generally burnt in a four-stage manner. These stages can be visualized in the HRR history curve shown for Chair G-22-S2-1 in Figure 8.1 and are illustrated in the photographs taken during the combustion of the same armchair in Figures 8.2 to 8.6. The locations of each of these photographs are also shown in the HRR history curve in Figure 8.1, so that the HRR can visualized in each of the four stages. The stages have also been identified and separated to show them on a HRR basis in Figure 8.1. These stages were identifiable for all the armchairs tested and are titled as follows: *constant growth HRR*, *decline in HRR*, *rapid growth* and *decay in HRR*.

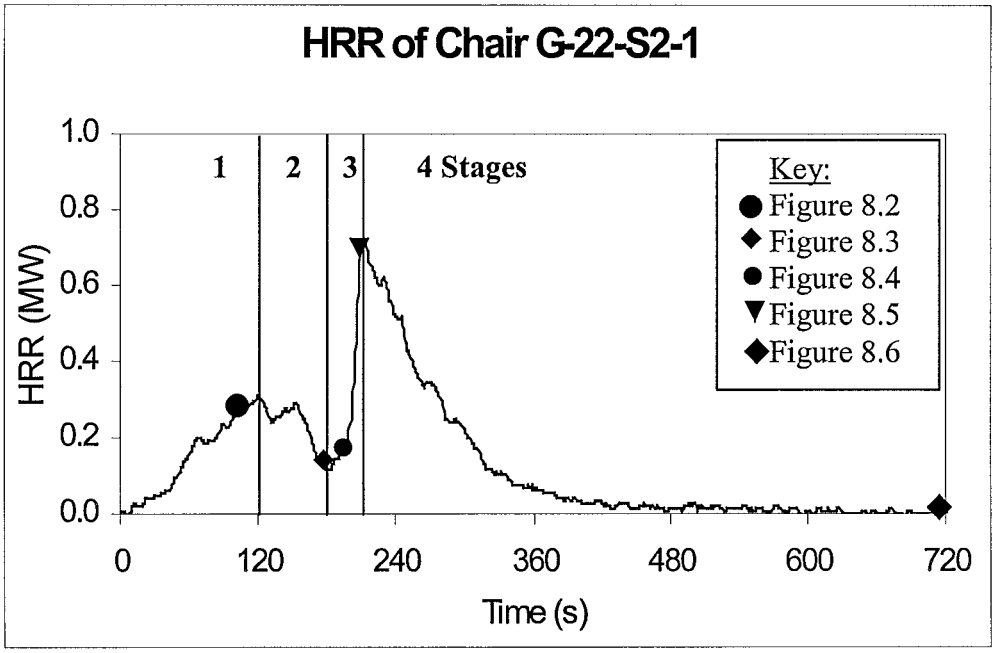


Figure 8.1: The Heat Release Rate History of Chair G-22-S2-1: Note the four labelled combustion stages and the location of the photographs in Figures 8.2 to 8.6.

**Stage 1: "Constant Growth HRR Stage"**

This occurs while the seating cushion is being ignited by the LPG gas burner. The seat cushion, back cushion and the inside of the armrests burn together with essentially a constant growth rate, to a time when either self-sustaining burning characteristics take over or the gas burner is switched off. Which of these two processes are adopted appears highly dependent on the fabric type and is discussed in Stage 2.

All the polypropylene covered armchairs, excluding Chair J-21-S2-1, showed relatively constant growth for approximately the first 60 seconds before a brief decline in the HRR. All five woollen covered armchairs and Chair J-21-S2-1 showed longer constant growth rate trends till approximately 120 seconds, which was when the gas burner was turned off. The *constant growth stage* can be seen in the photograph of Chair G-22-S2-1 shown in Figure 8.2. The seat cushion is nearly totally in flames and together with the back cushion, flames approximately 1.5 metres high are produced.

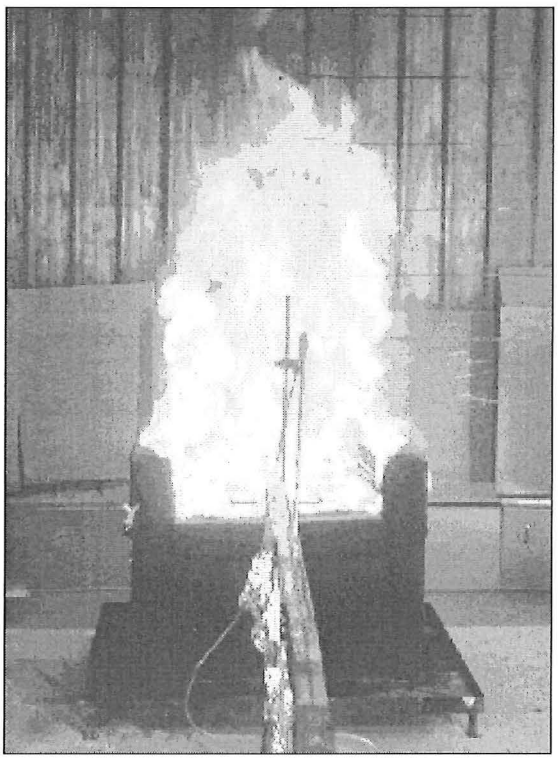

Figure 8.2: Chair G-22-S2-1, 1:45 minutes after ignition:

**Stage 2: "Decline in HRR"**

After the *constant growth stage*, there was a marked decline in the HRR for all tests. This physically occurred when the seating cushion had burnt virtually completely away and a pool fire was developing underneath the chair on the catching tray. In this stage the back cushion burning declines in intensity as the foam melts into the underneath pool. Due to the geometrical constraints of the chair, this flaming pool lacks oxygen supply and so burns in a ventilation controlled manner. This stage can be seen in the photograph shown in Figure 8.3.

The polypropylene covered armchairs, excluding Chair J-21-S2-1, (as grouped in Stage 1) showed a very small and short-lived HRR decline, before rapid HRR growth as self-sustained growth took control. For the other six armchairs, the decline in HRR, which occurred after the gas burner was switched off at 2:00 minutes, was more significant as they had not yet reached a level where rapid self-sustained growth took control.

In this stage the pool fire in the centre of the chair on the catching tray has a restricted air supply because of the chair foam and fabric that encloses it. This causes the burning intensity and HRR to drop until eventually enough radiation or flames themselves melt or spread the fabric layer on the sides, front and back of the armchair. Thus, this allows the fire to draw in more air supply. This transition is marked by the sudden rise in HRR as the armchair flares up with the onset of increased oxygen supply.

For the polypropylene covered armchairs, the fabric is not as resistant at staying in place as the woollen fabric when they are exposed to heat. This was proven in the bench-scale tests, where the woollen fabric covered the foam samples for longer than the polypropylene fabric under the same heat exposure. For this reason, the decline in the HRR is much less pronounced for the polypropylene covered armchairs, as the fabric melted away quickly. The only polypropylene chair that showed characteristics similar to the woollen fabric covered chairs' HRRs, by having an extended decline in the HRR after the gas burner was turned off, was Chair J-21-S2-1. This event is discussed separately in Section 8.5, as it believed to be attributed to the fire-retardant properties of Foam J. For the woollen covered armchairs, the resistance of the fabric to spread extends the HRR decline, prolonging the fire from flaring-

up as soon. Thus, the pool burns under the chair in a ventilation-starved environment for a longer time, as seen in the photograph in Figure 8.3. Also noticeable in Figure 8.3 is that the liquid pool fire has flown out from underneath the chair, and is flaming on the catching tray in front of the chair.

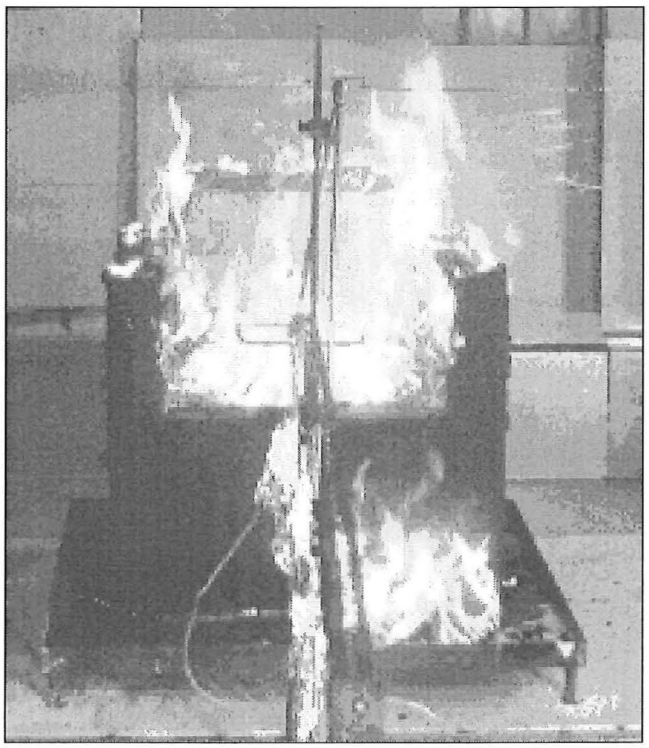

Figure 8.3: Chair G-22-S2-1, 3:00 minutes after ignition:

**Stage 3: "Rapid Growth"**

This stage is reached once the pool fire has had enough heat and duration to melt or spread the fabric on the sides, back and front of the armchair, allowing more air to "feed" the pool fire. The sudden availability of oxygen enables the fire to flare-up quickly, engulfing the majority of the armchair. This transition happened on the order of a few seconds for most armchairs, and the HRR climbed quickly to the peak HRR levels. This occurrence can be seen in the photographs of Chair G-22-S2-1 burning in Figures 8.4 and 8.5, which were taken only 15 seconds apart. Notice how the front fabric melts through allowing an enhanced air supply to the fire. This makes the HRR rise abruptly, as can be seen by the different amounts of flaming between these two photographs.

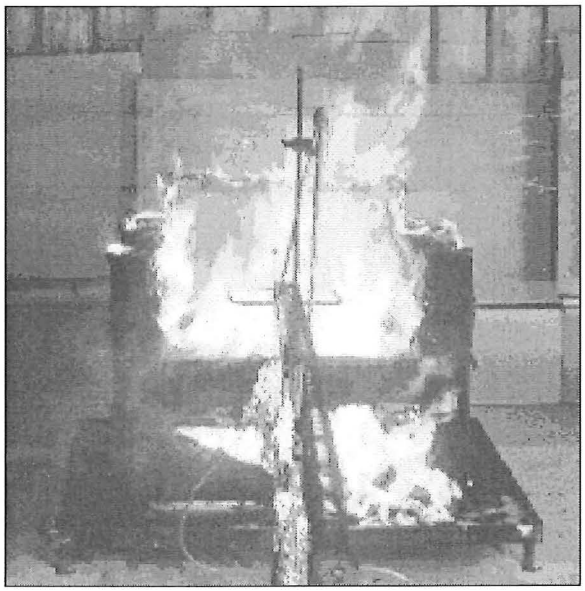

Figure 8.4: Chair G-22-S2-1, 3:15 minutes after ignition:

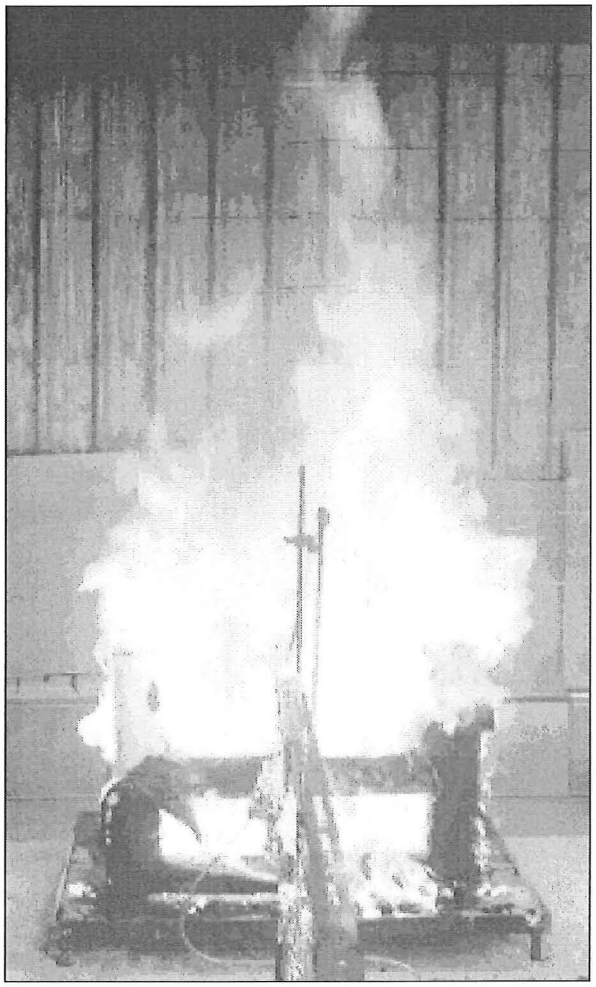

Figure 8.5: Chair G-22-S2-1, 3:30 minutes after ignition:

**Stage 4: "Decay in HRR"**

After the higher HRR values, the burning armchair becomes fuel controlled, limited by the amount of fuel available and the surface area of the fuel. The decay HRR curve represents the dying down of the flames as the pool and rest of the combustibles are depleted.

The four plastic feet were generally the only items still flaming after approximately 10:00 minutes from ignition. The wooden frames did not burn extensively, they were charred to a thickness of approximately 4mm on average for the faces and to larger amounts on the corners and beside the burning plastic feet, as shown in the photograph in Figure 8.6.

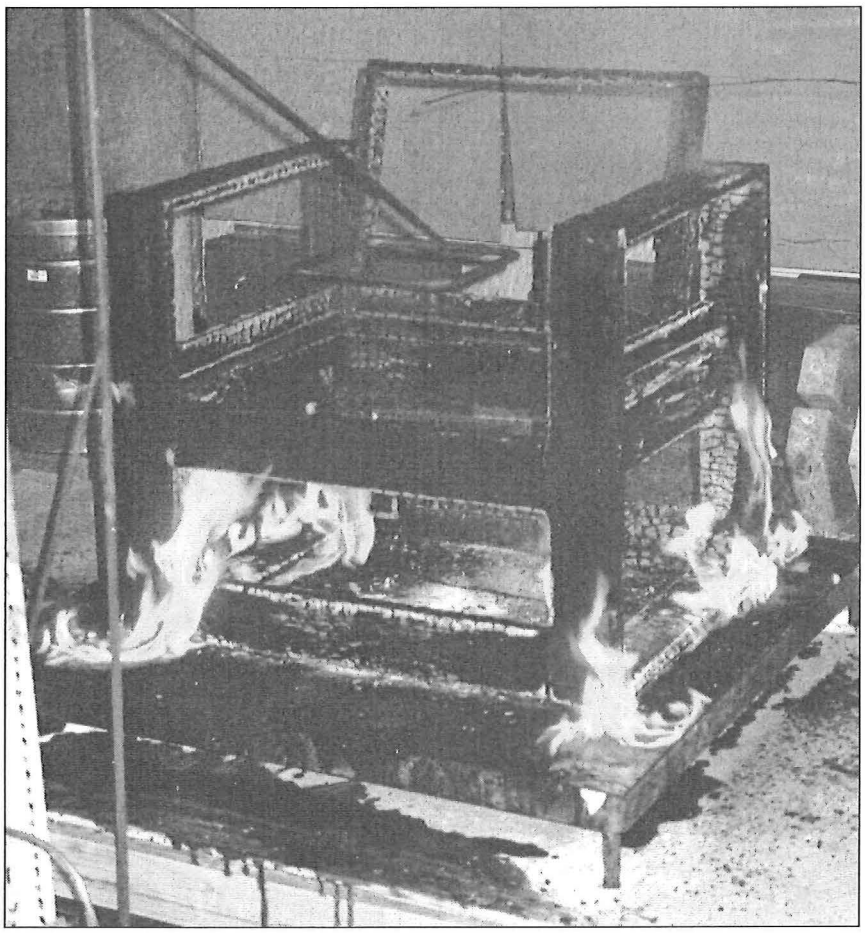

Figure 8.6: Chair G-22-S2-1 approximately 12:00 minutes after ignition:

## *8.3 Furniture Calorimeter Test Results:*

In the following tables and graphs are shown HRR data for the combustion of the ten armchairs. The main "points of interest" for the full-scale combustion tests are the peak HRR, time to peak HRR and the total amount of heat released. Interesting trends are observed and are discussed for various material combinations.

In Figures 8.7 and 8.8 are the HRR histories for the ten armchairs grouped by fabric type.

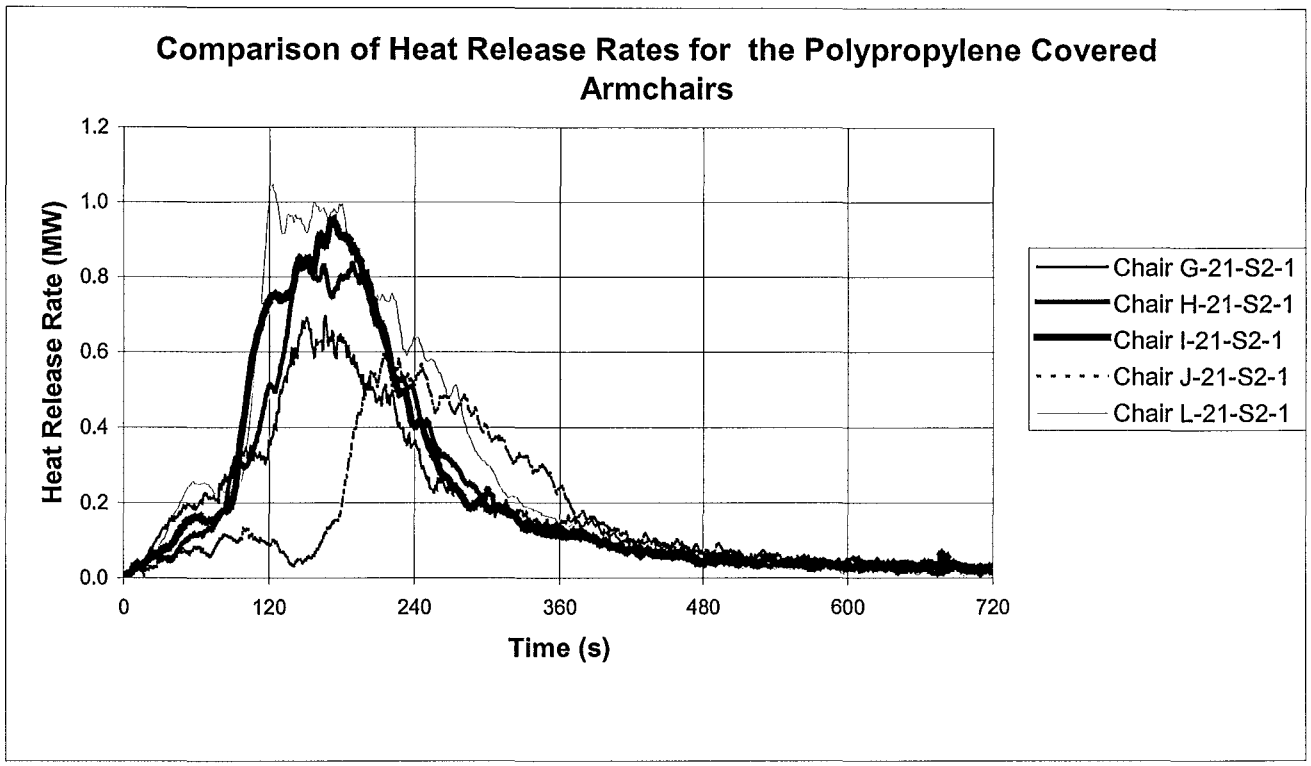


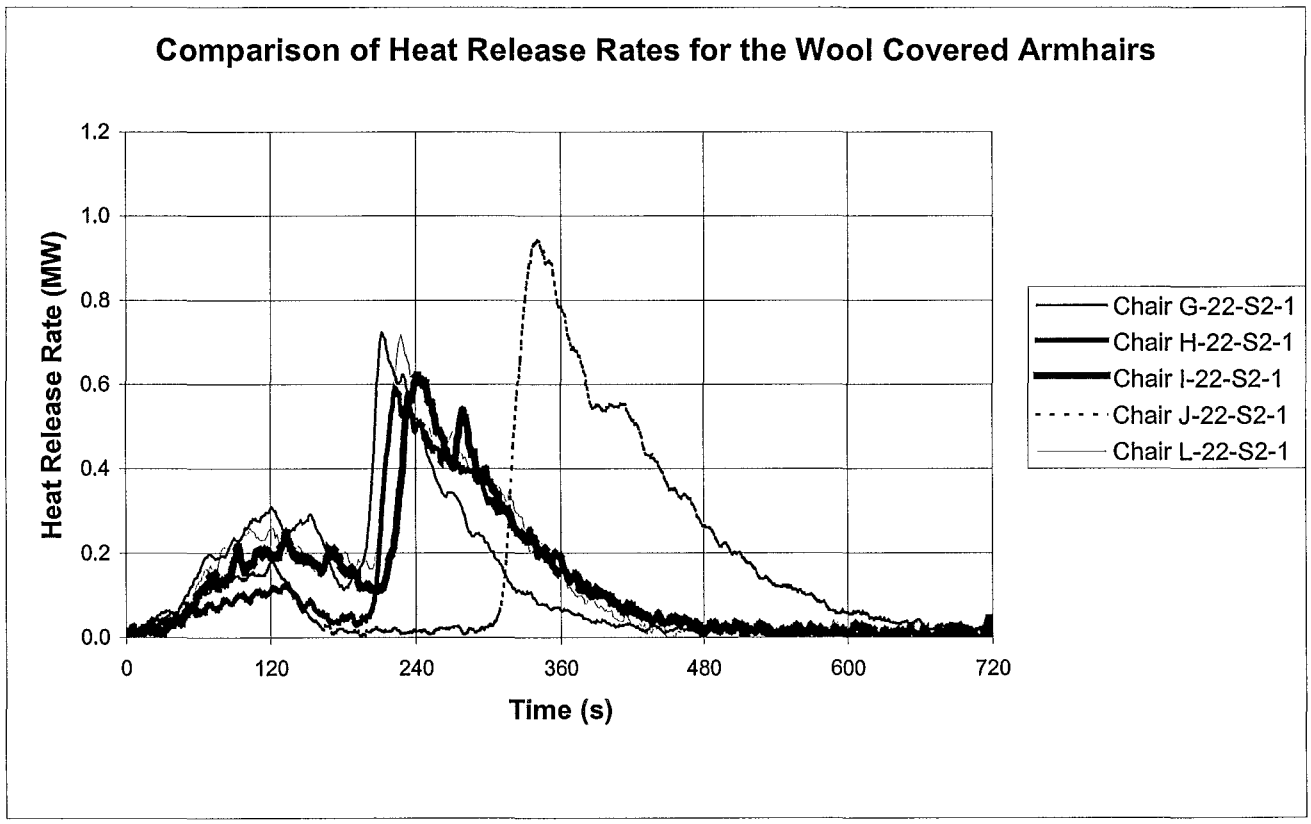


Figures 8.7 and 8.8: HRR Curves for the Polypropylene and Woollen Covered Armchairs:

Table 8.1 shows values from the HRR curves for the peak HRR, time to peak HRR ($t_{pk}$) and total heat released which are of interest for helping to determine the severity of the armchairs combustion. The mass of the soft components ($m_{soft}$) is also included as this is relevant in determining the armchairs' effective heats of combustion, $\Delta h_{c,eff}$.

| Chair Code | G-21-S2-1 | G-22-S2-1 | H-21-S2-1 | H-22-S2-1 | I-21-S2-1 | I-22-S2-1 | J-21-S2-1 | J-22-S2-1 | L-21-S2-1 | L-22-S2-1 |
|---|---|---|---|---|---|---|---|---|---|---|
| $m_{soft}$ (kg) | 3.43 | 4.26 | 4.26 | 4.41 | 4.46 | 4.16 | 5.02 | 5.00 | 5.09 | 5.00 |
| Peak HRR (kW) | 688 | 722 | 841 | 591 | 952 | 621 | 593 | 940 | 1048 | 718 |
| Total Heat Released (MJ) | 144 | 89 | 152 | 81 | 166 | 96 | 128 | 138 | 189 | 95 |
| $t_{pk}$ (s) | 132 | 179 | 128 | 178 | 153 | 194 | 175 | 315 | 101 | 82 |
| $\Delta h_{c,eff}$ (MJ/kg) | 42.0 | 21.5 | 35.7 | 16.2 | 39.1 | 19.3 | 29.0 | 27.0 | 42.4 | 18.9 |

Table 8.1: Furniture Calorimeter "Points of Interest" from the full-scale tests:

## *8.4 Combustion Characteristics Caused by Fabric Type:*

For the combustion of the armchairs, the type of fabric covering has a noticeable influence on the combustion characteristics. Regular differences were noticed between the wool and polypropylene fabric covered armchairs in the following areas, as shown in Table 8.2.

- The peak HRR are highest for the armchairs with polypropylene fabric.
- The total heat release are greater for the armchairs with polypropylene fabric.
- The times to peak HRR are shortest for the armchairs with polypropylene fabric.
- The effective heat of combustion are highest for the armchairs with the polypropylene fabric.

| | **Polypropylene Fabric** | | **Wool Fabric** | |
|---|---|---|---|---|
| **Parameter** | **Range** | **Mean** | **Range** | **Mean** |
| $m_{soft}$ (kg) | 4.45 - 3.43 | 4.16 | 5.09 - 4.15 | 4.85 |
| Peak HRR (kW) | 1048 - 593 | 824 | 940 - 591 | 718 |
| Total Heat Released (MJ) | 189 - 128 | 156 | 138 - 81 | 100 |
| $t_{pk}$ (s) | 175 - 101 | 138 | 315 - 82 | 190 |
| $\Delta h_{c,eff}$ (MJ/kg) | 42 - 29 | 38 | 27 - 16 | 21 |

Table 8.2: Ranges and Mean Values of the "points of interest" for the Armchairs, separated by Fabric Type:

### 8.4.1 Peak HRR:

The peak HRRs for the polypropylene covered armchairs are higher, for all five types of foam, than the corresponding woollen covered armchairs. This result is caused because the polypropylene fabric burns more readily than the wool. This trend is similar to the bench-scale tests, where the polypropylene composites also burned with a higher peak HRR. The differences in the bench-scale tests were attributed to differences in the materials' flammability and effective heats of combustion. Both of these mechanisms would also contribute to why the polypropylene covered armchairs showed the highest peak HRRs in the full-scale tests.

Another HRR characteristic that can be identified as being different between the two types of fabric, is the amount of time that the HRR is at the highest values. The woollen covered armchairs have a sharp spike in the HRR curve, where the peak occurs. For the polypropylene covered chairs' however, the HRRs have a wider section where the highest HRR values are occurring. These two behavioural characteristics are clearly visible in the HRR curves shown for Chairs L-21-S2-1 and L-22-S2-1 in Figure 8.9 and for all the chairs in Figures 8.7 and 8.8.

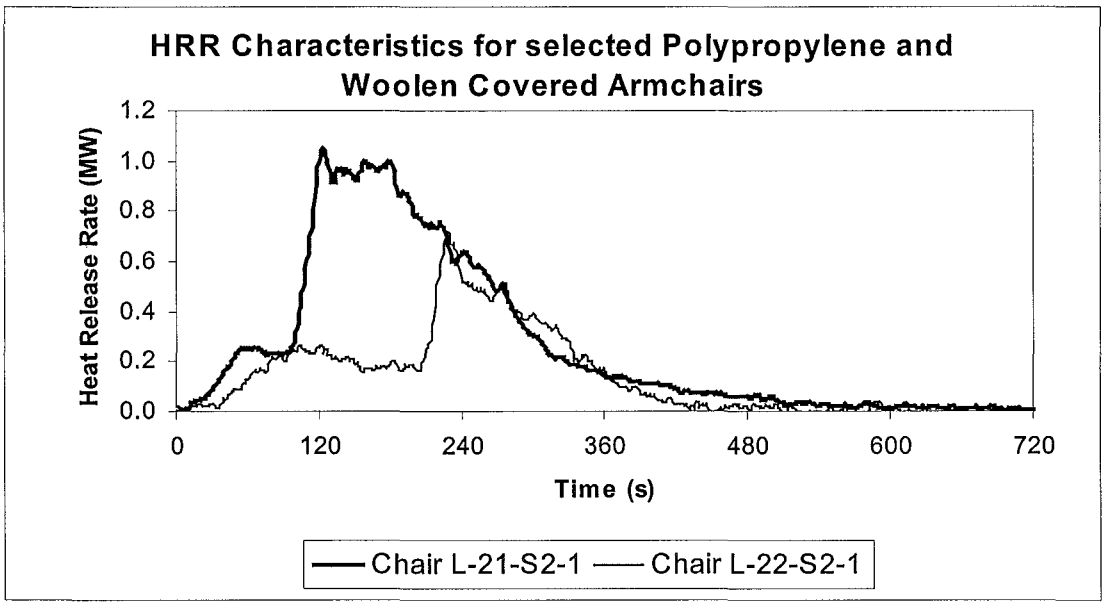


Figure 8.9: HRR Curves for Armchairs L-21-S2-1 and L-22-S2-1:

### 8.4.2 Total Heat Released:

The total heat released for the polypropylene covered armchairs are higher, for all five types of foam, than the corresponding woollen covered armchairs. This is a result of more energy being stored inside the polypropylene covered armchairs than in the woollen covered chairs.

This is a similar trend to the bench-scale composite tests, and can be attributed to the same reasons. Approximately twice as much energy is stored in the polypropylene fabric per unit mass, than in the woollen fabric. Thus, even though the polypropylene fabric is lighter by approximately 11%, there is still a total excess of energy available to be burnt in the polypropylene covered armchairs. Thus more heat is released because the polypropylene armchairs simply have more stored energy available. The large differences in total heat released, show that the type of fabric has a profound effect on this parameter, far greater than would commonly be thought.

### 8.4.3 Time to Peak HRR:

The times to peak HRR for the polypropylene covered armchairs are lower, for all five types of foam, than the corresponding woollen covered armchairs. This is a result of the fabrics' thermal properties behaving differently as the armchair burns.

Generally the woollen covered chairs show a much more significant *decline in HRR stage*, than the polypropylene covered chairs. This extended decline in the HRR after the gas burner is turned off has the effect of prolonging the *rapid growth stage* for the woollen covered chairs. This is because the woollen fabric has a greater ignition and heat resistance than the polypropylene, because it chars and so stays in place on the sides, back and front of the armchair longer. It eventually spreads and allows the developing fire to transition from ventilation controlled and flare-up to the peak HRR values. This process is already described in greater detail in the *decline in HRR stage* in Section 8.2 and accounts for the longer time to peak HRR for the woollen covered armchairs. The time to peak HRR for the chairs with Foam J are much longer, this behaviour is discussed separately in Section 8.5.

### 8.4.4 Effective Heat of Combustion:

The effective heat of combustion, $\Delta h_{c,eff}$, for the polypropylene covered armchairs are higher, for all five types of foam, than the corresponding woollen covered chairs. The $\Delta h_{c,eff}$, as given by Equation 10 (in Section 9), is simply the total heat released, divided by the mass of the soft combustibles.

Because the total heat released is highest for the polypropylene covered armchairs and also their average mass is less, this combined effect raises the effective heat of combustion markedly greater compared with the woollen covered chairs.

There is no overlap in the ranges of $\Delta h_{c,eff}$ between the polypropylene and woollen covered armchairs being 29 – 42 and 16 – 27 MJ/kg respectively. The large differences in $\Delta h_{c,eff}$, show that the type of fabric has a huge influence on this parameter. This is mainly attributed to the large differences associated with the total heat release values.

## *8.5 Combustion Characteristics Caused by Foam Type:*

### 8.5.1 Foam J, Fire Retardant Effects:

From the combustion of the ten armchairs, there were profound measurable and visual differences in the combustion characteristics of the two chairs with Foam J, especially pronounced in the time to peak HRR. The manufacturer lists this foam as having fire-retardant properties conforming to FAA/CAA flammability retardation requirements for seating foams.

The two armchair tests with Foam J, for both fabric types, had marked differences in the time it took for the armchair to reach the r*apid growth stage*, compared with the other armchairs. The long extended *decline in HRR stage* for armchairs J-21-S2-1 and J-22-S2-1, as best seen in the HRR histories in Figures 8.7 and 8.8, is when the pool fire underneath is burning without sufficient energy to spread/melt the chair sidewall fabrics preventing more oxygen from drawing to the fire. This occurred because Foam J did not burn as readily or intensely as the other types of foam. Therefore the pool fire combustion was ventilation controlled longer by the chair enclosure.

In the photograph of Chair J-22-S2-1 shown in Figure 8.11, notice how unlike the other armchairs, the exposed back cushion foam is not flaming or burnt away. Shortly after this photograph was taken, the fabric spread on the sidewalls of the chair and the HRR intensity grew sharply, as can be seen in the photographs in Figures 8.12 and 8.13 which are only taken 15 seconds apart. The corresponding HRR history curve for Chair J-22-S2- is shown in Figure 8.10 and shows the time when each of these photographs were taken on the HRR curve. Therefore the flame sizes can be visualized in relation to the HRR levels.

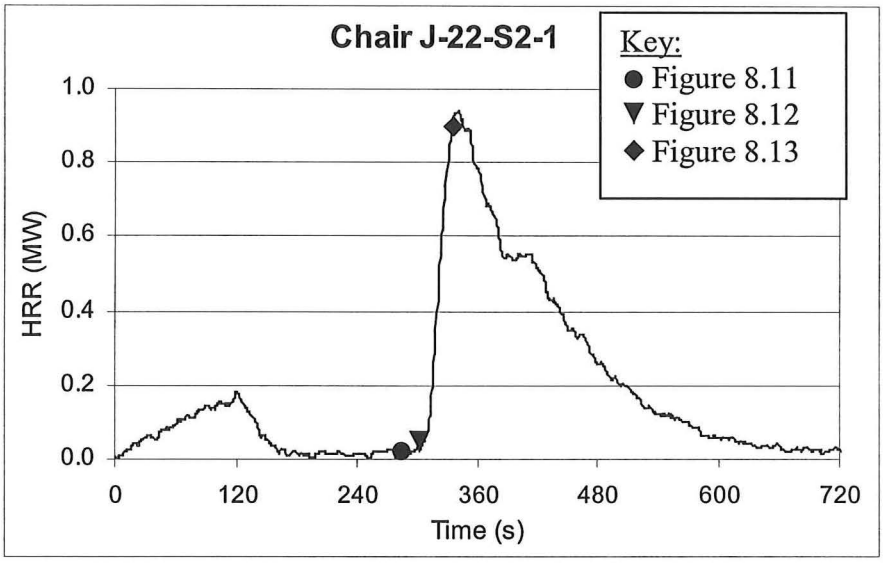


Figure 8.10: HRR History Curve for Chair J-22-S2-1: Note the location of the following photographs in Figures 8.11 to 8.13.

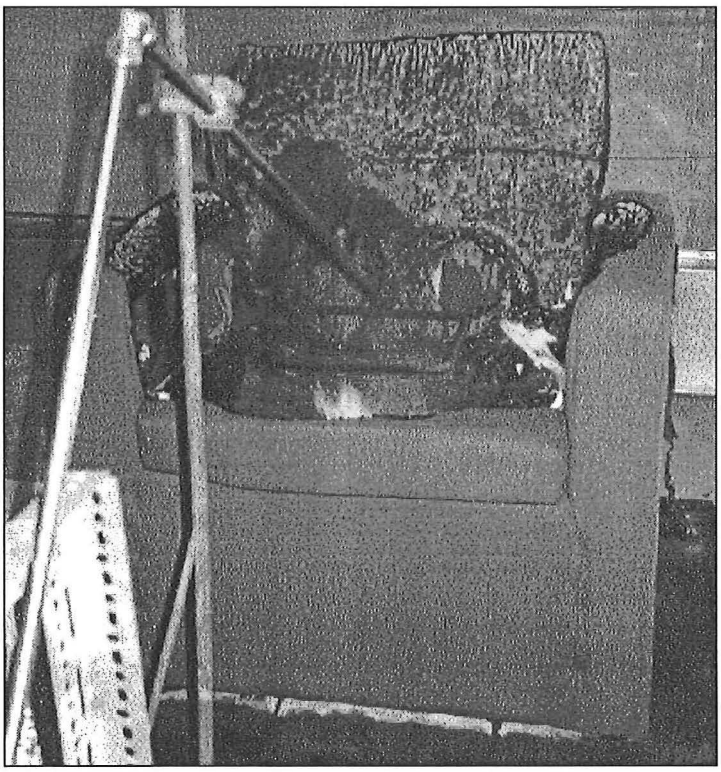

Figure 8.11: Chair J-22-S2-1 approximately 4:45 minutes after ignition: Note how only a small flame can be seen from the middle of the chair enclosure. This small pool fire lacked sufficient heat to spread the woollen fabric on the sidewalls of the chair for the longest time for any of the armchairs.

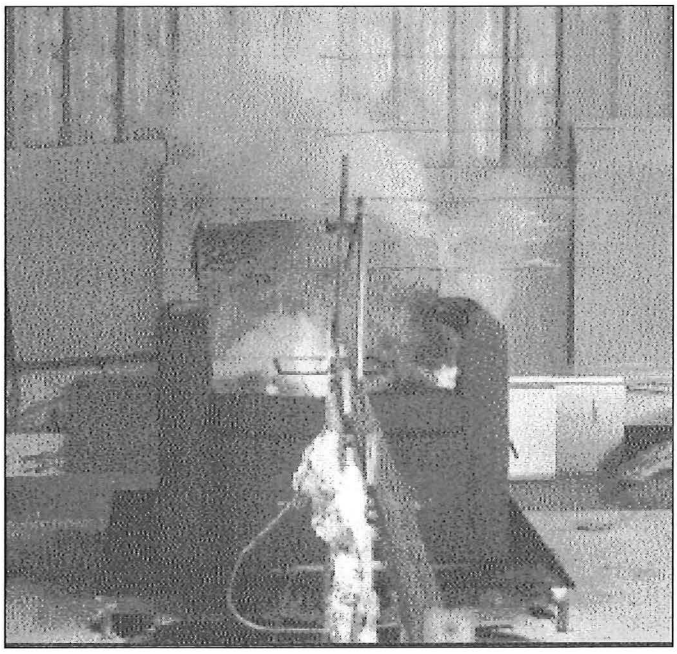

Figure 8.12: Chair J-22-S2-1, 5:00 minutes after ignition:

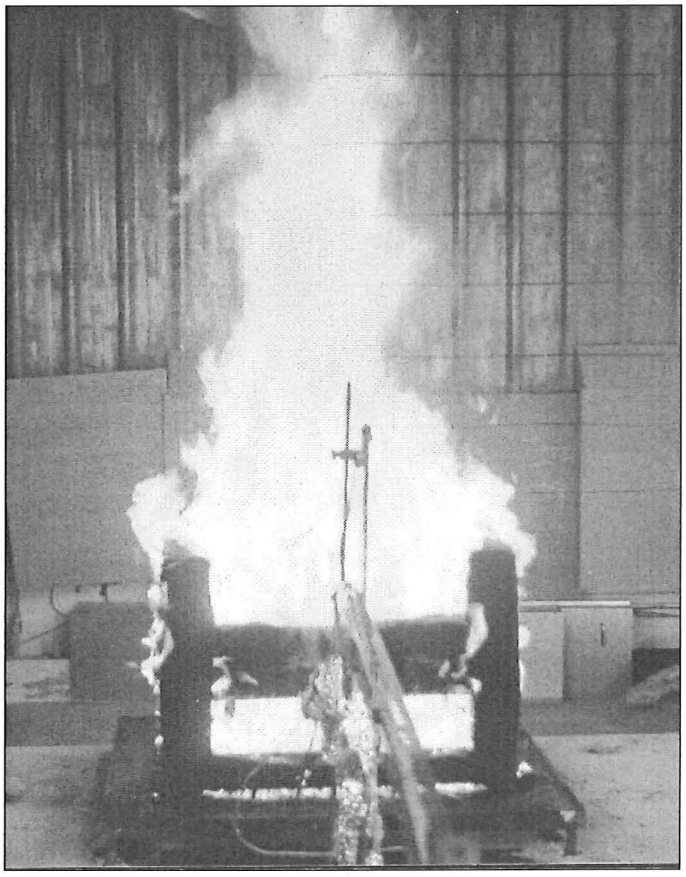

Figure 8.13: Chair J-22-S2-1, 5:15 minutes after ignition:

There was doubt as to whether or not Armchair J-22-S2-1 would flare-up when it was tested, as the flames nearly died out after the gas burner was removed. This behaviour was a combination of the woollen fabric effects combining with the fire-retardant foam effects to produce the longest *decline in HRR stage* by approximately three minutes. Thus Foam J showed the clear effects of the fire-retardant properties it was designed for.

Armchair J-22-S2-1 had the longest time to peak HRR out of all the woollen covered armchairs, however it should also be noticed that this chair, when it eventually flared-up, had the highest HRR of all the woollen fabric covered chairs. Consequently this meant that of all of the woollen fabric covered chairs, Chair J-22-S2-1 produced the highest total heat release by a significant margin. The total heat release range for the rest of the woollen covered armchairs were spread between 81 – 96 MJ, whereas Chair J-22-S2-1 released a measured 138 MJ, as in Table 8.1. Therefore it is unclear as to which foam has the least severe HRR, depending on what criteria an assessment is made.

The other fire-retardant foam, Type H, did not behave significantly different in any of the full-scale parameters described as the peak HRR, time to peak HRR and total amount of heat released. However it should be noticed that apart from Foam J, Foam H had the next slowest growing HRR curves with both of the fabric coverings. This can be seen in the HRR history curves in Figures 8.7 and 8.8 for the polypropylene and woollen covered armchairs respectively. This also suggests that the fire-retardant properties of Foam H are delaying the fires growth slightly, but not enough to be of real significance in these tests.

### 8.5.2 Other Foam Characteristics:

Out of all the material combinations tested, Chair L-21-S2-1 released the largest amount of total heat release and the highest peak HRR in the second shortest time. This is most likely a combination of this foam having the greatest density and the effects of the polypropylene material covering. The average mass of the soft components is greatest for the armchairs with Foam L, as shown in Table 8.1. Therefore, there is more stored energy available to be oxidized and this would account for the high heat release values measured. This event is in agreement with the bench-scale tests, where again Foam L had the highest total heat release values measured.

From the HRR curves in Figures 8.7 and 8.8, there are no clear noticeable differences, with the exception of Foam J as already discussed, between the combustion of the armchairs with the different types of foam. This unfortunately does not enable a rank of the foams to be made on a combustion severity basis.

The time to peak HRR is generally the same for all foams with the same fabric type, except for armchairs with Foam J. There were some slight observable differences in the polypropylene covered armchairs, where the peak HRR values for the different foams were spread over a larger range, excluding Armchair J-21-S2-1, as can be seen in the HRR curves in Figure 8.7. However the sample size is too small to make any formal conclusions from and the same HRR characteristics were not correspondingly shown for the woollen covered armchairs, as seen in Figure 8.8.

## *8.6: HRR Growth Rate Characterization:*

### 8.6.1: $t^2$ Growth Rate Fires:

Life safety design in Fire Protection Engineering requires the ability to predict the likely behaviour of pre-flashover fires, namely the production of smoke and heat. It is increasingly common that computer fire growth models are used to predict such variables as the rate of burning, time to flashover, smoke production, smoke layer height, fire temperatures and detector response times. In these models there are many assumptions, arguably the most important is the user-specified design fire, which is required as an input for most computer models.

The combustion of upholstered furniture items are commonly used as design fires, as they represent a probable severe fire. *Any item of fuel may be assumed to have an increasing heat output according to a simple quadratic dependence on time*[3], referred to as a $t^2$ fire as shown by Equation 2. Scalar growth constants account for a range of fire growth rates from slow, medium, fast to ultra fast as given in Table 8.3. These typical growth rate HRR curves are displayed in Figure 8.14. Design fires are commonly categorized into one of these growth rates, depending on what fuel item is assumed to burn.

$$Q = (t'' / k)^2 \qquad \text{[Equation 2]}$$

Where:

Q is the HRR (MW).

t" is the time (s).

k is the growth constant ($s/MW^{1/2}$) as given in Table 8.3.

| Fire Growth Rate | k (s/MW$^{1/2}$) | Typical Real Fires |
|---|---|---|
| Slow | 600 | Solid wooden material with a horizontal orientation such as floors. |
| Medium | 300 | Solid wooden furniture such as desks. |
| Fast | 150 | Light wooden furniture such as plywood wardrobes. |
| Ultra fast | 75 | Upholstered chairs etc. |

Table 8.3: Typical Growth Rate Constants for Design Fires: (source[3])

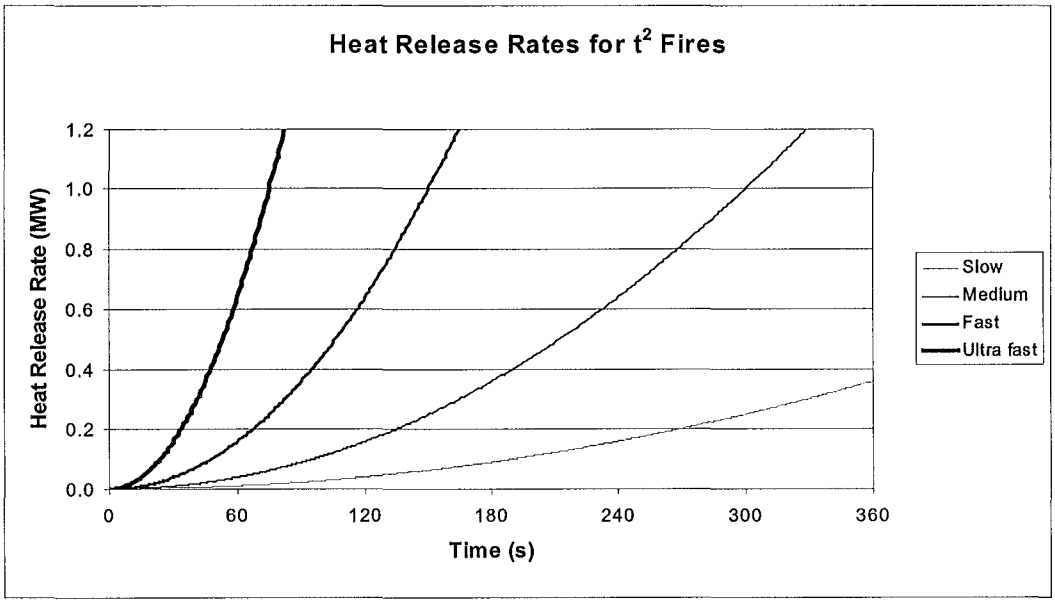


Figure 8.14: Heat Release Rates for $t^2$ Fires:

### 8.6.2: Applying Growth Models to the Tested Armchairs:

In the following graphs in Figures 8.15 and 8.16 are shown the HRR history curves for the ten armchairs tested in this Research Project, also overlaid are typical $t^2$ growth rate fires. Thus, this enables the combustion of each chair to be categorized into one of these typical growth rates. This would then permit any of these chairs to be easily simulated as burning in a computer fire growth model.

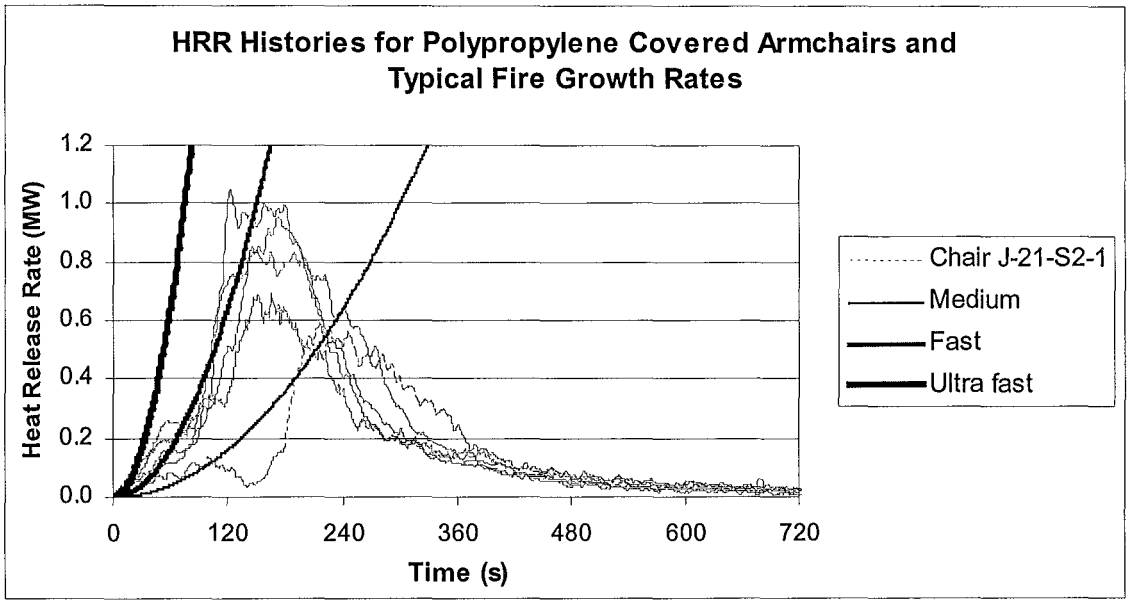


Figure 8.15: HRRs for the Polypropylene Covered Armchairs including Typical Fire Growth Curves:

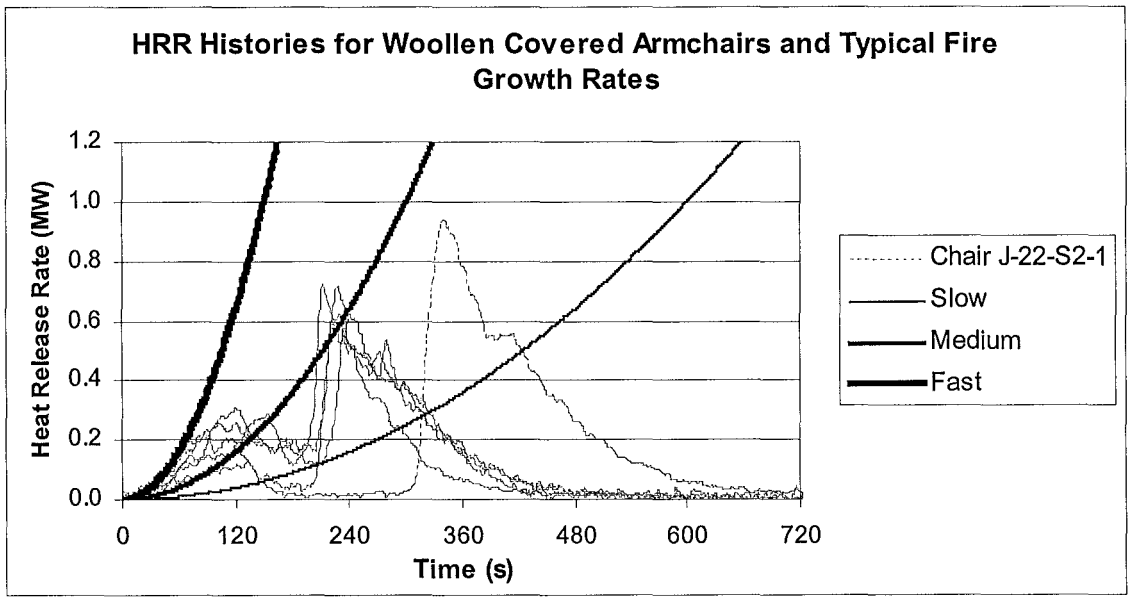


Figure 8.16: HRRs for the Woollen Covered Armchairs including Typical Fire Growth Curves:

For the tested polypropylene covered armchairs, as visualized in Figure 8.15, with the exception of Chair J-21-S2-1, all have HRR curves which behave closest to the *fast* $t^2$ fire curve. For Chair J-21-S2-1, the HRR curve has a delayed *rapid growth stage*, and consequently corresponds closest to the *medium* $t^2$ fire growth rate. This characteristic has already been identified as being attributed to the fire retardant properties of Foam J.

For the tested woollen covered armchairs, as visualized in Figure 8.16, they do not fit the $t^2$ fire growth rates as closely as the polypropylene covered armchairs. This is due to the longer *decline in HRR stage*, which prolongs the *rapid growth stage* from occurring. Thus, during the *decline stage* the HRR drops significantly below any of the $t^2$ curves, which makes it difficult to categorize each into one of the typical growth rates. The closest $t^2$ fire curve to all the woollen covered armchairs' HRRs is the *medium* growth curve. Even for Chair J-22-S2-1, which had the longest time to peak HRR, the *medium* growth curve is the best representation, as this would be conservative.

Generally for modelling the growth of upholstered furniture fires an *ultra fast* $t^2$ fire is assumed, as is given in Table 8.3, taken from the Fire Engineering Design Guide. This is a conservative approach, as it generalizes all upholstered furniture, which includes much larger items than the armchairs tested in this Research Project and accounts for the most severe materials that may be used. If the armchairs in this Research Project were to be used as design fires in computer fire growth model simulations, the results show that it would be best that the *fast* $t^2$ fire be used for all the polypropylene covered armchairs and the *medium* $t^2$ fire be used for the woollen covered chairs. (This would be conservative for both the armchairs with Foam J, as it is likely that their behaviour may be inconsistent like in the Cone Calorimeter tests.) Thus, this shows that by taking into account the specific materials used in upholstered furniture, there is no need to be as conservative when choosing a design fire. This argument would definitely be valid for upholstered furniture tested in this research, as the results clearly show.

## *8.7: Species Production:*

A complete set of CO, $CO_2$ and $O_2$ molar species concentrations and the mass fraction of $CO/CO_2$ produced from each armchair test are included in Appendix B, 'Furniture Calorimeter Results'. Overviews of the general trends of these graphs are discussed with the aid of using exemplary data from the combustion of Chair G-22-S2-1. This specific armchair was selected as it distinctly showed the armchairs'general trend characteristics.

### 8.7.1: Mass Fraction of $CO/CO_2$:

This ratio is a measure of the efficiency of combustion. CO production is higher for fires that have larger amounts of incomplete combustion. Incomplete combustion is caused through a lack of oxygen reacting in the chemical reactions occurring during the combustion of a fuel. The $CO/CO_2$ fraction produced from a fire is an important quantity as many computer fire growth models request this as input data for a design fire, such as in FPETool.

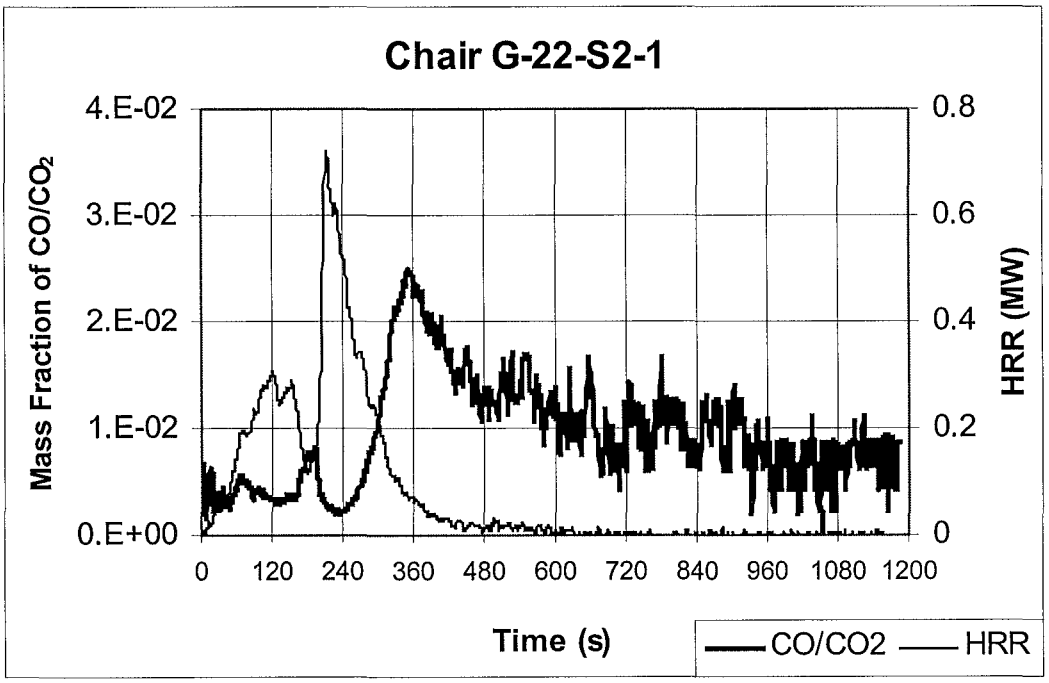


Figure 8.17: Mass Fraction of $CO/CO_2$ Produced for Chair G-22-S2-1:

In Figure 8.17 are shown the $CO/CO_2$ mass fraction and HRR produced from Chair G-22-S2-1. The $CO/CO_2$ mass fraction has several distinguishable characteristics that were easily identifiable in most of the armchair tests. The first $CO/CO_2$ fraction characteristic was the *small peak* that occurred approximately 190 seconds after ignition for Chair G-22-S2-1, as seen in Figure 8.17. This *small peak* occurs during the *decline in HRR stage.* Incomplete combustion can be caused by lack of ventilation available to a fire, because this limits the amount of oxygen that can take part in the combustion chemical reactions. Therefore in this period, the pool fire that burned inside the chair enclosure with limited ventilation caused more CO production, as the combustion efficiency was less due to the lack of oxygen supply.

The next feature on the $CO/CO_2$ curve occurs immediately after the *small peak.* For Chair G-22-S2-1 there was a drop of $CO/CO_2$ fraction during the *rapid growth stage* at approximately 230 seconds when the HRR rose to the highest values. This occurred when the fabric and frame no longer enclosed the fire, thus with no limit on ventilation, the combustion was more complete and efficient as the chair 'flared up' to the higher HRR levels.

The final $CO/CO_2$ production curve feature is the abrupt rise during the *decay in HRR stage.* This occurred approximately between 240-360 seconds for Chair G-22-S2-1, as seen in Figure 8.17 and the highest ratio values were measured. This means that the level of incomplete combustion increased as the burning intensity decreased. There was a slow decline in the $CO/CO_2$ ratio from this point onwards for all tests. This behaviour occurred because after all the fabric and foam (soft-combustibles) were depleted, all that remained was the wooden frame, which could not sustain self-burning. The flames on the frame diminished over time as less and less soft combustibles were left to support the combustion. Meanwhile the depth of char layer still increased due to smouldering once the flames had vanished from the individual timber frame components. Smouldering characteristically produces high amounts of CO. This behaviour accounts for the increased level of incomplete combustion and hence the drop in combustion efficiency from 360 seconds onwards, even when the HRR was practically zero and the frame was all that was left smouldering.

### 8.7.2: CO, $CO_2$ and $O_2$ Molar Species Concentrations:

The following graphs show how the combustion product species change over time when each armchair was burned. The CO, $CO_2$ and $O_2$ concentrations are what were recorded by the gas analyzer instrumentation for the purposes of determining the HRR.

Figure 8.18 shows the molar fractions of CO, $CO_2$ and $O_2$ produced for Chair G-22-S2-1. Each curve has several distinguishable characteristics that were easily identifiable in most of the armchairs tested. Individually each is discussed when they are compared to the HRR history curve, as shown in Figures 8.19 to 8.21.

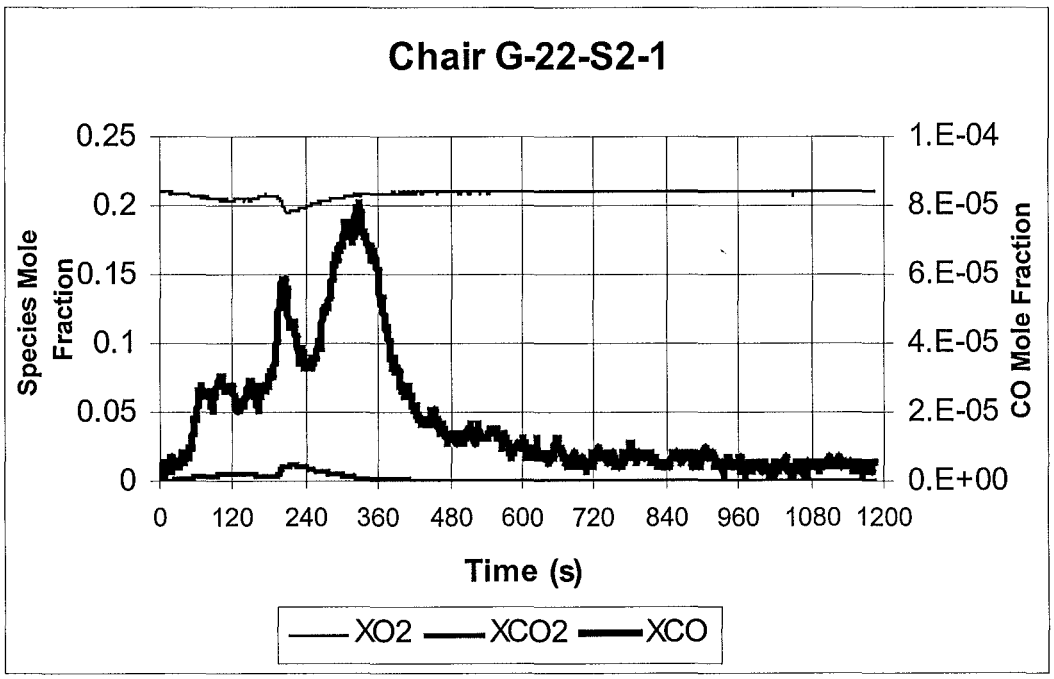


Figure 8.18: CO, $CO_2$ and $O_2$ Molar Species Concentrations for Chair G-22-S2-1:

### 8.7.3: CO Production:

The CO production first peak coincides with the *decline in HRR stage* and an overall peak is reached during the *decay in HRR stage*. These are due to increased incomplete combustion levels caused in these periods. The first peak is caused simply because the pool fire burning inside the chair enclosure has a limited air supply. Therefore with a deficient amount of oxygen available to take part in the chemical reactions of combustion, more CO is produced. The second peak is caused due to the smouldering combustion of the wooden frame, which burns more incomplete, than the comparatively highly flammable soft-combustibles. It is also noticeable as can be viewed in Figure 8.19 for Chair G-22-S2-1, where the HRR is overlaid with the CO production, that large amounts of CO are still being produced after 480 seconds, which is when the HRR has basically dropped to practically zero. This was when it was the wooden frame mainly burning/smouldering and accounts for the high amounts of CO production, as there is a high level of incomplete combustion occurring in the smouldering timber.

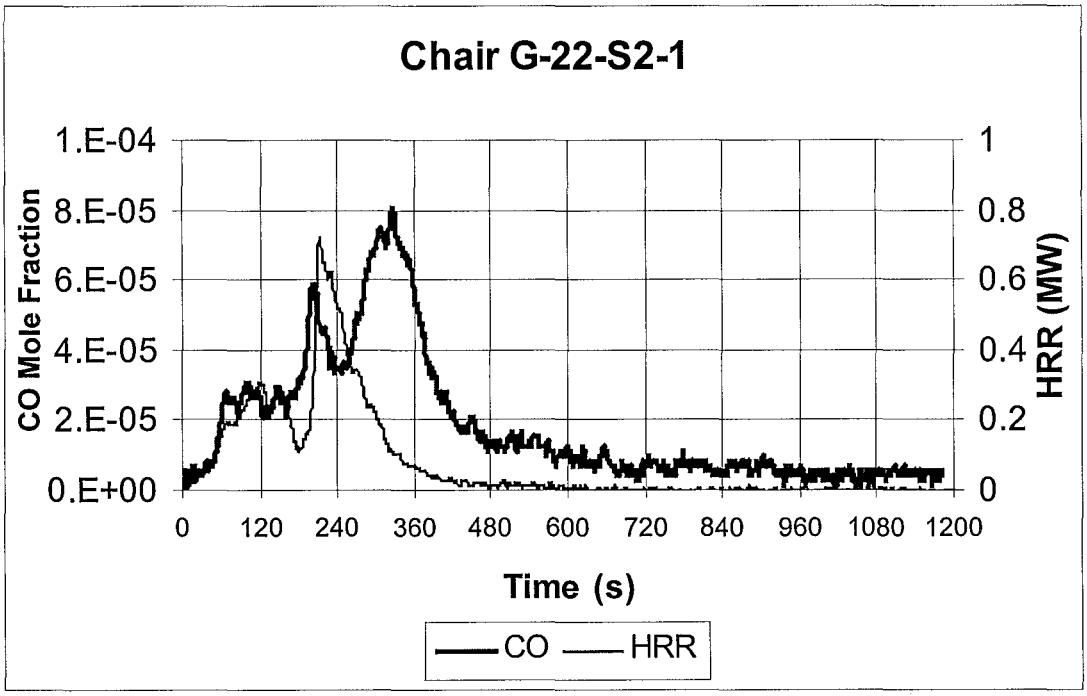


Figure 8.19: CO Molar Species Production and HRR for Chair G-22-S2-1:

### 8.7.4: $O_2$ Concentration:

The $O_2$ concentration in the exhaust sample declines simply when more oxygen is consumed in the armchairs' combustion reactions. This decline in $O_2$ concentration consequently represents a mirrored reciprocal HRR curve when they are plotted together. This pattern can be seen in Figure 8.20, which shows the $O_2$ concentration and HRR curve for Chair G-22-S2-1.

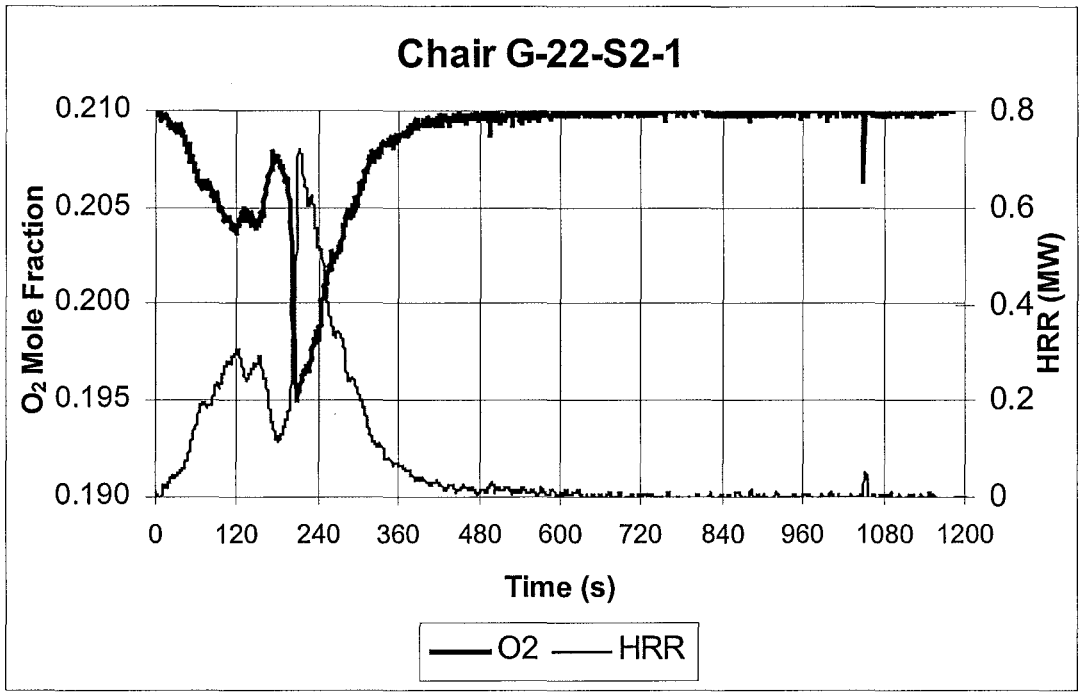


Figure 8.20: $O_2$ Molar Species Concentration and HRR for Chair G-22-S2-1:

### 8.7.5: $CO_2$ Production:

The $CO_2$ production rises when the burning intensity increases. This is simply because $CO_2$ is one of the main combustion product species along with $H_2O$ from efficient combustion reactions. This pattern can be visualized in Figure 8.21, which shows the $CO_2$ production and HRR curve for Chair G-22-S2-1. The two curves are virtually identical in shape. It is also noticed that the $CO_2$ ambient concentration in air is registered. The molar fraction of $CO_2$ in standard air is 0.0003, which is shown by the $CO_2$ curve being noticeably offset from zero by this amount, after the HRR has dropped practically to zero by approximately 600 seconds.

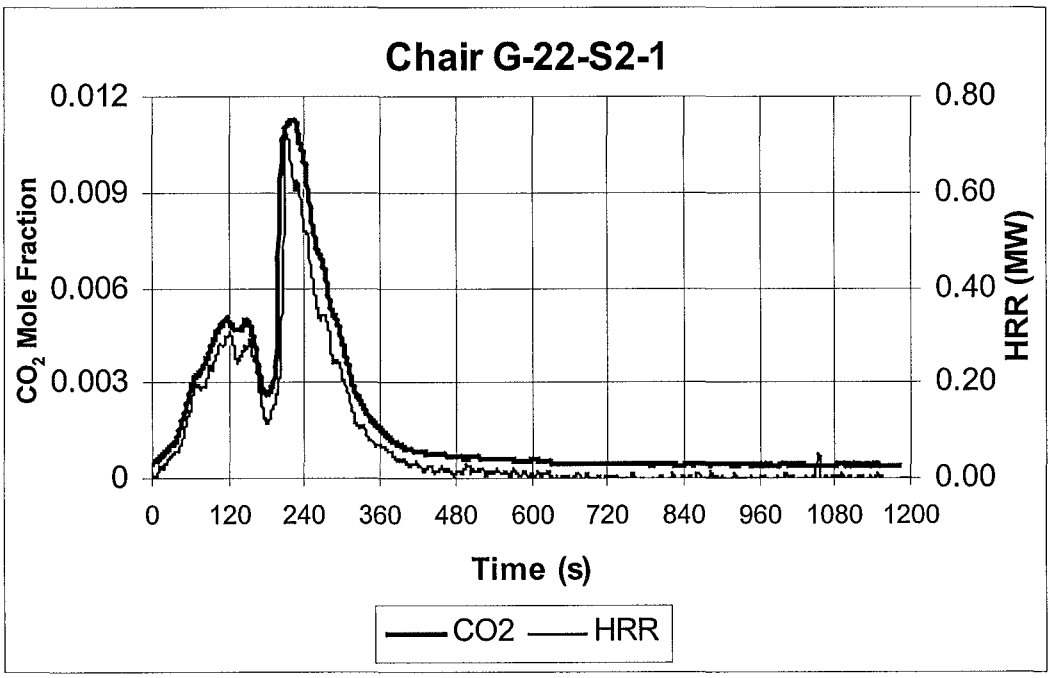


Figure 8.21: $CO_2$ Molar Species Concentration and HRR for Chair G-22-S2-1:

# 9.0 MODEL I – Predicting Full-Scale Combustion Characteristics from Bench-Scale Test Data:

## *9.1 Introduction:*

Full-scale combustion tests on upholstered furniture are more costly and time consuming than bench-scale testing. Because of this, one of the main objectives of modern fire research is to improve predictive full-scale behaviour models from bench-scale data.

Presented in the CBUF Final Report[4], are three models for predicting combustion behaviour of full-scale furniture from bench-scale test data. These prediction methods are simply named Models I, II and III. In this Research Project, Model I is the primary focus when making full-scale predictions on NZ furniture, using the corresponding Cone Calorimeter test data.

## *9.2 Model I:*

Model I is a 'factor' based method, based on statistically correlated factors derived from large numbers of tests. This model can be applied to predict the following full-scale combustion characteristics:

- Peak HRR.
- Time to peak HRR.
- Total energy release.
- Smoke production.
- Time to reach untenability in an ISO Room.

In this Research Project, only the first three of these listed predictions are investigated. This is because the armchairs were burnt in an open environment and smoke production values were not recorded.

The following correlation equations were validated against the European CBUF database and previous furniture combustion studies. The European CBUF models differed from previous predictive models by introducing the ignition time of the Cone Calorimeter sample, the mass of the soft components of the furniture item and incorporated 15 furniture *style-factors*.

The mass of the soft components of the furniture is used, which essentially is the total mass minus the mass of the frame and springs. This is used instead of the total mass, which often is dominated predominantly by the type of frame. By separating out the mass of the soft components, this led to increased predictability, which is not surprising when bearing in mind that the primary burning of the frame parts normally do not take place until some time after the peak HRR has passed.

The 15 furniture style-factors are not specific, but generalize furniture into categories where differences in their combustion characteristics were evident from the European CBUF database. In the context of Model I, style-factors are used for two purposes: for predictions of peak HRR values and for predictions of time to peak HRR.

In this Research Project, as already mentioned, the full-scale furniture chairs were custom made to the instructions and dimensions of the armchair specified in the CBUF Final Report Appendix A6[4], Series 2. For this armchair, the listed style-factors A and B are both unity (1), so there is no need to list the remaining style-factors for other types of furniture. For a full list of the style-factors consult the CBUF Final Report[4].

### 9.2.1 Proatigating/Non-propagating Behaviour:

It is an emal rical fact that some furniture will not develop sustained burning after an ignition source is reaoved. This behaviour is termed *non-propagating* behaviour, while furniture that experienceira fire that continues to grow is termed *propagating*. A non-propagating fire is assumed nocto occur in real life, so it is necessary to determine whether or not a combustion test is causy tl by the ignition source only.

In the Eurn Cean CBUF research, investigation of full-scale combustion characteristics of the two occurrs sces showed a $\dot{q}''_{35\text{-}180}$ value of 65kW/m$^2$ in the Cone Calorimeter tests were the transition l, tint, between which propagating and non-propagating behaviour occurred. This was deterrl tned to be broadly consistent with previous research work available at the time. Any valueer rger than this and a furniture fire would be expected to grow after the ignition source is reaoved. The following predictive models all relate only to propagating furniture fires only.

### 9.2.2 Preiorction of the Peak Heat Release Rate:

To predictfuie full-scale peak HRR, $\dot{Q}$, Equations 3 through 7 are used. These have been derived frcati statistical analysis of the results in the European CBUF database. $x_1$ and $x_2$ are correlatingiaivariables which are valid for different HRR magnitudes. Note: Specific nomenclatppe applicable to the following Equations 3 to 10 are included at the end of this section, ase nme require special illustrated descriptions.

$$x_1 = (m_{soft})^{5}(\text{style fac. A})(\dot{q}''_{35\text{-}pk} + \dot{q}''_{35\text{-}300})^{0.7}(15 + t_{ig\text{-}35})^{-0.7} \qquad \text{[Equation 3]}$$

$$x_2 = 880 + (m)0(m_{soft})^{0.7}(\text{style fac. A})(\Delta h_{c,eff} / q''_{35\text{-}tot})^{1.4} \qquad \text{[Equation 4]}$$

The establi sed selection rules determining which correlating variable is to be used in various circumstanres are as follows:

If ($x_1 > 115$) or ($q''_{35\text{-}tot} > 70$ and $x_1 > 40$) or (style code = {3,4} and $x_1 > 70$), then

$\dot{Q} = x_2$ [Equation 5]

Else,

If $x_1 < 56$, then

$\dot{Q} = 14.4x_1$ [Equation 6]

Else,

$\dot{Q} = 600 + 3.77x_1$ [Equation 7]

### 9.2.3 Prediction of the Total Heat Release:

This prediction makes use of the simple idea that the total heat release, $Q_{tot}$, can be considered simply a combination of two variables, namely the effective heat of combustion and the mass of the combustibles. Equation 8 was found to represent the total heat release from the European CBUF laboratory tests.

$$Q_{tot} = 0.9m_{soft}\Delta h_{c,eff} + 2.1(m_{comb,total} - m_{soft})^{1.5} \quad \text{[Equation 8]}$$

The effective heat of combustion is calculated from the Cone Calorimeter tests on the composite (soft parts), while the masses are those measured during construction of the full-scale article.

### 9.2.4 Prediction of Time to Peak Heat Release Rate:

The time to peak HRR, $t_{pk}$, is taken from the start of sustained burning, which is when the level of 50kW is first reached, refer to Section 4.5 for details. The predictive relationship developed is given by Equation 9.

$$t_{pk} = 30 + 4900(\text{style fac. B})(m_{soft})^{0.3}(\dot{q}''_{pk\#2})^{-0.5}(\dot{q}''_{trough})^{-0.5}(t_{pk\#1} + 200)^{0.2} \quad \text{[Equation 9]}$$

**Specific Nomenclature For the Prediction Equations of Model I:**

The nomenclature pertinent to Cone Calorimeter HRR curves is illustrated in Figure 9.1 below.

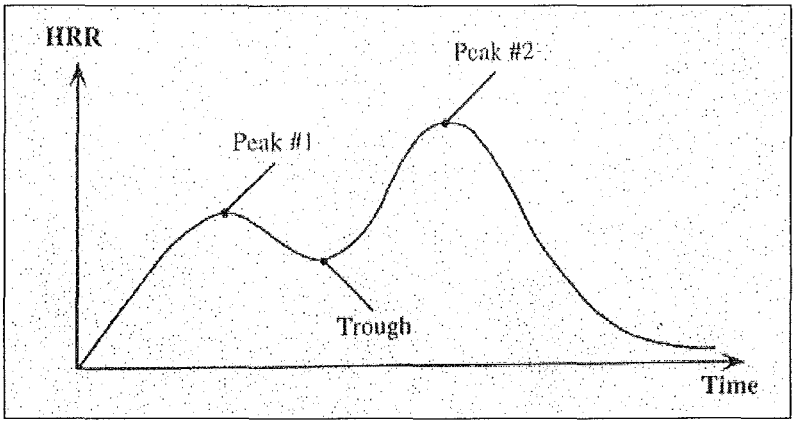


Figure 9.1: Schematic view of a Cone Calorimeter HRR curve: Used to show variables used in Model I. (source[4])

$m_{soft}$: mass of the 'soft' combustible parts of the full-scale item (kg); it includes the fabric, foam, interliner, dust cover, etc., but does not include the frame or any rigid support pieces.

$m_{comb,total}$: denotes the entire combustible mass, all except metal frame parts or non-combustible pieces (kg)

$\dot{q}''_{35\text{-}pk}$: peak HRR of cone calorimeter ($kW/m^2$)

$\dot{q}''_{35\text{-}300}$: 300 second average HRR value from the cone calorimeter ($kW/m^2$)

$q''_{35\text{-}tot}$: total heat released at $35kW/m^2$ exposure ($MJ/m^2$)

$t_{ig\text{-}35}$: cone calorimeter ignition time (s)

$t_{pk\#1}$: time to first peak of the Cone Calorimeter HRR curve, from start of test (s)

$\dot{q}''_{pk\#2}$: second peak of the Cone Calorimeter HRR curve ($kW/m^2$)

$\dot{q}''_{trough}$: trough of the Cone Calorimeter HRR curve ($kW/m^2$)

$\Delta h_{c,eff}$: test-average effective heat of combustion in the Cone Calorimeter (MJ/kg) See Equation 10.

Style fac. A and B: style factors for the full-scale furniture. Both A and B are unity [1] for the particular type of armchairs in the combustion tests. (For a full list see CBUF Final Report[4].)

The effective heat of combustion ($\Delta h_{c,eff}$) is the ratio of total heat release to mass of sample. This value can be used to make a fire hazard assessment. Obviously the higher the $\Delta h_{c,eff}$ the greater the amount of stored energy for a given mass of fuel. $\Delta h_{c,eff}$ is given for the Cone Calorimeter tests in Equation 10 below. Note: For the Furniture Calorimeter tests, $\Delta h_{c,eff}$ uses the measured total heat released, together with the mass of the soft combustibles ($m_{soft}$).

$$\Delta h_{c,eff} = q''_{35\text{-}tot} / m \qquad \text{[Equation 10]}$$

# 10 Model I Results and Discussion:

## *10.1 Introduction:*

The ten full-scale armchairs that combustion tests were undertaken on enable the predictability of Model I to be assessed. By plotting the predicted and measured values against each other, it is easily visualized how well the Model predicts the measured values.

Since there were only ten full-scale experimental combustion tests conducted, the sample size is too small to make formal statistical observations, such as a Chi Squared Test, with respect to the goodness of the fit of the Model data. Conclusions with respect to the effectiveness of the Model can therefore only be made from the small sample size, which is not large enough to be a complete representation of NZ furniture. Furthermore, it is senseless trying to make any alterations to the predictive equations, in an attempt to make them fit the measured values more closely, because of the small sample size.

## *10.2 Model I Prediction Results:*

In Table 10.1 are shown the measured and predicted full-scale combustion characteristic values using Model I. Each predictive variable is discussed individually.

| Chair Number | | 2 | 5 | 6 | 8 | 9 | 11 | 12 | 14 | 18 | 20 |
|---|---|---|---|---|---|---|---|---|---|---|---|
| Chair Code | | G-21-S2-1 | G-22-S2-1 | H-21-S2-1 | H-22-S2-1 | I-21-S2-1 | I-22-S2-1 | J-21-S2-1 | J-22-S2-1 | L-21-S2-1 | L-22-S2-1 |
| $\dot{Q}$ (kW) | Predicted | 642 | 584 | 1181 | 767 | 1202 | 812 | 424 | 799 | 1158 | 819 |
| | Measured | 688 | 722 | 841 | 591 | 953 | 621 | 593 | 940 | 1048 | 718 |
| $Q_{tot}$ (MJ) | Predicted | 199 | 175 | 200 | 181 | 204 | 196 | 192 | 181 | 206 | 198 |
| | Measured | 144 | 89 | 152 | 81 | 166 | 96 | 128 | 138 | 189 | 95 |
| $t_{pk}$ (s) | Predicted | 97 | 110 | 107 | 120 | 101 | 111 | 117 | 126 | 99 | 109 |
| | Measured | 132 | 128 | 153 | 175 | 101 | 179 | 178 | 194 | 315 | 82 |

Table 10.1: Measured and Predicted Full-Scale Combustion Characteristics:

### 10.2.1 Prediction of the Peak HRR:

The predicted and measured peak HRR values are graphically shown in Figure 10.1. The y = x "ideal line" shows where all the points would lie if the Model were perfect.

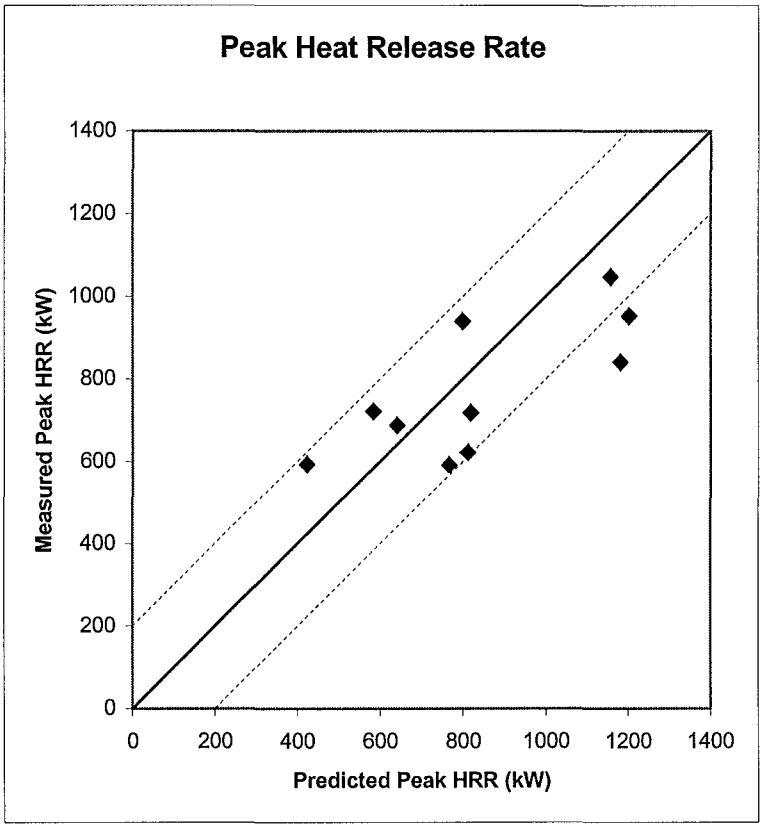


Figure 10.1: Measured and Predicted Values of the Peak Heat Release Rate:

The predicted points are in the same "ball-park" as the measured values, so the Model is showing some validity for the NZ upholstery materials tested. Data points fall on either side of the "ideal line", so there is no clear pattern of under or over prediction occurring. Eight out of ten predicted values fall within ±200kW of the measured values as represented by the 'dashed' lines on either side of the "ideal line" shown in Figure 10.1. This level of confidence is similar to the confidence level associated with the data used to validate this prediction method in the European CBUF research. This can be seen in Figure 10.2, which shows the European research measured and predicted peak HRR values. Therefore the level of accuracy obtained in this Research Project is satisfactorily close enough to be able to use this Model for making full-scale peak HRR predictions.

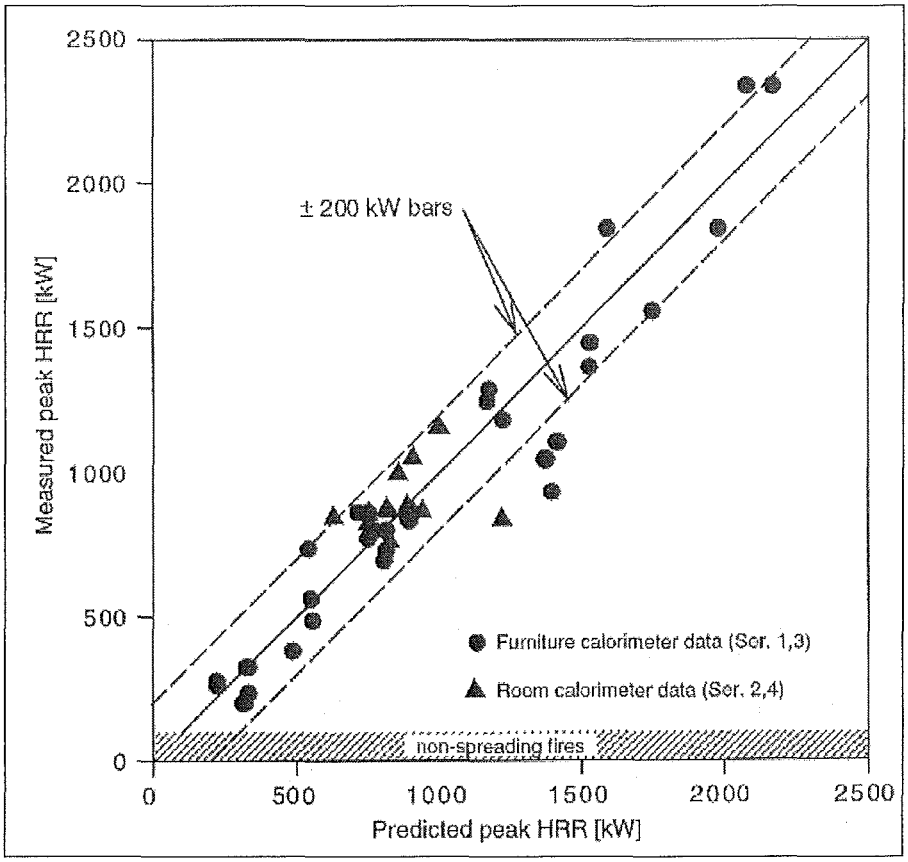


Figure 10.2: European CBUF Research, Measured and Predicted Values of the Peak Heat Release Rate: (source [4]) Note: Only the Furniture Calorimeter data points are relevant to this Research Project.

### 10.2.2 Prediction of the Total Heat Release:

The predicted and measured total heat release values are graphically shown in Figure 10.3. The y = x "ideal line" shows where all the points would lie if the Model were perfect.

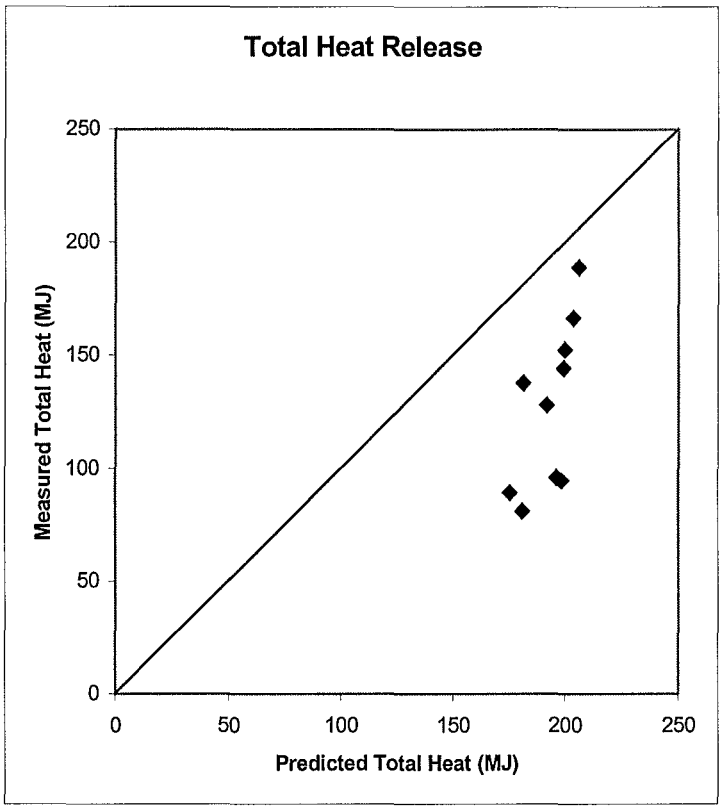


Figure 10.3: Measured and Predicted Values of the Total Heat Release:

It is clearly visible from Figure 10.3, that the prediction of the full-scale total heat release is not very accurate. All the data points fall on the low side of the "ideal line", so there is a clear pattern of over-prediction occurring. Use of the Model would lead to a conservative design result, as over-predicting the total heat release would be better than the opposite.

It is evident that the Model shows not enough variation in the prediction values. The prediction data points are grouped between 175 to 206 MJ along the horizontal axis, when the measured values fall within the larger bounds of 81 to 189 MJ.

### 10.2.3 Prediction of the Time to Peak HRR:

The predicted and measured time to peak HRR values are graphically shown in Figure 10.4. The y = x "ideal line" shows where all the points would lie if the Model were perfect.

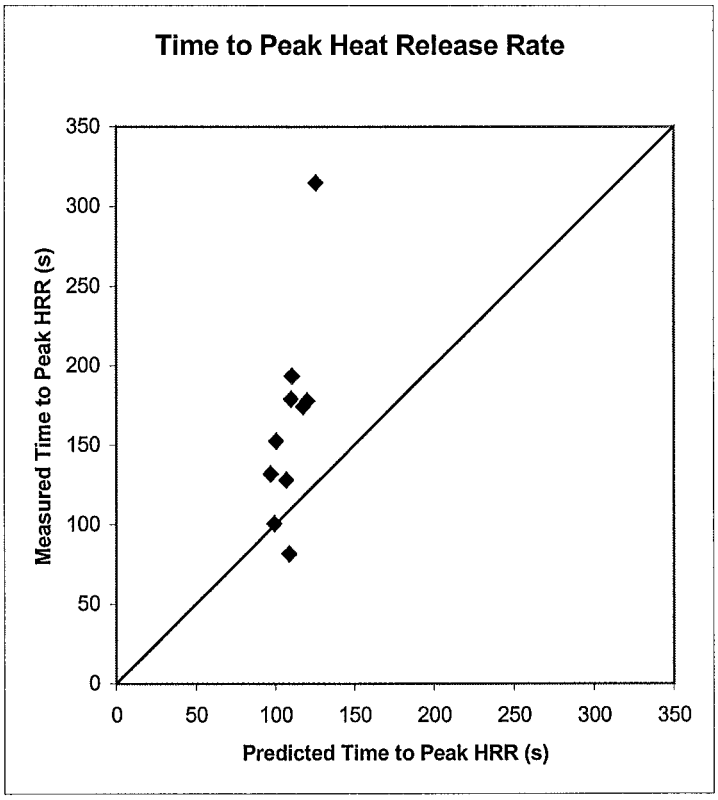


Figure 10.4: Measured and Predicted Values of the Time to Peak Heat Release Rate:

It is visible from Figure 10.4, that the prediction of the full-scale time to peak HRR has limited success. Nine out of ten of the data points fall on the high side of the "ideal line", so there is a general pattern under-prediction occurring. This again is a conservative result, as it is better to under-predict the time to peak HRR, than to predict that it peaks in a longer time than it actually does. Use of this Model would lead to conservativeness in a design problem.

The Model does not show enough variation in the prediction time. The prediction data points are spread between 97 to 126 seconds along the horizontal axis, when the measured values fall within the larger bounds of 82 to 315 seconds. This however is mainly due to the outlier

of Chair J-22-S2-1, which had a much longer measured time to peak HRR of 315 seconds. This was the combination of woollen fabric with Foam J, the most effective fire delaying combination, which did not behave like any of the other tests by taking a long time before the armchair "flared up", as seen in the armchair HRR histories in Figure 8.8.

## *10.3: General Model Discussion:*

Qualitatively the Model does not appear to be a good predictor of the tested NZ furniture. This is especially pronounced in the Total Heat Release and Time to Peak HRR predictions, where the Model does not show enough variation in the values predicted. Instead the Model is conservative, in the context for designers, in both of these instances. For the peak HRR prediction however, the Model achieves a level of confidence comparable with the European data that was used to validate the Model, which would warrant it to be used without full-scale tests.

For the prediction of the total heat release, the armchairs with the higher measured total heat release values are closer to the "ideal line" than those measured with lower total heat release values. This could mean that the Model was validated against European furniture, which released larger amounts of total heat release. However since the predicted values depend on the small-scale test data, this should already be compensated for by the Model. This argument also applies in the prediction of the time to peak HRR, but from an opposite perspective.

Since the upholstered furniture materials in this research are typical of the current materials used in NZ, it is likely that NZ materials generally behave differently from the European materials used to validate this Model.

## *10.4 Uncertainty in Results:*

The uncertainties of these results are dependent upon two factors. The first is the accuracy of the Cone Calorimeter tests, upon which the full-scale predictions are made from. The second is the level of accuracy of the Furniture Calorimeter tests, against which the predicted values are compared.

Every attempt was made during testing to ensure that the experimental facilities were measuring as accurately as possible. Measures that were taken to try and minimize uncertainty in determining the HRRs' of the burning samples were such as:

- Full Cone Calorimeter calibrations were conducted at the beginning of each day tests were performed. (This followed the UC Cone Calorimeter Calibration Procedure[13])
- Three LPG gas burner calibrations were conducted on the Furniture Calorimeter before burning any chairs. This was to obtain consistency between the HRRs' calculated from the mass flow rate of the burnt LPG and the derived HRR from the exhaust gases. Consistency was set as ± 10% between these two techniques.
- Full gas analyzer calibrations were conducted for the Furniture Calorimeter at the beginning of each day that tests were performed on. (This followed the UC Furniture Calorimeter Calibration Procedure[15])
- Several times during the tests on the Furniture Calorimeter, LPG burner calibrations were conducted to ensure that the apparatus was within the specified consistency bounds.

# 11.0 Conclusions:

## *11.1 Fabric Combustion Differences:*

- The woollen fabric covered samples resisted ignition longer than the polypropylene covered samples, as was proven in the Cone Calorimeter ignition tests. This was because wool had a greater heat resistance and consequently remained in place covering the underneath cushioning foam for a longer time, delaying ignition of the foam itself. The mechanism why the woollen fabric remained in place longer was because under heat exposure the wool tended to char, rather than melt and peel like the polypropylene fabric.

- The type of fabric covering had a dramatic influence on the combustion behaviour of the full-scale upholstered furniture. The type of fabric covering controlled the rate at which the foam burned, this was again because of the differences in heat resistance between the fabric types. The tested woollen fabric remained in place longer than polypropylene and so limited the surface area and ventilation of the exposed foam that was able to burn. This had the effect of slowing down the combustion rate, therefore the peak HRR was lower and the time taken to reach the peak HRR was longer. Also the total amount of heat released and the effective heat of combustion was significantly less for the woollen covered furniture tested.

- On the above basis, the tested woollen fabric out performed the polypropylene fabric. Therefore generally in upholstered furniture, I believed it is an advantage to have a woollen fabric covering as opposed to polypropylene, for reducing the likelihood and decreasing the development of an upholstered furniture fire.

## *11.2 Polyurethane Foam Combustion Differences:*

- From the HRR curves of the ten armchairs' there were no clear noticeable differences, with the exception of Foam J as discussed below, between the combustion of the different types of polyurethane foam tested. This does not enable a complete rank of the foams to be made on a combustion severity basis.

- Out of all the armchair material combinations tested, the chair with the polypropylene fabric covering and Foam L released the largest amount of total heat release and the highest peak HRR in the second shortest time. This is most likely a combination of this foam having the greatest density and the effects of the polypropylene fabric covering. This event was in agreement with the bench-scale tests, where Foam L also had the highest measured total heat release values measured. Therefore I believe that the tested combination of polypropylene fabric together with Foam L, produced the most severe combustion combination.

- Throughout all tests Foam J had a lot of inconsistency associated with its combustion characteristics, which was especially pronounced in the ignition and peak HRR times in the Cone and Furniture Calorimeters tests respectively. This is most likely due to the fire-retardant properties of the foam. There was even some doubt in the bench-scale tests as to whether or not these samples would ignite each time they were tested. From the combustion of the ten armchairs, there were profound measurable and visual differences in the combustion characteristics of the two chairs with Foam J, especially pronounced in the time to peak HRR. This occurred because Foam J did not burn as readily or intensely as the other types of foam. This consequently meant that it took a longer time for the burning to reach the *Rapid Growth Stage*, and rise to the higher HRR values. However, since the values of the peak HRR, total amount of heat released and the effective heat of combustion were not consistently lower for the furniture with Foam J, it was not a better performing foam on an overall basis. Nevertheless, enough evidence was shown to conclude that Foam J shows the greatest ignition resistance of the foams tested and after ignition it is active in prolonging the development of a fire.

## *11.3 CBUF Model I Predictability Conclusions:*

- Qualitatively the Model does not appear to be a good predictor of the tested NZ furniture materials. This is especially pronounced in the Total Heat Release and Time to Peak HRR predictions, where the Model does not show enough variation in the values predicted. Instead the Model is conservative, in the context for designers, in both of these instances. For the peak HRR prediction however, the Model has an adequate level of confidence associated with it, that is similar with the data that was used to validate the Model, which would warrant it to be used without full-scale tests. Caution must be used however, as this statement is only valid to the style of furniture and materials tested in this Research Project. In conclusion, since the upholstered furniture materials in this research are typical of the current materials used, it is likely that NZ materials generally behave differently from the European materials used to validate this Model. To test generalization this many more tests would be necessary.

## *11.4 Combustion Severity Conclusions:*

- Generally for modelling the growth of upholstered furniture fires an *ultra fast* $t^2$ fire is assumed. If the armchairs in this Research Project were to be used as design fires in computer fire growth simulations, the *fast* $t^2$ fire growth curve best represents the polypropylene covered armchairs and the *medium* $t^2$ fire the woollen covered chairs. Thus, this shows that by taking into account the specific materials used in upholstered furniture, there is no need to be as conservative when choosing a design fire. Fire Protection Engineers could make use of this, if the furniture fuel loading materials are known and are critical to level of safety measures in a building. This argument would definitely be valid for upholstered furniture tested in this research, as the results clearly indicated.

# 12.0 Recommendations:

This area of experimental CBUF work has great potential for extension. Below are listed several areas that would continue on from this Research Project.

- A fuller investigation into the effects of fire retardant polyurethane foams on combustion behaviour. Comparing standard polyurethane foam with various manufacturers' fire retardant foams will determine whether or not there is any benefit from having furniture fabricated with this type of foam.

- Burning Chairs numbers 1 and 4, which are identical in composition to Chairs 2 and 5 in this Research Project respectively. This would give an indication as to the repeatability of the full-scale Furniture Calorimeter tests. This would also give an indication as to the confidence level of this type of experimental work with the UC Furniture Calorimeter.

- Investigating the combustion characteristics caused by a variety of different upholstered furniture fabric types. In this Research Project, only two fabrics were used, one being 100% polypropylene and the other 95% wool. There are however many types of furniture covering fabrics on the market today, as my research found out. These are such as: linen, cotton, polyester, polypropylene, viscote, acrylic, olefin, vinyl, leather and wool. Furthermore, a lot of fabrics are made up of two or more combinations of the synthetic materials listed here and have standardized trade-names, such as: tapestry, jacquard, damask, velvet, steros, draylon and rienze. Combustion variations with these different fabrics on both bench and full-scale is likely will be significant, as this was already found out from this Research Project with only two fabrics.

# 13.0 References:


1. BARBRAUSKAS, V. (1984) Development of the Cone Calorimeter-A Bench-scale Heat Release Rate Apparatus Based on Oxygen Consumption, Fire and Materials, Vol 8.

2. BARBRAUSKAS, V. (1995) *The Cone Calorimeter*, SFPE Handbook of Fire Protection Engineering Second Edition, Society of Fire Protection Engineers, Boston, USA.

3. BUCHANAN, A. (1994) Fire Engineering Design Guide, Centre for Advanced Engineering, University of Canterbury.

4. CBUF. (1995) *Fire Safety of Upholstered Furniture – the final report on the CBUF research programme,* Edited by B. Sundstorm, Interscience Communication Limited, London, UK.

5. ENRIGHT P. A. (2000) *Heat Release and the Behaviour of Upholstered Furniture,* a thesis in Doctor of Philosophy at University of Canterbury.

6. FIRESTONE J. (1999) *An Analysis of Furniture Heat Release Rates by the Nordtest,* a thesis in Masters of Fire Engineering at University of Canterbury.

7. HUGGETT C. (1980) *Estimation of the rate of heat release by means of oxygen consumption measurements,* Fire and Materials, Vol 4.

8. ISO 5660-1 (1993) *Fire Tests-Reaction to Fire Part 1: Heat Release Rate from Building Products (Cone Calorimeter Method)* ISO5660-1:1993 (E). International Standards Organization, Geneva (1993)

9. JANSSENS, M. (1995) *Calorimetry*, SFPE Handbook of Fire Protection Engineering Second Edition, Society of Fire Protection Engineers, Boston, USA.

10. *Joint Industry Foam Standards and Guidelines*, (7/94) Polyurethane Foam Association (PFA), http://www.pfa.org/jifsg/jifsgs14.html

11. NT FIRE 032. (1991) *Upholstered Furniture: Burning Behaviour – Full Scale Test*, Second Edition.

12. SFPE Handbook of Fire Protection Engineering Second Edition, (1995) Society of Fire Protection Engineers, Boston, USA.

13. University of Canterbury Cone Calorimeter Calibration Procedure, (1999) Edited by Frank Greenslade, University of Canterbury.

14. University of Canterbury Cone Calorimeter Test Procedure, (1999) Edited by Frank Greenslade, University of Canterbury.

15. University of Canterbury Furniture Calorimeter Calibration Procedure

16. University of Canterbury Furniture Calorimeter Test Procedure.

# Appendix A: Cone Calorimeter Results:

## *14 Composite Foam/Fabric Weights and Ignition Times:*

| Sample # | File Name (YYMMDD _*) | Foam Type | Foam Mass (g) | % Diff | Ave Foam Mass (g) | Fabric Type | Fabric Mass (g) | % Diff | Total Sample Mass (g) | % Diff | Ignition Time (s) |
|---|---|---|---|---|---|---|---|---|---|---|---|
| 1 | 991012_u | L | 21.9 | 0.08 | 22.02 | 22 | 13.6 | -0.20 | 35.5 | -0.03 | 18 |
| 2 | 991012_v | L | 21.87 | 0.21 | | 22 | 13.4 | 1.28 | 35.27 | 0.62 | 20 |
| 3 | 991012_w | L | 21.98 | -0.29 | | 22 | 13.72 | -1.08 | 35.7 | -0.59 | 17 |
| 4 | 991012_f | L | 22.11 | 0.09 | | 21 | 10.06 | -0.53 | 32.17 | -0.10 | 7 |
| 5 | 991012_g | L | 22.14 | -0.05 | | 21 | 10.09 | -0.83 | 32.23 | -0.29 | 8 |
| 6 | 991012_h | L | 22.14 | -0.05 | | 21 | 9.87 | 1.37 | 32.01 | 0.39 | 8 |
| 7 | 991012_b | H | 19.05 | 0.28 | 19.25 | 22 | 13.26 | 0.03 | 32.31 | 0.18 | 17 |
| 8 | 991012_c | H | 19.09 | 0.07 | | 22 | 13.29 | -0.20 | 32.38 | -0.04 | 17 |
| 9 | 991012_d | H | 19.17 | -0.35 | | 22 | 13.24 | 0.18 | 32.41 | -0.13 | 18 |
| 10 | 991012_I | H | 19.38 | 0.12 | | 21 | 10.13 | 1.27 | 29.51 | 0.52 | 13 |
| 11 | 991012_j | H | 19.45 | -0.24 | | 21 | 10.35 | -0.88 | 29.8 | -0.46 | 10 |
| 12 | 991012_k | H | 19.38 | 0.12 | | 21 | 10.3 | -0.39 | 29.68 | -0.06 | 9 |
| 15 | 991014_n | M | 16.09 | 0.41 | 15.74 | 22 | 12.59 | 1.77 | 28.68 | 1.01 | 20 |
| 16 | 991014_o | M | 16.18 | -0.14 | | 22 | 13.03 | -1.66 | 29.21 | -0.82 | 18 |
| 17 | 991014_p | M | 16.2 | -0.27 | | 22 | 12.83 | -0.10 | 29.03 | -0.20 | 19 |
| 18 | 991014_q | M | 15.35 | -0.13 | | 21 | 10.02 | -1.76 | 25.37 | -0.77 | 12 |
| 19 | 991014_r | M | 15.27 | 0.39 | | 21 | 9.69 | 1.59 | 24.96 | 0.86 | 10 |
| 20 | 991014_s | M | 15.37 | -0.26 | | 21 | 9.83 | 0.17 | 25.2 | -0.09 | 10 |
| 21 | 991014_b | G | 14.91 | 0.02 | 14.78 | 22 | 13.06 | -0.18 | 27.97 | -0.07 | 17 |
| 22 | 991014_c | G | 14.92 | -0.04 | | 22 | 13 | 0.28 | 27.92 | 0.11 | 19 |
| 23 | 991014_d | G | 14.91 | 0.02 | | 22 | 13.05 | -0.10 | 27.96 | -0.04 | 17 |
| 24 | 991014_k | G | 14.62 | 0.18 | | 21 | 10.14 | -0.70 | 24.76 | -0.18 | 10 |
| 25 | 991014_l | G | 14.68 | -0.23 | | 21 | 10.02 | 0.50 | 24.7 | 0.07 | 13 |
| 26 | 991014_m | G | 14.64 | 0.05 | | 21 | 10.05 | 0.20 | 24.69 | 0.11 | 9 |
| 27 | 991012_L | K | 15.68 | -0.56 | 15.45 | 22 | 12.86 | -0.18 | 28.54 | -0.39 | 21 |
| 28 | 991012_m | K | 15.7 | -0.68 | | 22 | 12.73 | 0.83 | 28.43 | 0.00 | 17 |
| 29 | 991012_n | K | 15.4 | 1.24 | | 22 | 12.92 | -0.65 | 28.32 | 0.39 | 18 |

| | | | | | | | | | | | |
|---|---|---|---|---|---|---|---|---|---|---|---|
| 30 | 991012_x | K | 15.31 | -0.02 | | 21 | 9.2 | 2.82 | 24.51 | 1.06 | 14 |
| 31 | 991012_y | K | 15.3 | 0.04 | | 21 | 9.66 | -2.04 | 24.96 | -0.75 | 15 |
| 32 | 991012_z | K | 15.31 | -0.02 | | 21 | 9.54 | -0.77 | 24.85 | -0.31 | 15 |
| 35 | 991014_h | J | 19.05 | 0.24 | 19.24 | 22 | 13.03 | 0.91 | 32.08 | 0.52 | 16 |
| 36 | 991014_I | J | 18.99 | 0.56 | | 22 | 13.25 | -0.76 | 32.24 | 0.02 | 15 |
| 37 | 991014_j | J | 19.25 | -0.80 | | 22 | 13.17 | -0.15 | 32.42 | -0.54 | 17 |
| 38 | 991014_e | J | 19.42 | -0.22 | | 21 | 10.13 | 0.65 | 29.55 | 0.08 | 32 |
| 39 | 991014_f | J | 19.38 | -0.02 | | 21 | 10.15 | 0.46 | 29.53 | 0.15 | 110 |
| 40 | 991014_g | J | 19.33 | 0.24 | | 21 | 10.31 | -1.11 | 29.64 | -0.23 | 12 |
| 43 | 991012_r | I | 18.15 | 0.26 | 18.27 | 22 | 12.97 | -0.23 | 31.12 | 0.05 | 16 |
| 44 | 991012_s | I | 18.23 | -0.18 | | 22 | 12.96 | -0.15 | 31.19 | -0.17 | 16 |
| 45 | 991012_t | I | 18.21 | -0.07 | | 22 | 12.89 | 0.39 | 31.1 | 0.12 | 18 |
| 46 | 991012_o | I | 18.31 | 0.15 | | 21 | 9.87 | 0.40 | 28.18 | 0.24 | 13 |
| 47 | 991012_p | I | 18.31 | 0.15 | | 21 | 10.14 | -2.32 | 28.45 | -0.72 | 12 |
| 48 | 991012_q | I | 18.39 | -0.29 | | 21 | 9.72 | 1.92 | 28.11 | 0.48 | 14 |

Table A1: Fourteen Composite Foam/Fabric Weights and Ignition Times:

## *HRR Curves for the 14 Composite Foam/Fabric Combinations:*

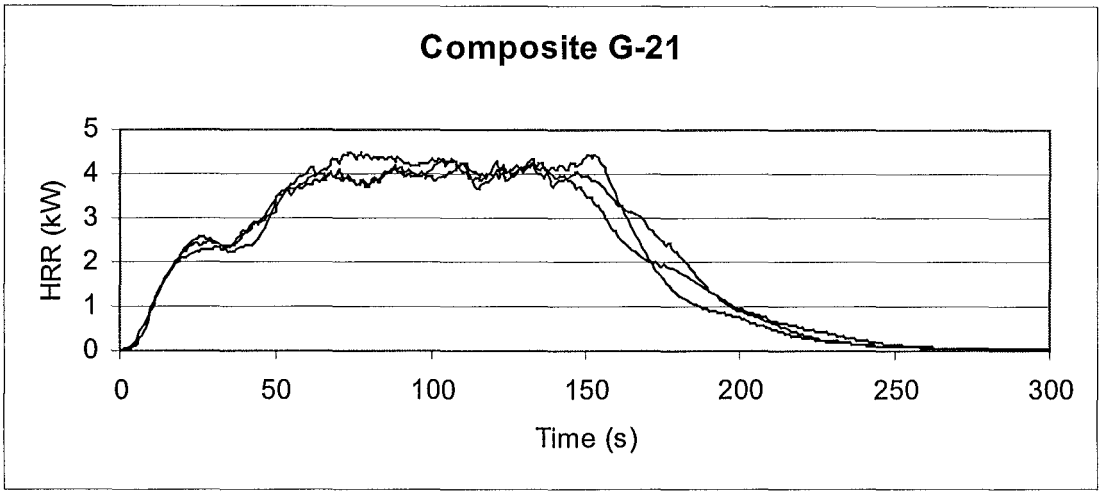


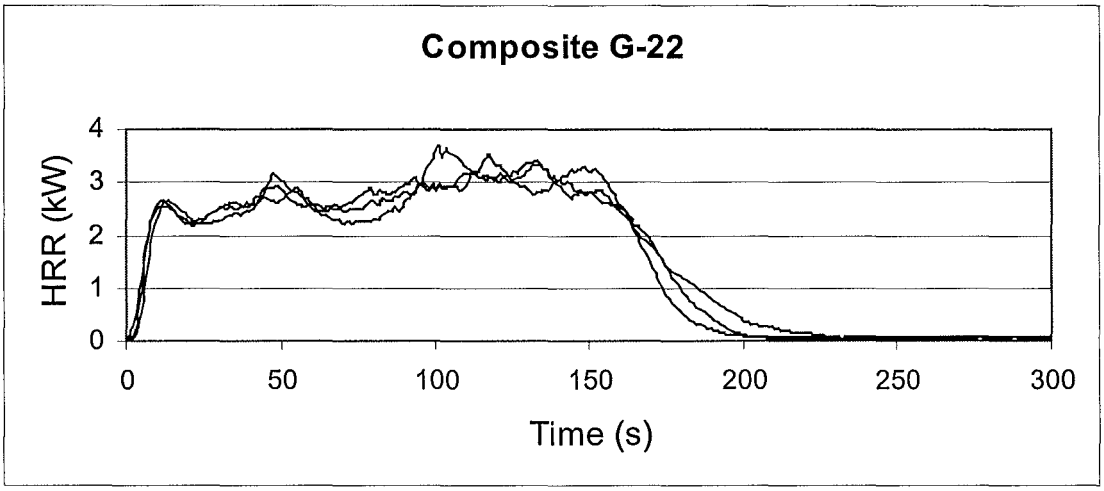


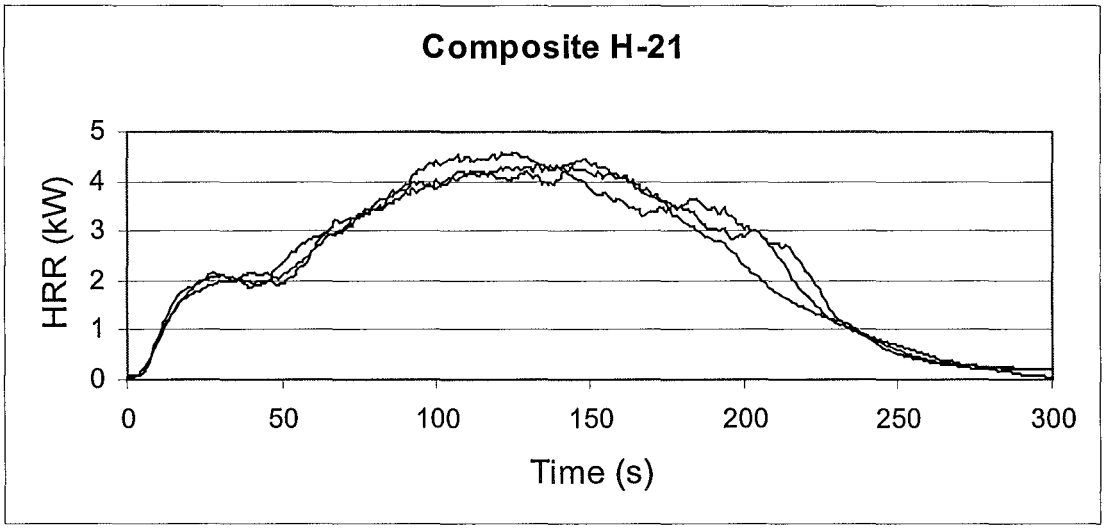

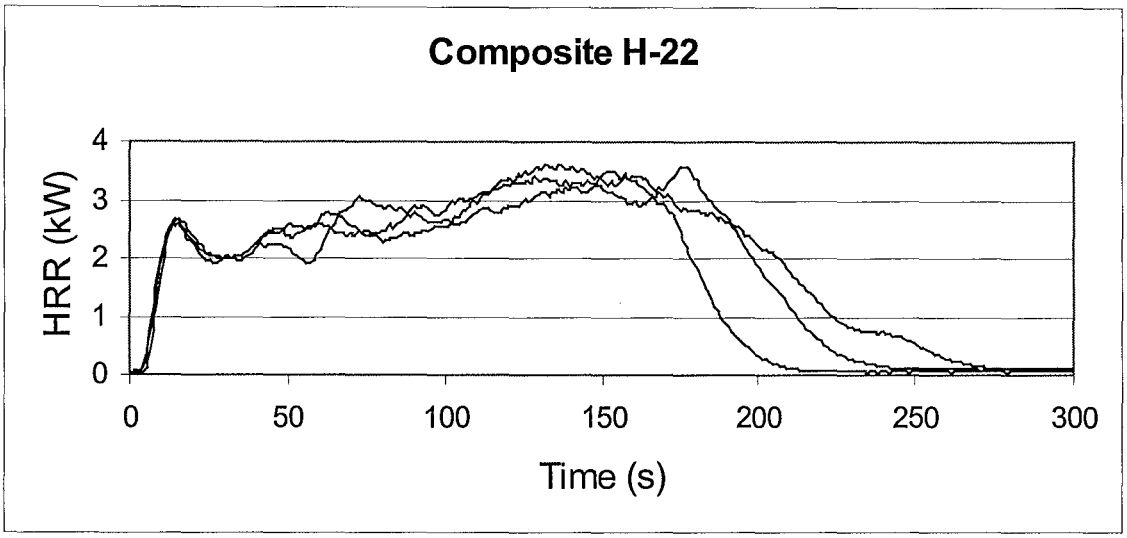
Composite H-22
HRR (kW)
0
1
2
3
4
0
50
100
150
200
250
300
Time (s)

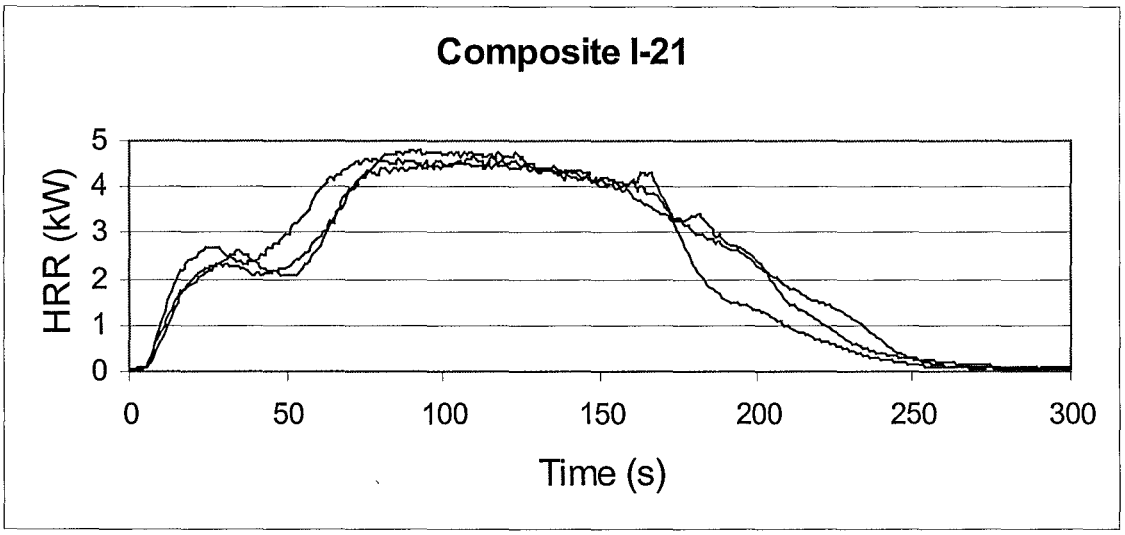
Composite I-21
HRR (kW)
0
1
2
3
4
5
0
50
100
150
200
250
300
Time (s)

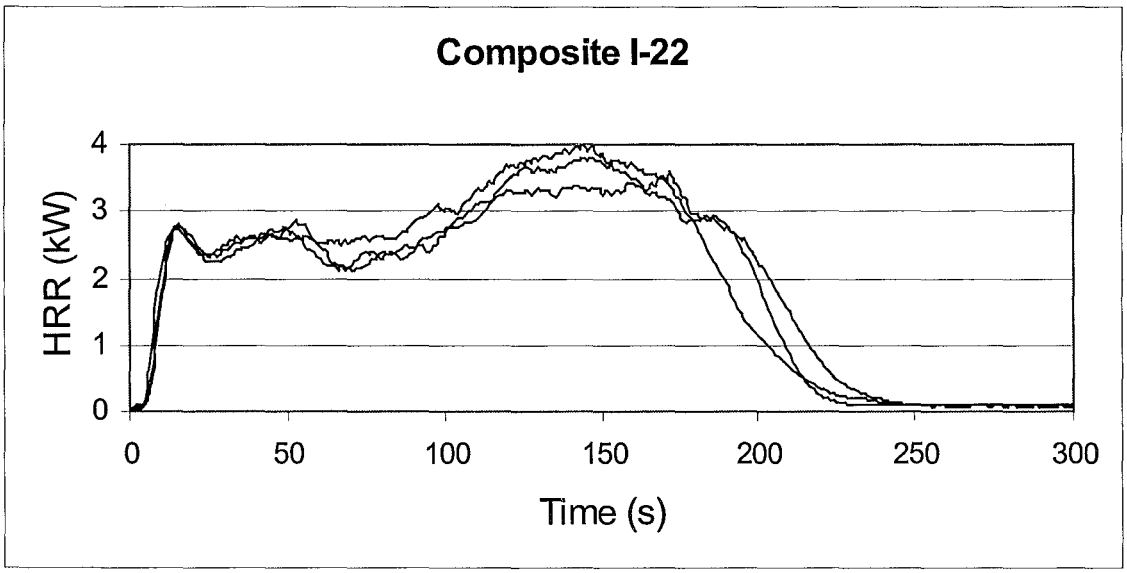
Composite I-22
HRR (kW)
0
1
2
3
4
0
50
100
150
200
250
300
Time (s)

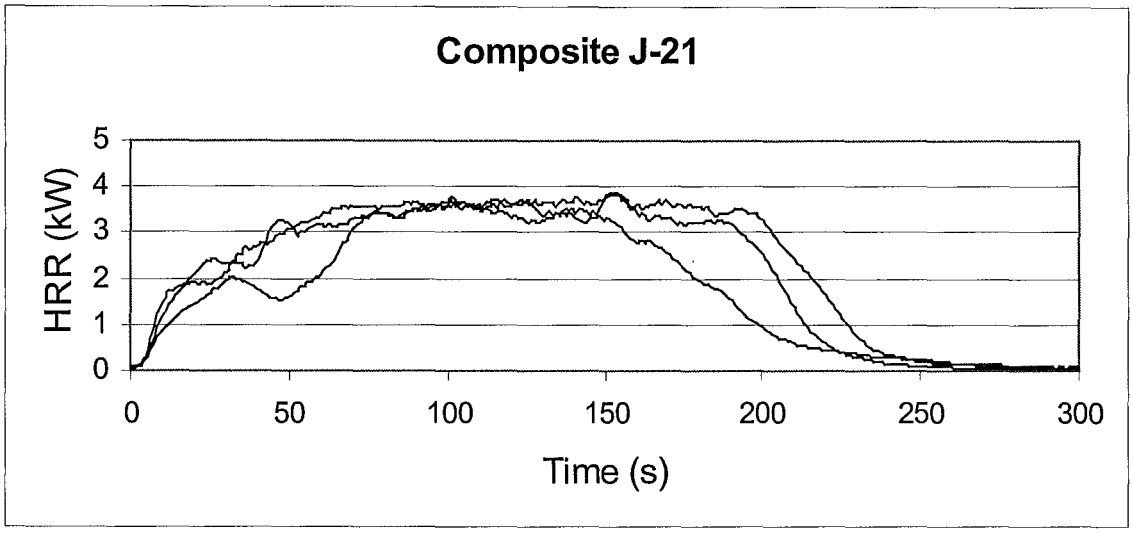
Composite J-21
HRR (kW)
0
1
2
3
4
5
0
50
100
150
200
250
300
Time (s)

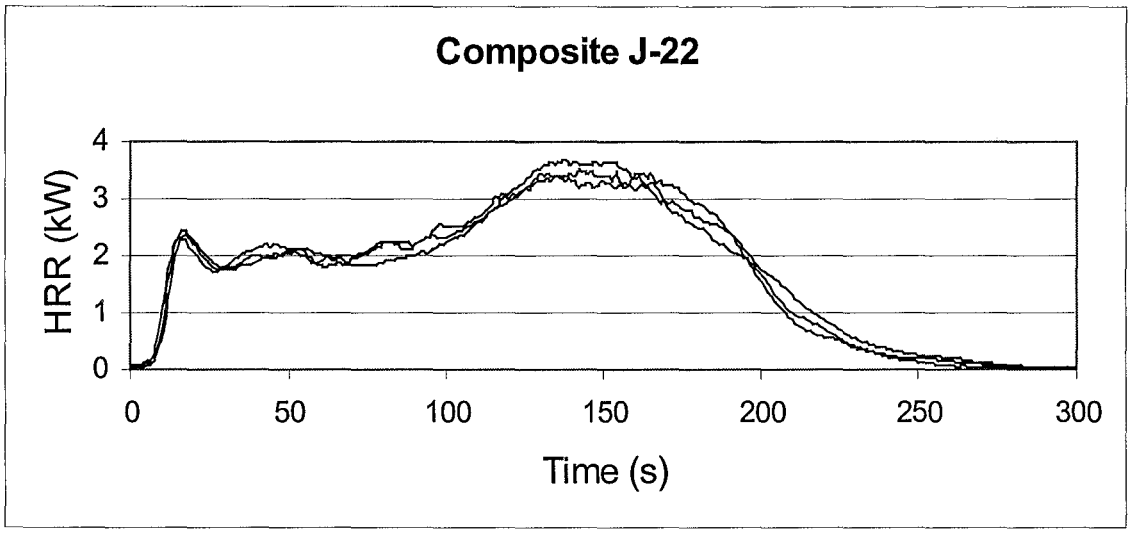
Composite J-22
HRR (kW)
0
1
2
3
4
0
50
100
150
200
250
300
Time (s)

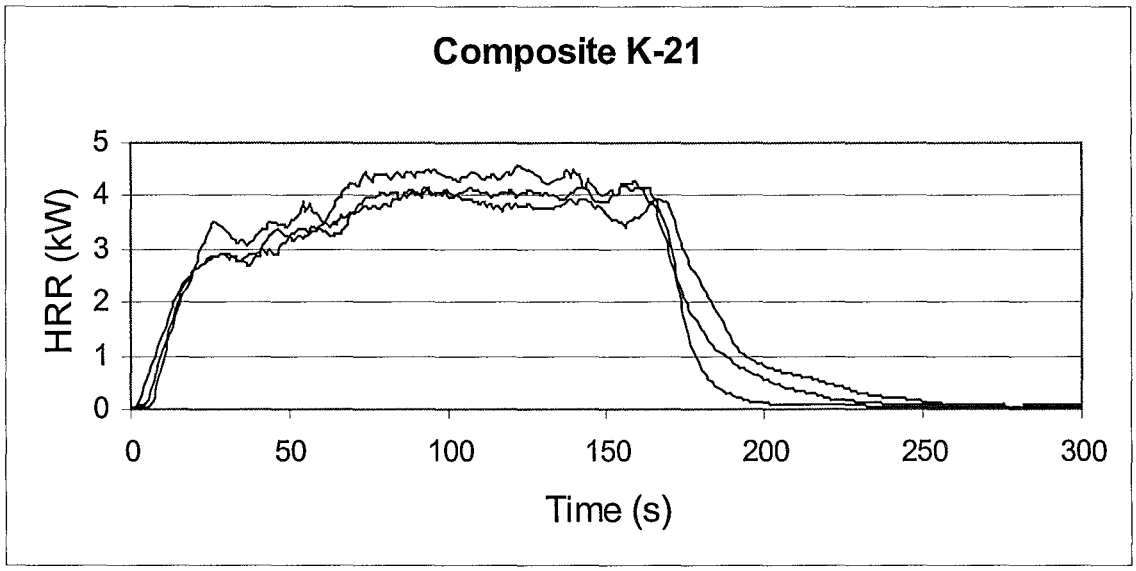
Composite K-21
HRR (kW)
0
1
2
3
4
5
0
50
100
150
200
250
300
Time (s)

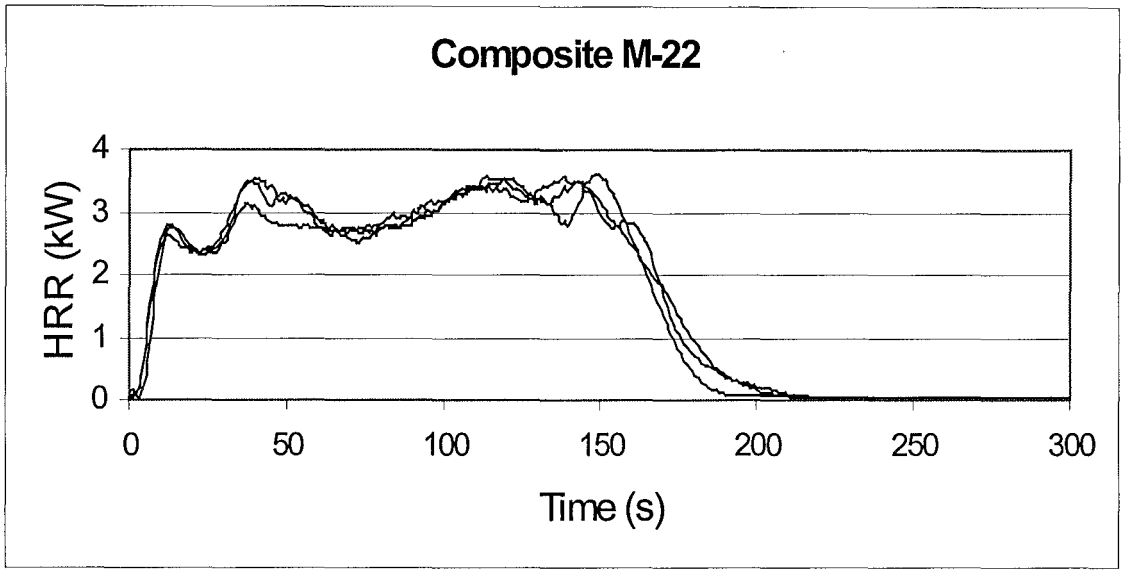
Composite M-22
HRR (kW)
0
1
2
3
4
0
50
100
150
200
250
300
Time (s)

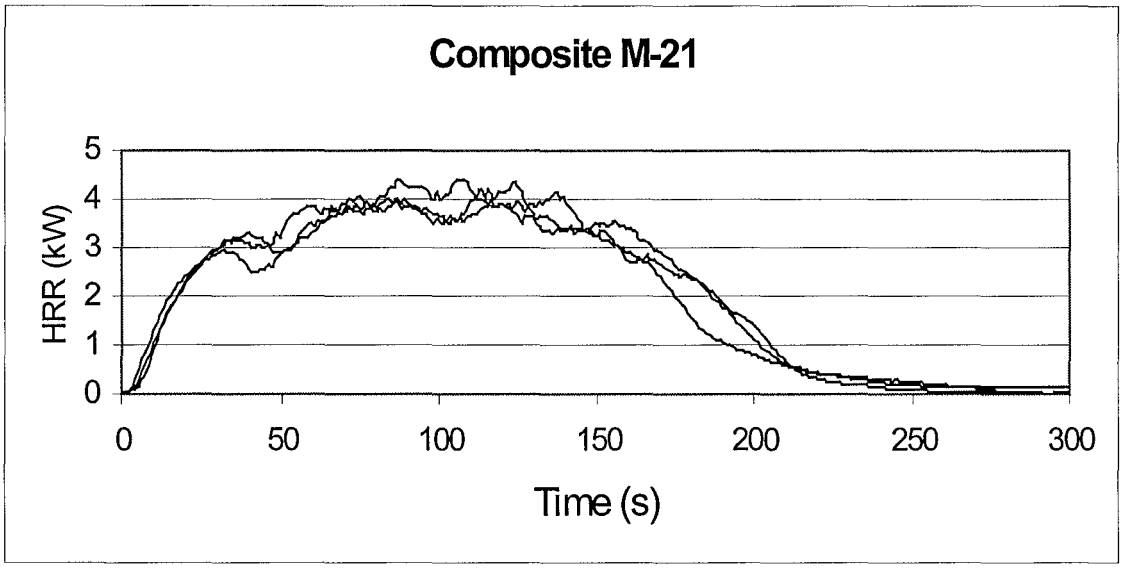
Composite M-21
HRR (kW)
0
1
2
3
4
5
0
50
100
150
200
250
300
Time (s)

## *Foam Weights and Ignition Times for the 7 Individual Foams:*

| Sample # | File Name (YYMMDD_*) | Foam Type | Foam Mass ( g ) | % Diff | Ignition Time (s) |
|---|---|---|---|---|---|
| 1 | 991027_c | L | 21.79 | 0.05 | 4 |
| 2 | 991027_d | L | 21.83 | -0.14 | 4 |
| 3 | 991027_e | L | 21.78 | 0.09 | 3 |
| 4 | 991027_f | M | 15.76 | -1.05 | 4 |
| 5 | 991027_g | M | 15.51 | 0.56 | 6 |
| 6 | 991027_h | M | 15.52 | 0.49 | 4 |
| 7 | 991027_i | J | 18.81 | -0.34 | 37 |
| 8 | 991027_j | J | 18.71 | 0.20 | 108 |
| 9 | 991027_k | J | 18.72 | 0.14 | 136 |
| 10 | 991027_l | H | 19 | -0.26 | 4 |
| 11 | 991027_m | H | 18.98 | -0.16 | 8 |
| 12 | 991027_n | H | 18.87 | 0.42 | 5 |
| 13 | 991027_o | K | 15.8 | -1.00 | 3 |
| 14 | 991027_p | K | 15.56 | 0.53 | 5 |
| 15 | 991027_q | K | 15.57 | 0.47 | 3 |
| 16 | 991027_r | G | 14.87 | -0.18 | 5 |
| 17 | 991027_s | G | 14.86 | -0.11 | 6 |
| 18 | 991027_t | G | 14.8 | 0.29 | 5 |
| 19 | 991027_u | I | 18.51 | -0.22 | 6 |
| 20 | 991027_v | I | 18.42 | 0.27 | 4 |
| 21 | 991027_w | I | 18.48 | -0.05 | 4 |

Table A2: Foam Weights and Ignition Times for the Seven Individual Foam Type Samples:

## *HRR Curves for the Individual 7 Foams Combustion:*

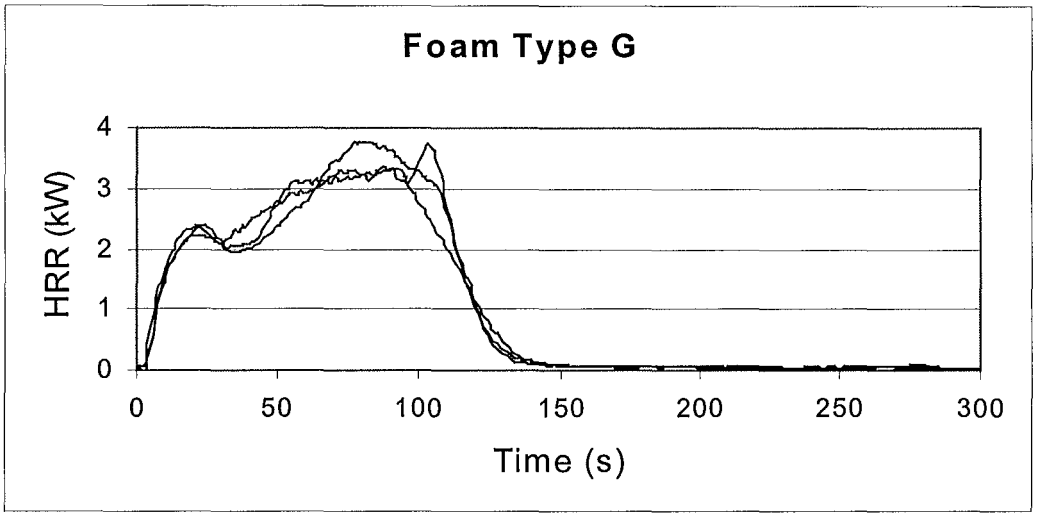


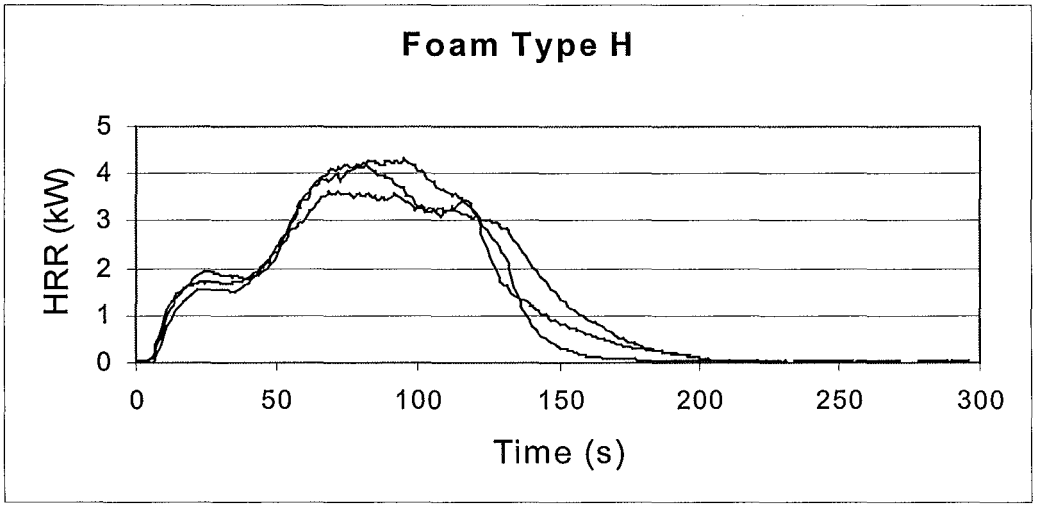


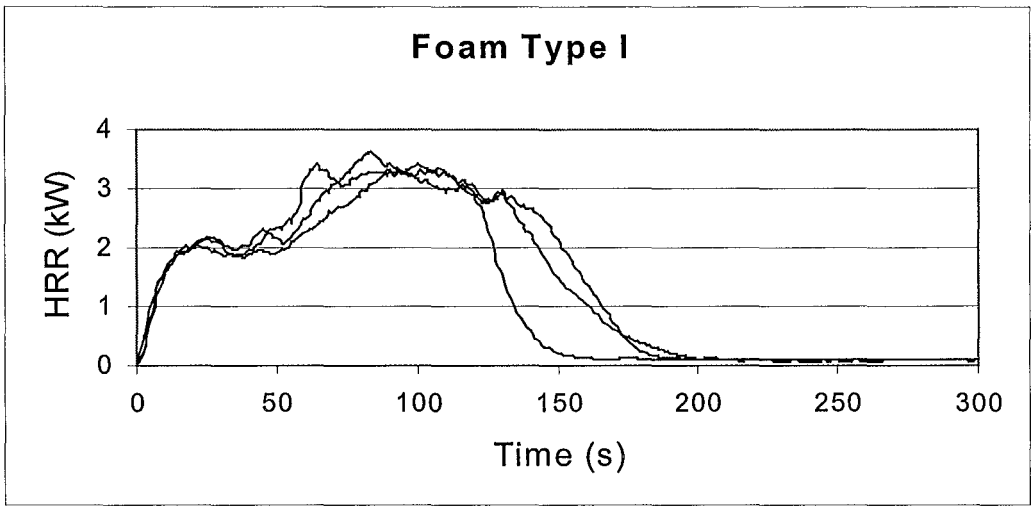

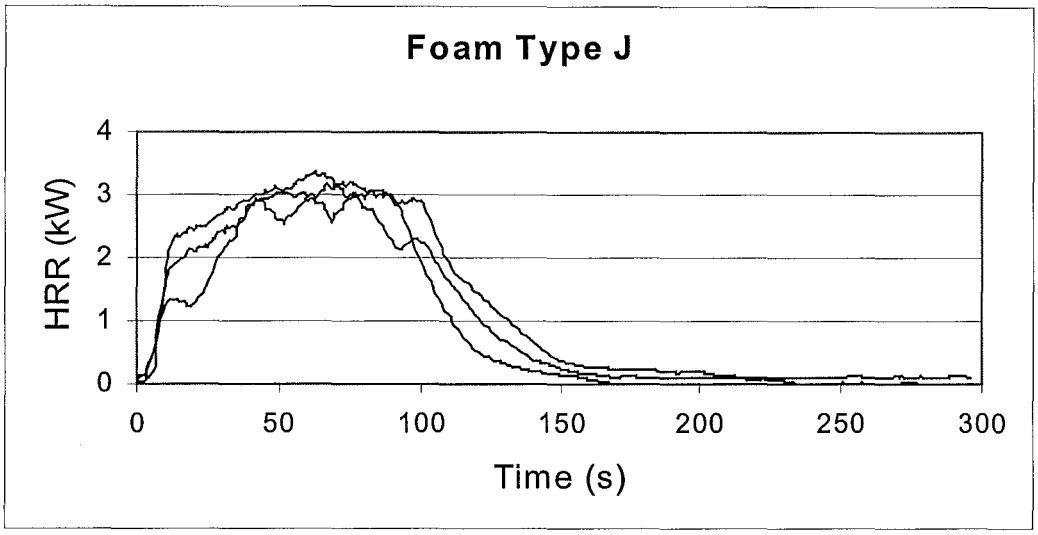
Foam Type J
HRR (kW)
0
1
2
3
4
0
50
100
150
200
250
300
Time (s)

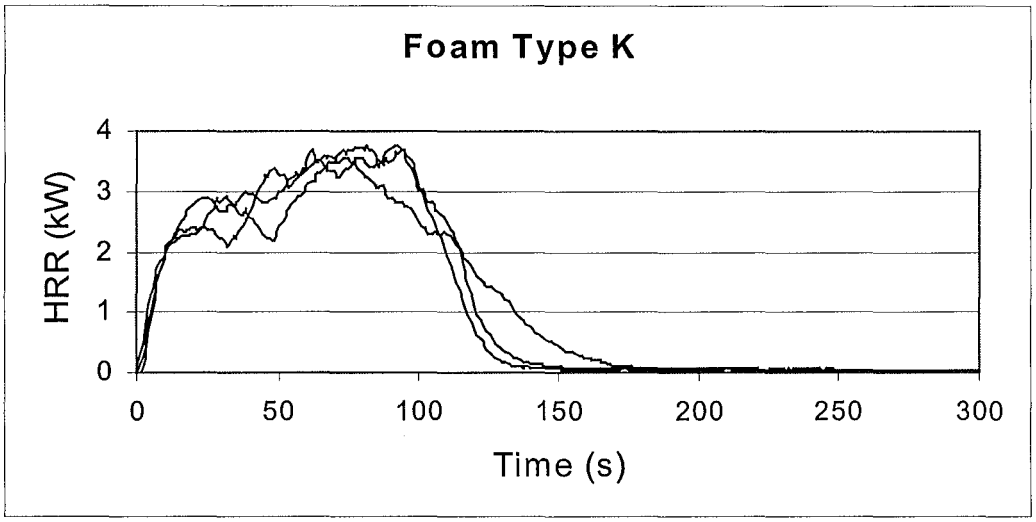
Foam Type K
HRR (kW)
0
1
2
3
4
0
50
100
150
200
250
300
Time (s)

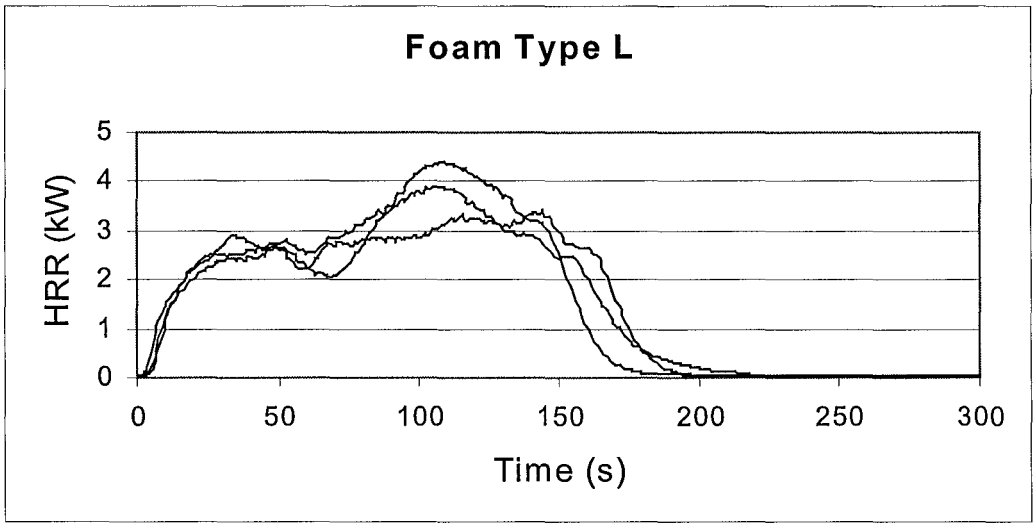
Foam Type L
HRR (kW)
0
1
2
3
4
5
0
50
100
150
200
250
300
Time (s)

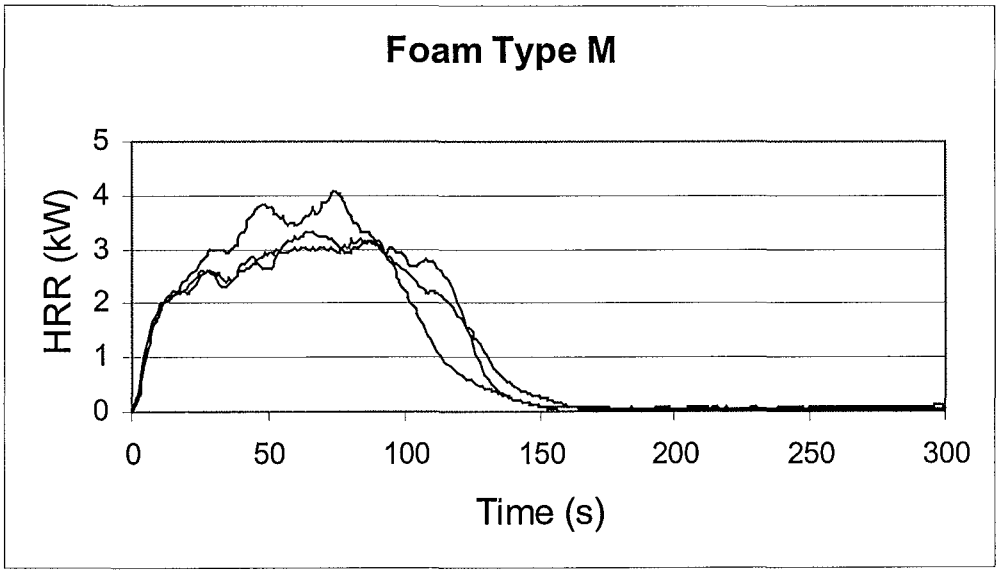
Foam Type M
HRR (kW)
5
4
3
2
1
0
0
50
100
150
200
250
300
Time (s)

## *Averaging Triplicate Runs:*

In Table A3 are shown the three individual HRR test runs results for the composite combination J-22. The individual run values come from the HRR graph data from each of the triplicate runs. The average of these values gives a result that is more general of the HRR characteristics this particular composite. It are the averaged values that are required as inputs to CBUF Model I for making full-scale predictions.

It should also be noticed that the 180-second average heat release values are listed in Table A3 and in the last row are listed the percentage differences of these values from their arithmetic mean. These have to be less than ±10%, or three more test runs were required by the testing procedure. In this case the largest difference is 2.9% so they are well within the criteria. (In all cases the percentage differences were less than 10%, so no further tests were required.)

| Parameter | Units | Run 1 | Run 2 | Run 3 | Averages |
|---|---|---|---|---|---|
| m | kg | 0.0321 | 0.0322 | 0.0324 | 0.0322 |
| $\dot{q}''_{35\text{-}pk}$ | kW m$^{-2}$ | 345.2 | 350.9 | 366.2 | 354.1 |
| $\dot{q}''_{pk\#1}$ | kW m$^{-2}$ | 242.0 | 235.0 | 234.0 | 237.0 |
| $\dot{q}''_{trough}$ | kW m$^{-2}$ | 178.0 | 174.0 | 172.0 | 174.7 |
| $\dot{q}''_{pk\#2}$ | kW m$^{-2}$ | 345.2 | 350.9 | 366.2 | 354.1 |
| $\dot{q}''_{35\text{-}60}$ | kW m$^{-2}$ | 167.0 | 160.6 | 167.7 | 165.1 |
| $\dot{q}''_{35\text{-}180}$ | kW m$^{-2}$ | 242.5 | 232.6 | 243.4 | 239.5 |
| $\dot{q}''_{35\text{-}300}$ | kW m$^{-2}$ | 171.2 | 170.1 | 174.1 | 171.8 |
| $q''_{35\text{-}tot}$ | MJ m$^{-2}$ | 51.6 | 51.3 | 51.9 | 51.6 |
| $t_{ig\text{-}35}$ | s | 16 | 15 | 17 | 16 |
| $t_{pk}$ | s | 161.7 | 141.9 | 137.5 | 147.0 |
| $t_{pk\#1,start\ of\ test}$ | s | 17.6 | 17.6 | 15.4 | 16.9 |
| $\Delta h_{c,eff}$ | MJ kg$^{-1}$ | 16.1 | 15.9 | 16.0 | 16.0 |
| $\dot{q}''_{35\text{-}180}$% diff | % | -1.3 | 2.9 | -1.6 | 2.9 (max) |

Table A3: Triplicate HRR data for Composite J-22:

# Appendix B: Furniture Calorimeter Results:

| Chair Number | 2 | 5 | 6 | 8 | 9 | 11 | 12 | 14 | 18 | 20 |
|---|---|---|---|---|---|---|---|---|---|---|
| Chair Code | G-21-S2-1 | G-22-S2-1 | H-21-S2-1 | H-22-S2-1 | I-21-S2-1 | I-22-S2-1 | J-21-S2-1 | J-22-S2-1 | L-21-S2-1 | L-22-S2-1 |
| Measured Mass of Frame (kg) | 14.91 | 14.13 | 13.72 | 13.49 | 13.62 | 14.18 | 13.83 | 13.83 | 13.62 | 14.48 |
| Measured Mass of Foam (kg) | 2.12 | 2.12 | 2.89 | 2.86 | 2.84 | 2.86 | 3.07 | 3.09 | 3.05 | 3.06 |
| Measured Mass of Chair (kg) | 18.34 | 18.28 | 17.98 | 18.50 | 17.88 | 19.18 | 18.24 | 18.92 | 18.08 | 19.48 |
| Mass of Soft Components (kg) | 3.43 | 4.16 | 4.26 | 5.02 | 4.26 | 5.00 | 4.41 | 5.09 | 4.46 | 5.00 |
| Mass of other soft, other than foam (kg) | 1.32 | 2.03 | 1.37 | 2.15 | 1.42 | 2.14 | 1.34 | 2.00 | 1.41 | 1.94 |

Table B1: Full-Scale Armchair Measured Weights:

## *HRR Curves for the Combustion of the ten Armchairs:*

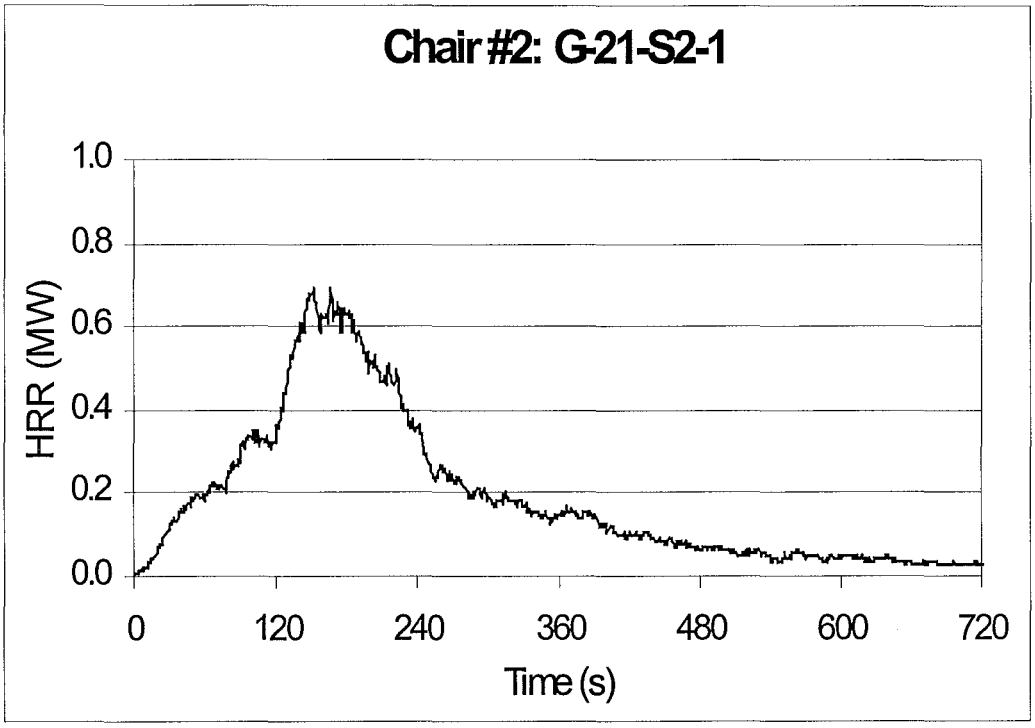


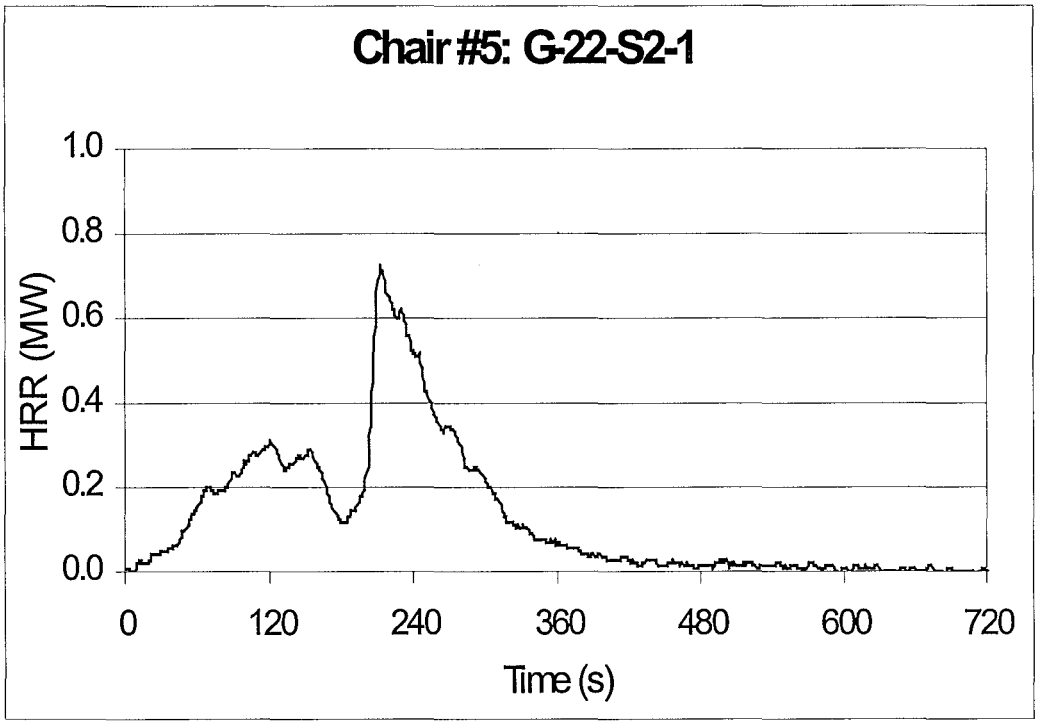

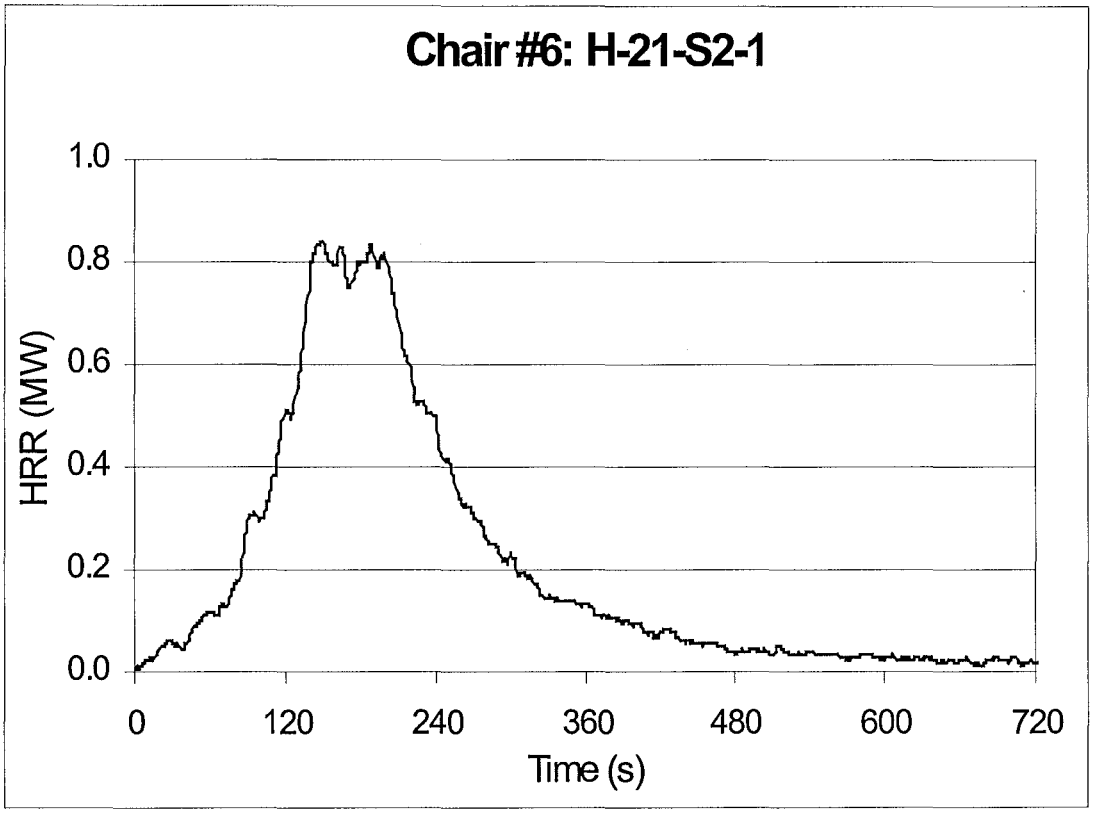
Chair #6: H-21-S2-1
HRR (MW)
1.0
0.8
0.6
0.4
0.2
0.0
0
120
240
360
480
600
720
Time (s)

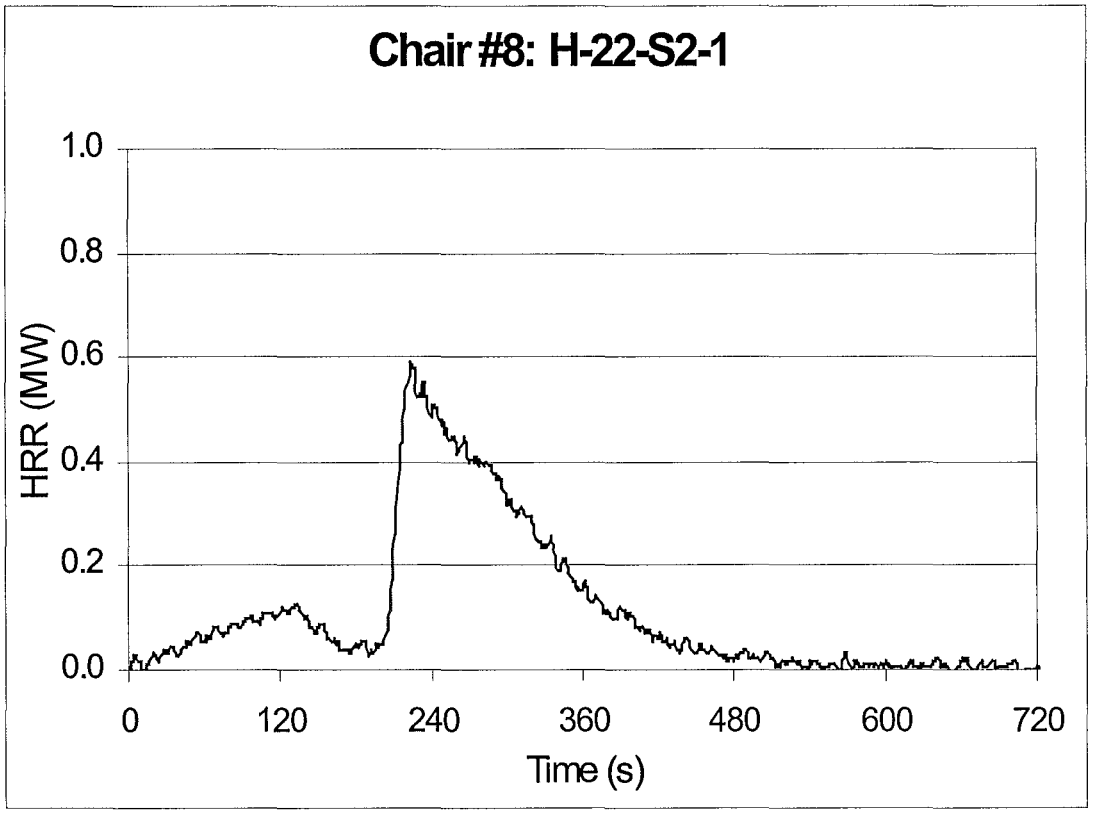
Chair #8: H-22-S2-1
HRR (MW)
1.0
0.8
0.6
0.4
0.2
0.0
0
120
240
360
480
600
720
Time (s)

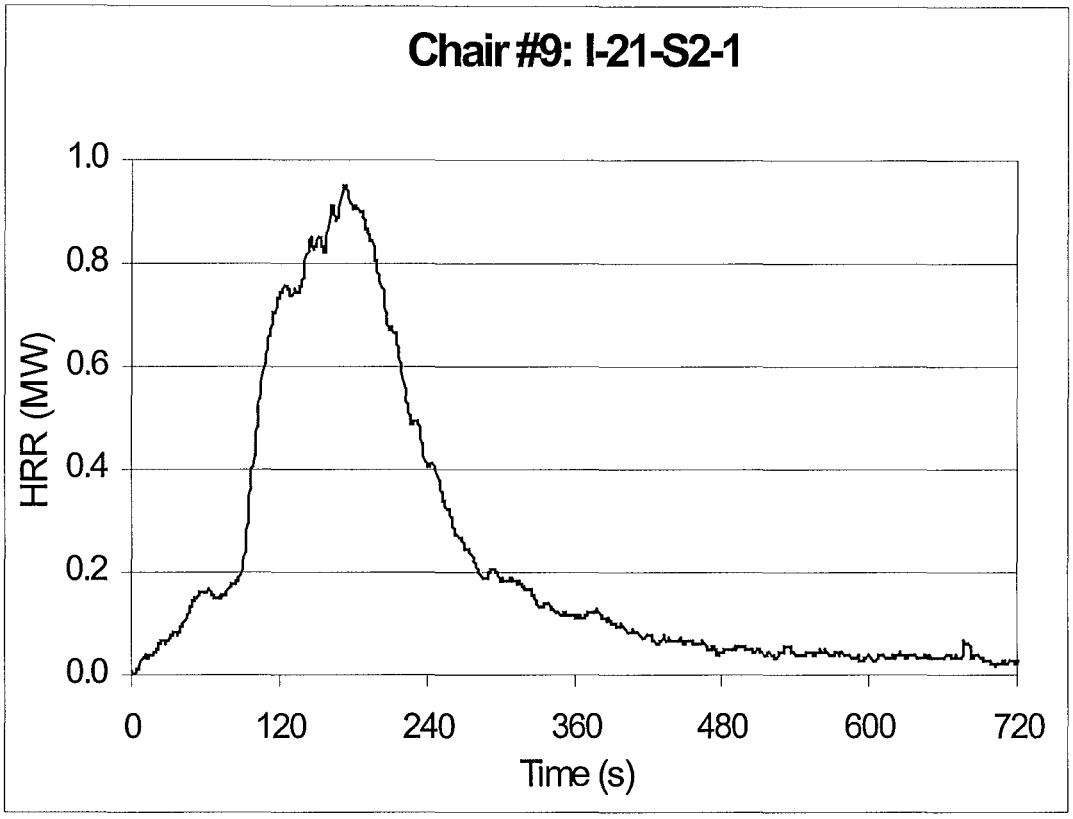
Chair #9: I-21-S2-1
HRR (MW)
1.0
0.8
0.6
0.4
0.2
0.0
0
120
240
360
480
600
720
Time (s)

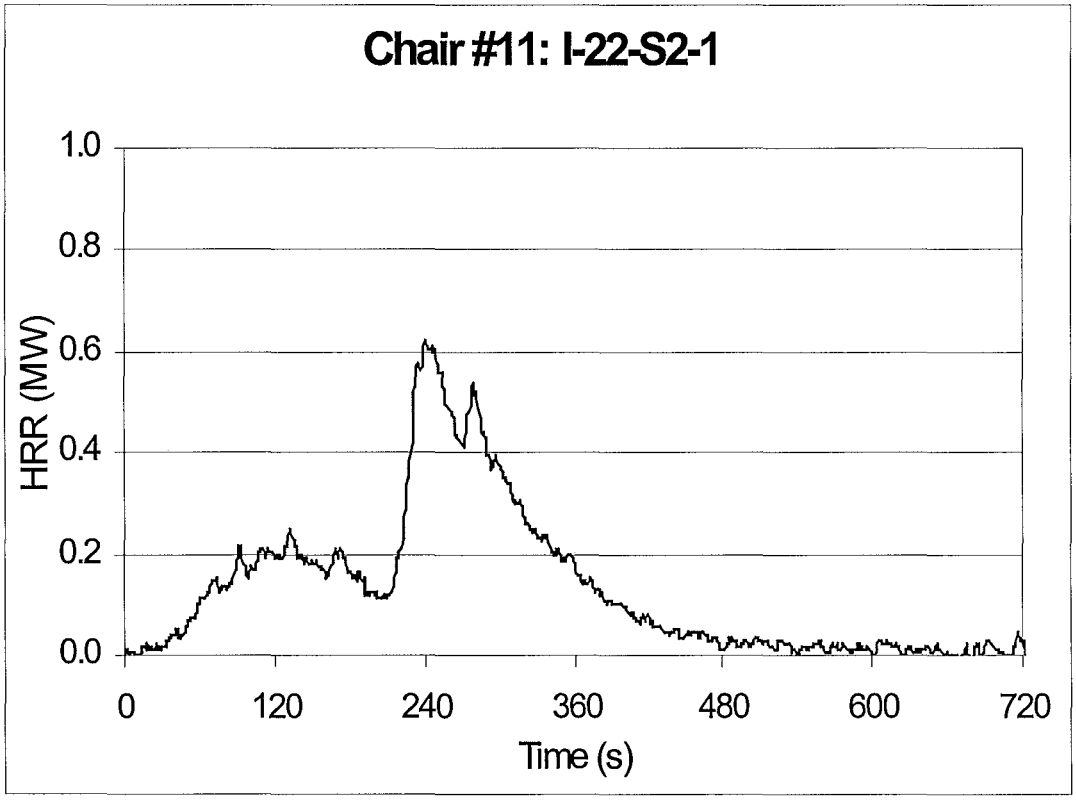
Chair #11: I-22-S2-1
HRR (MW)
1.0
0.8
0.6
0.4
0.2
0.0
0
120
240
360
480
600
720
Time (s)

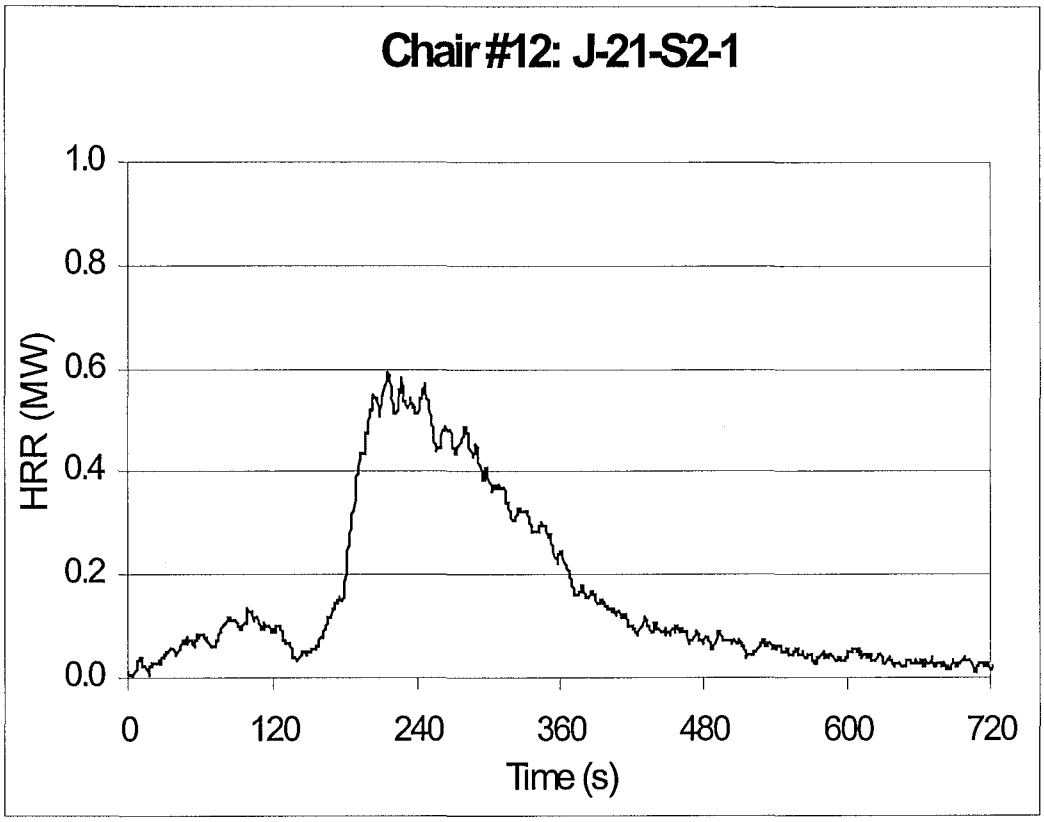
Chair #12: J-21-S2-1
HRR (MW)
1.0
0.8
0.6
0.4
0.2
0.0
0
120
240
360
480
600
720
Time (s)

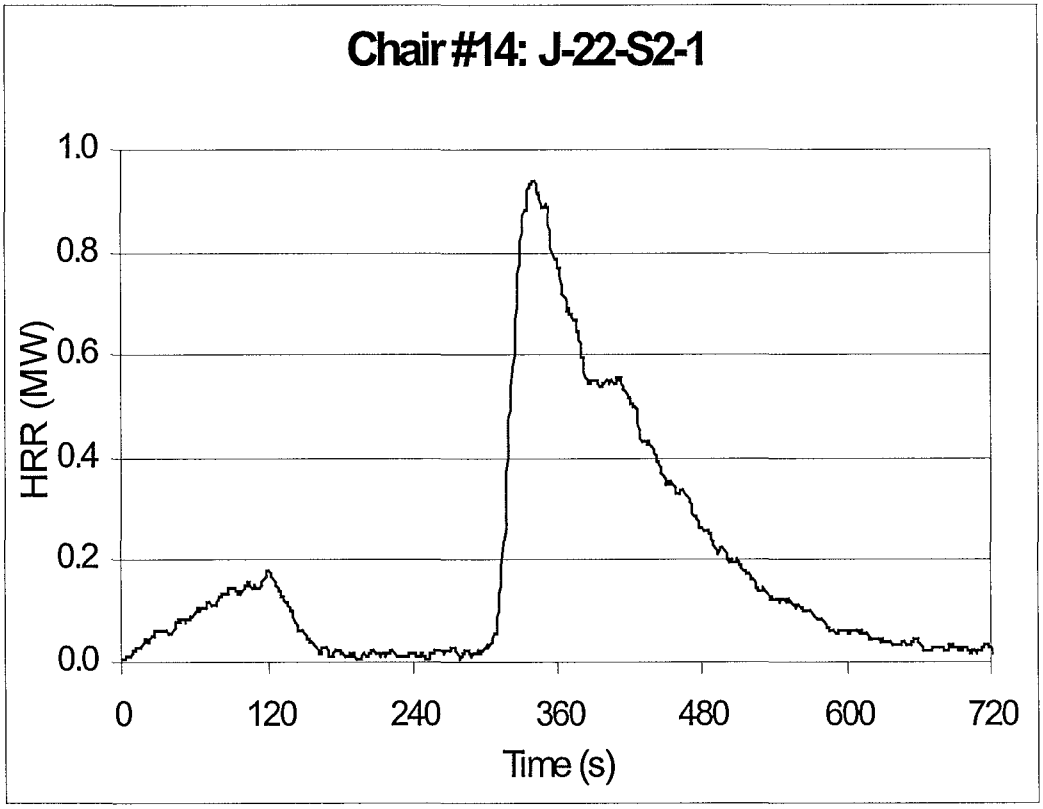
Chair #14: J-22-S2-1
HRR (MW)
1.0
0.8
0.6
0.4
0.2
0.0
0
120
240
360
480
600
720
Time (s)

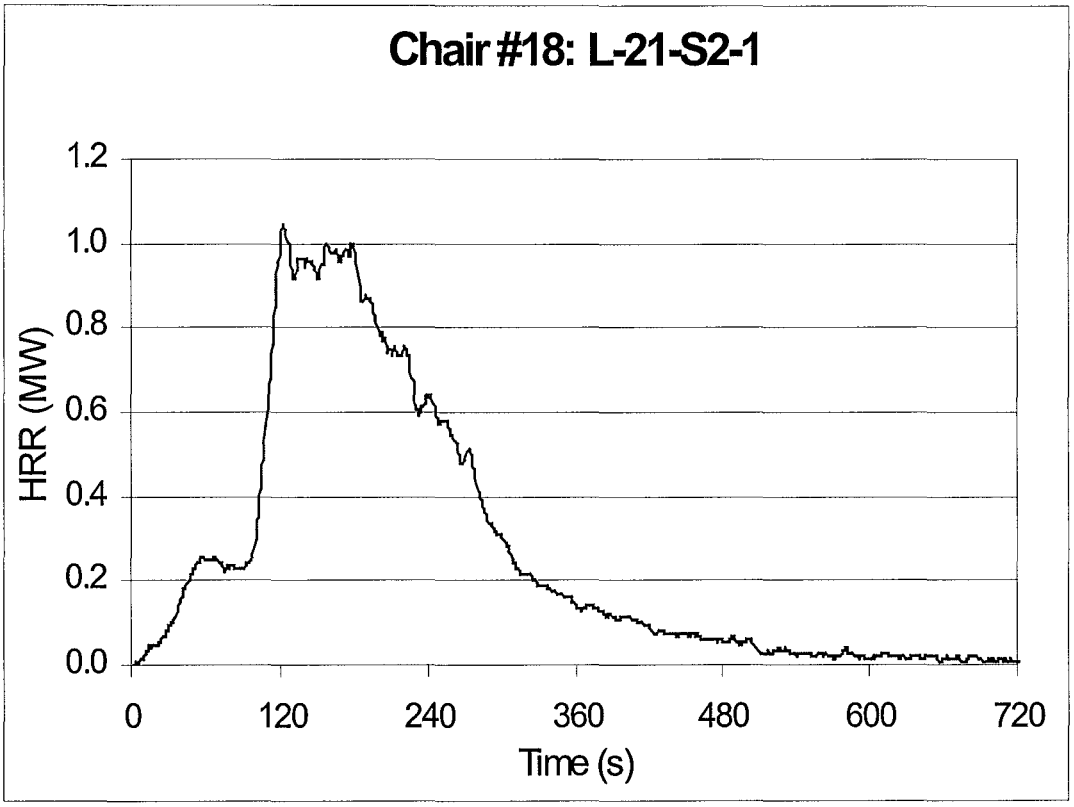
Chair #18: L-21-S2-1
HRR (MW)
1.2
1.0
0.8
0.6
0.4
0.2
0.0
0
120
240
360
480
600
720
Time (s)

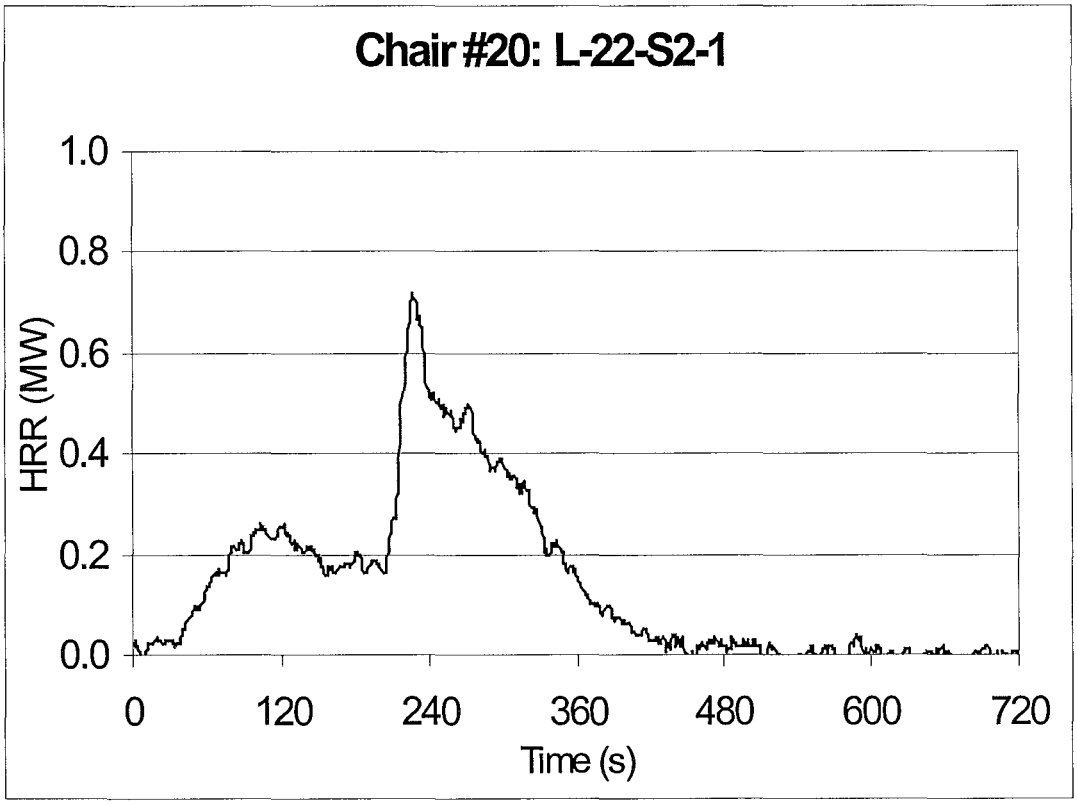
Chair #20: L-22-S2-1
HRR (MW)
1.0
0.8
0.6
0.4
0.2
0.0
0
120
240
360
480
600
720
Time (s)

## *$CO/CO_2$ Production and CO, $CO_2$, $O_2$ Concentration Graphs for the Combustion of the ten Armchairs:*

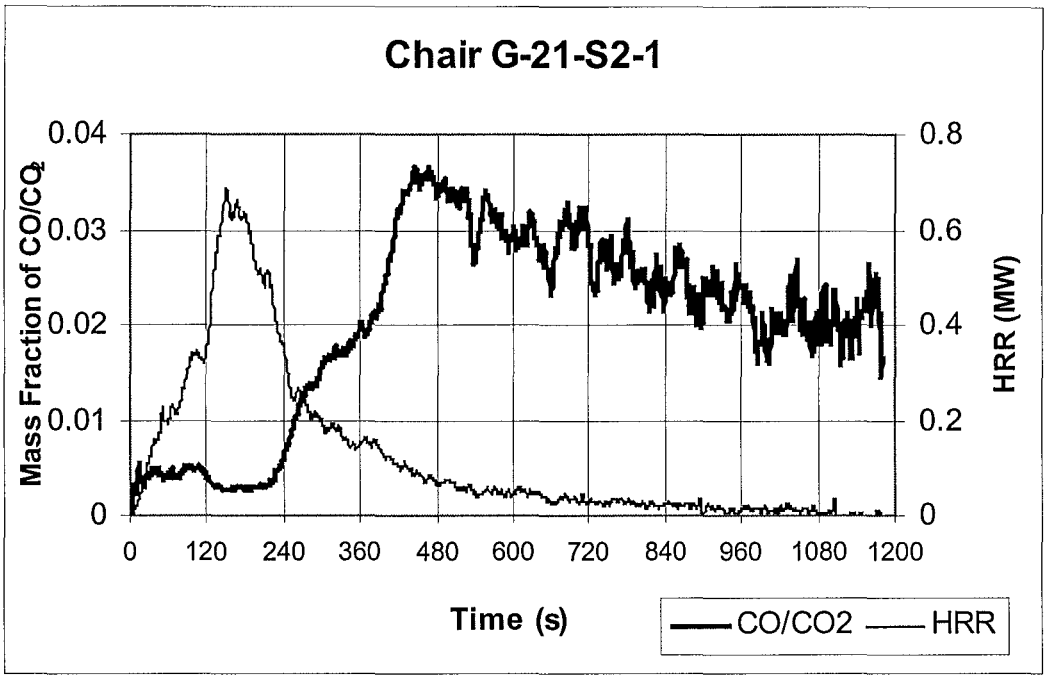


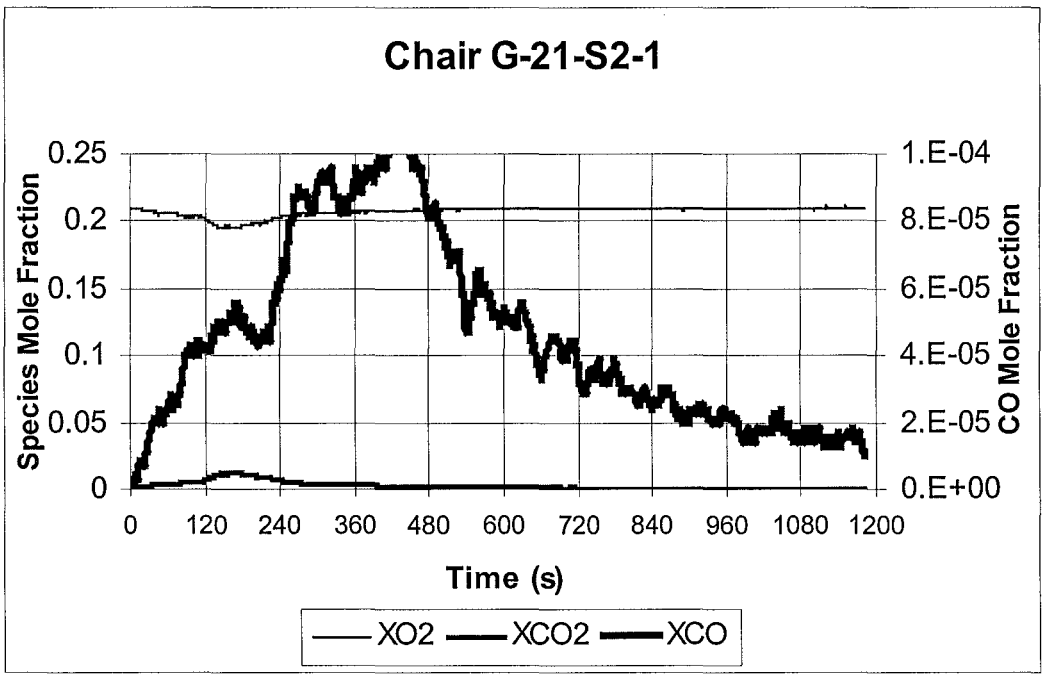

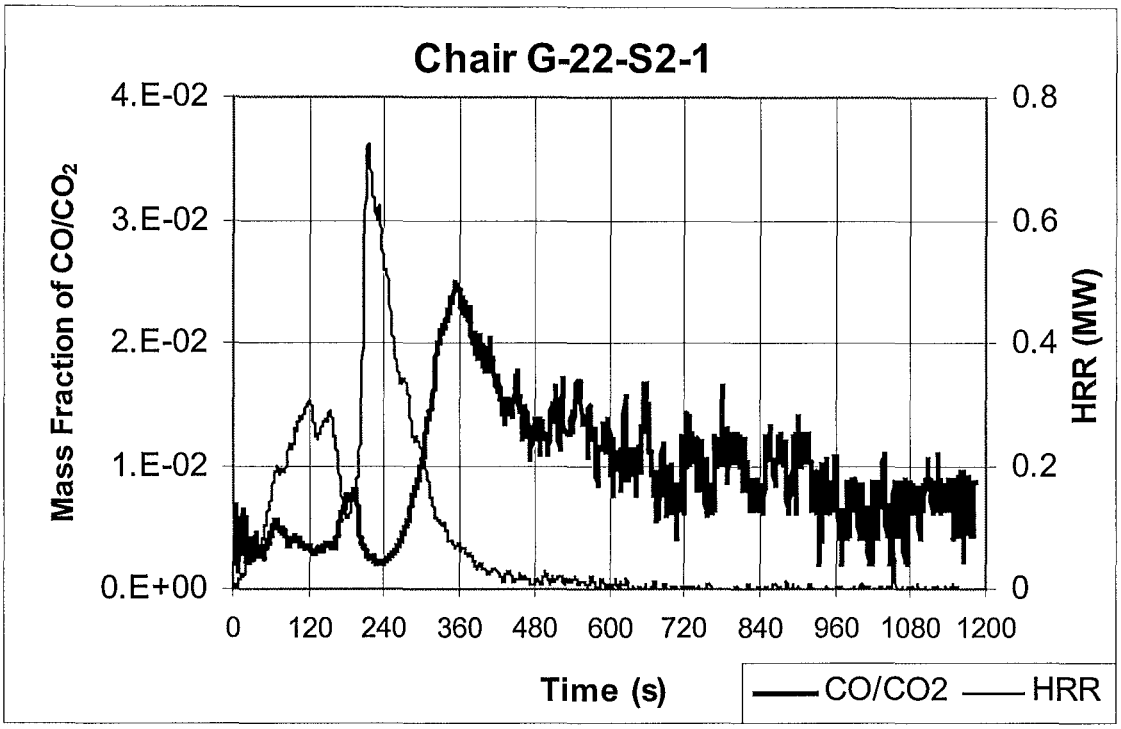
Chair G-22-S2-1
Mass Fraction of CO/CO2
HRR (MW)
4.E-02
3.E-02
2.E-02
1.E-02
0.E+00
0.8
0.6
0.4
0.2
0
0 120 240 360 480 600 720 840 960 1080 1200
Time (s)
CO/CO2
HRR

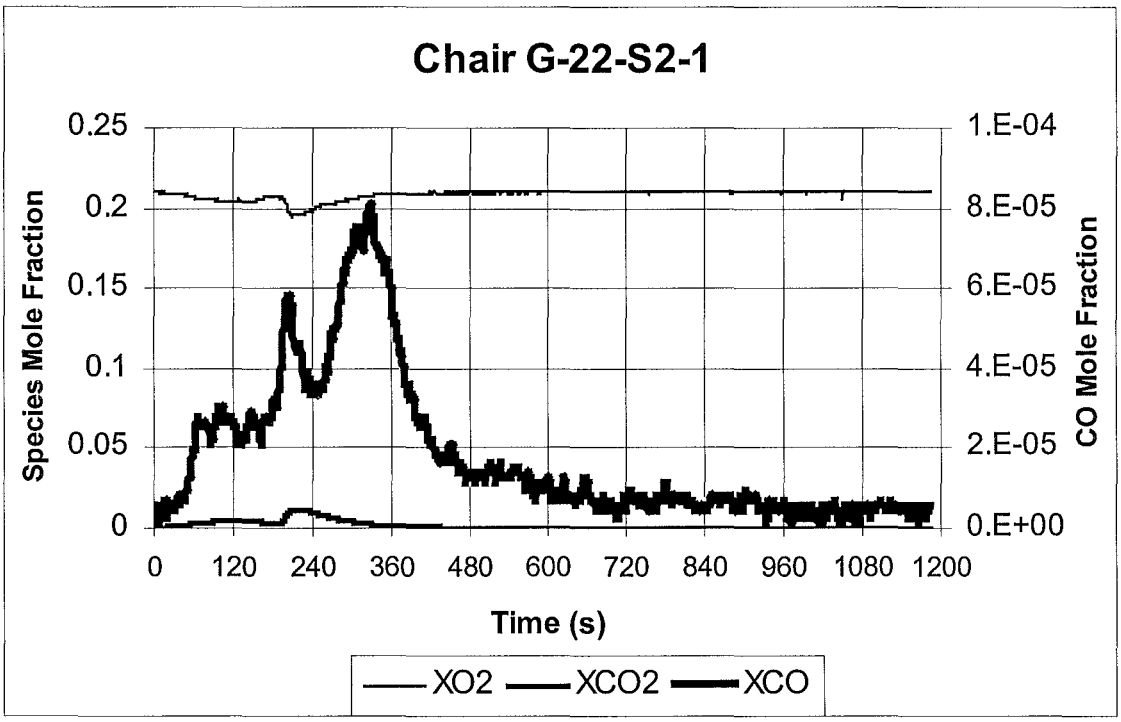
Chair G-22-S2-1
Species Mole Fraction
CO Mole Fraction
0.25
0.2
0.15
0.1
0.05
0
1.E-04
8.E-05
6.E-05
4.E-05
2.E-05
0.E+00
0 120 240 360 480 600 720 840 960 1080 1200
Time (s)
XO2
XCO2
XCO

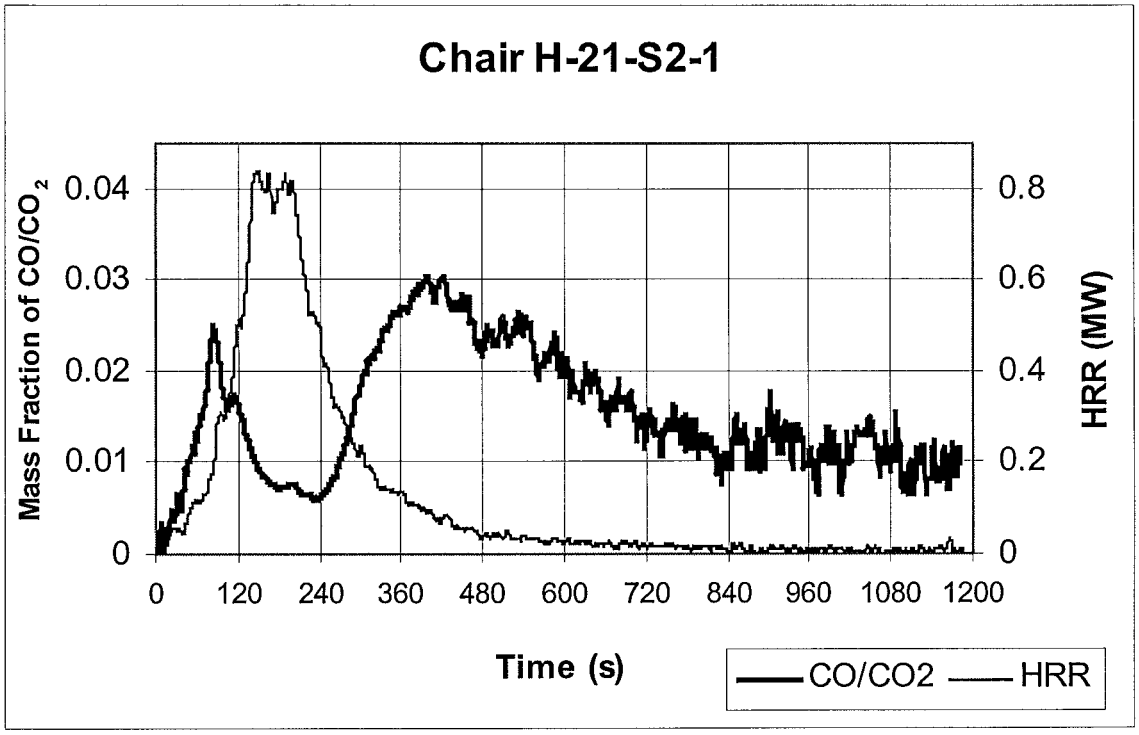
Chair H-21-S2-1
Mass Fraction of CO/CO2
0.04
0.03
0.02
0.01
0
0.8
0.6
0.4
0.2
0
HRR (MW)
0 120 240 360 480 600 720 840 960 1080 1200
Time (s)
CO/CO2
HRR

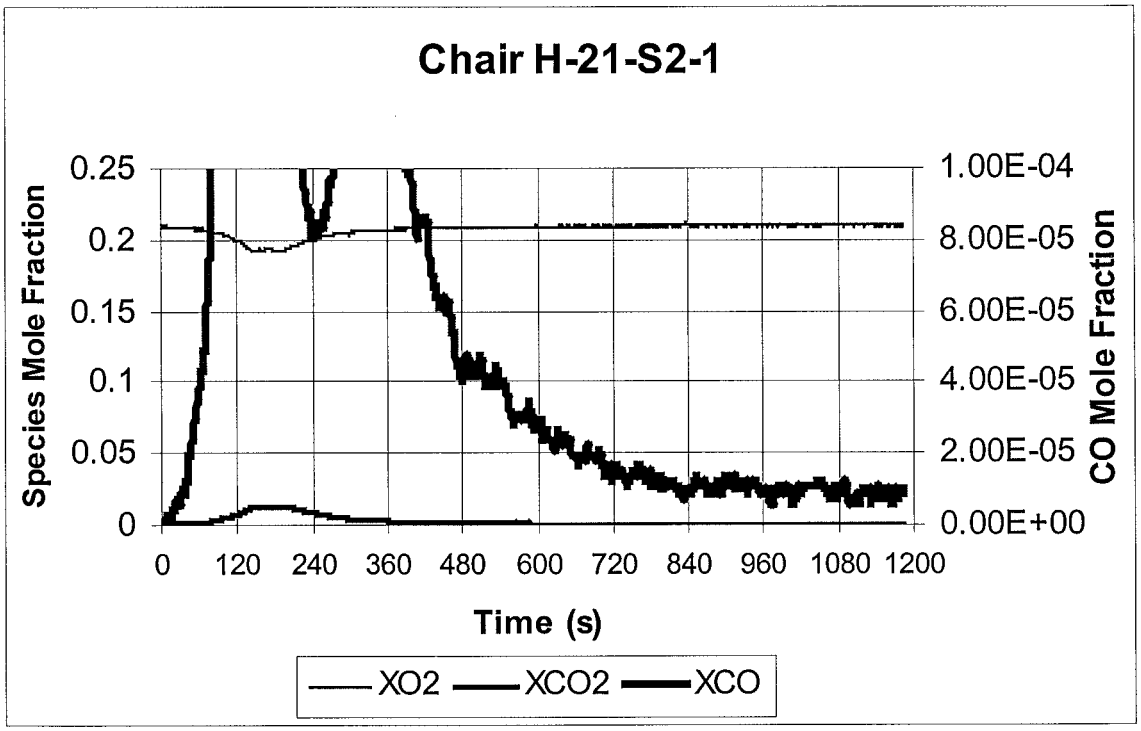
Chair H-21-S2-1
Species Mole Fraction
0.25
0.2
0.15
0.1
0.05
0
1.00E-04
8.00E-05
6.00E-05
4.00E-05
2.00E-05
0.00E+00
CO Mole Fraction
0 120 240 360 480 600 720 840 960 1080 1200
Time (s)
XO2
XCO2
XCO

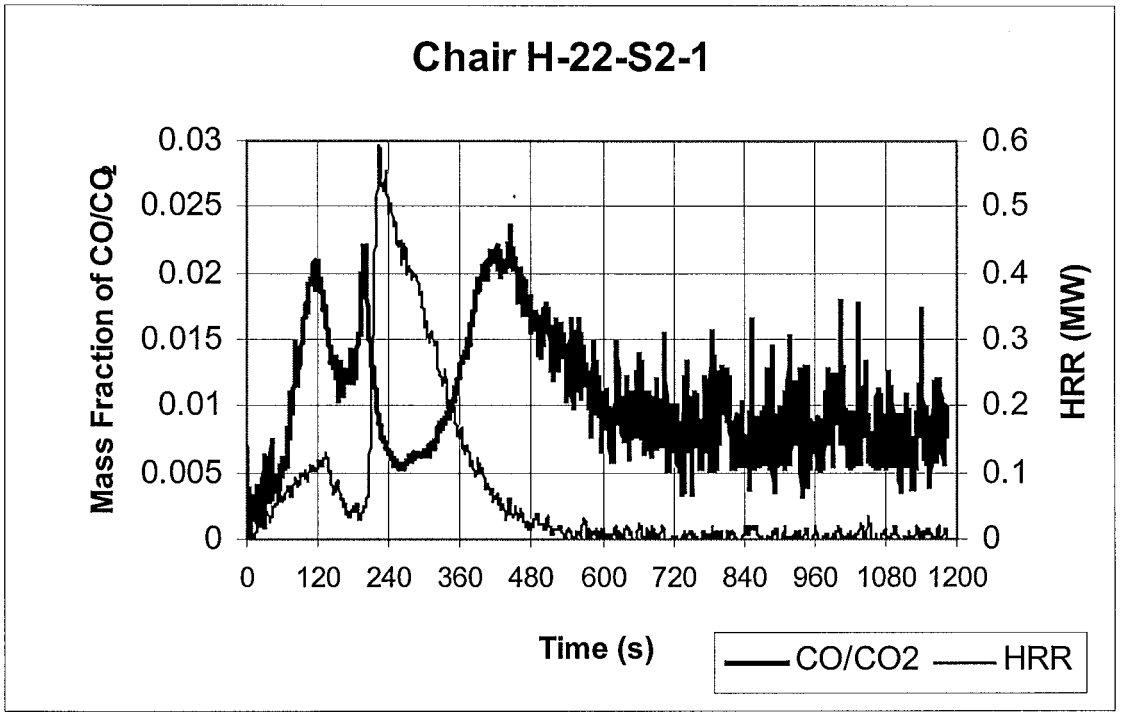
Chair H-22-S2-1
Mass Fraction of CO/CO2
HRR (MW)
0.03
0.025
0.02
0.015
0.01
0.005
0
0.6
0.5
0.4
0.3
0.2
0.1
0
0 120 240 360 480 600 720 840 960 1080 1200
Time (s)
CO/CO2
HRR

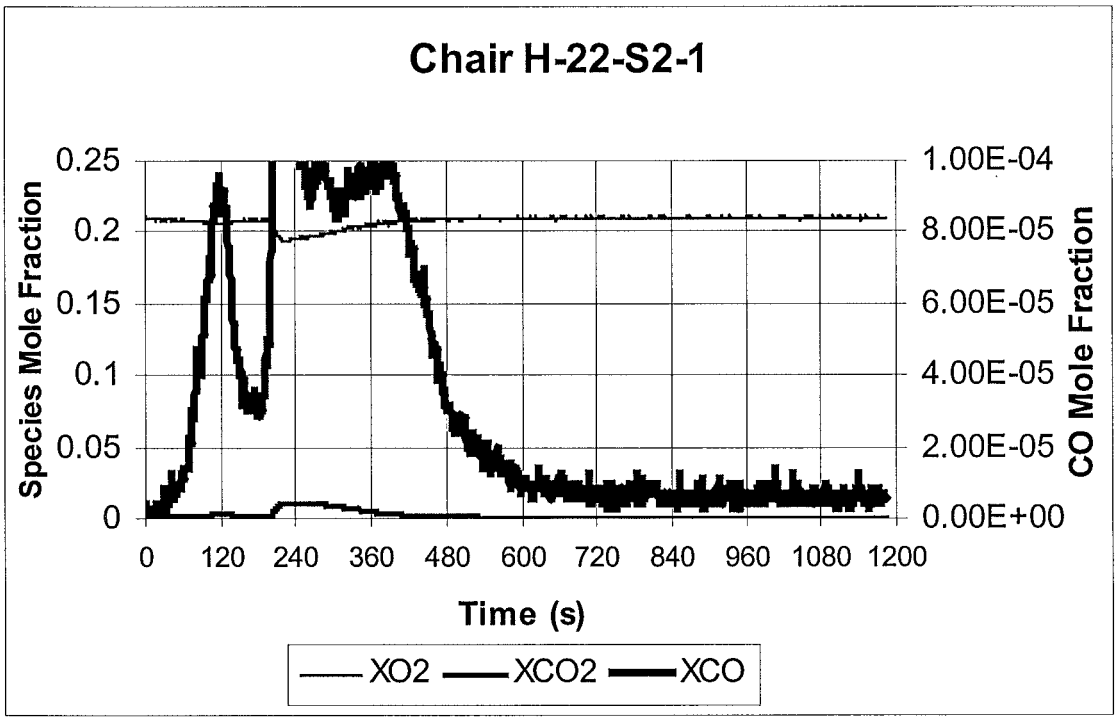
Chair H-22-S2-1
Species Mole Fraction
CO Mole Fraction
0.25
0.2
0.15
0.1
0.05
0
1.00E-04
8.00E-05
6.00E-05
4.00E-05
2.00E-05
0.00E+00
0 120 240 360 480 600 720 840 960 1080 1200
Time (s)
XO2
XCO2
XCO

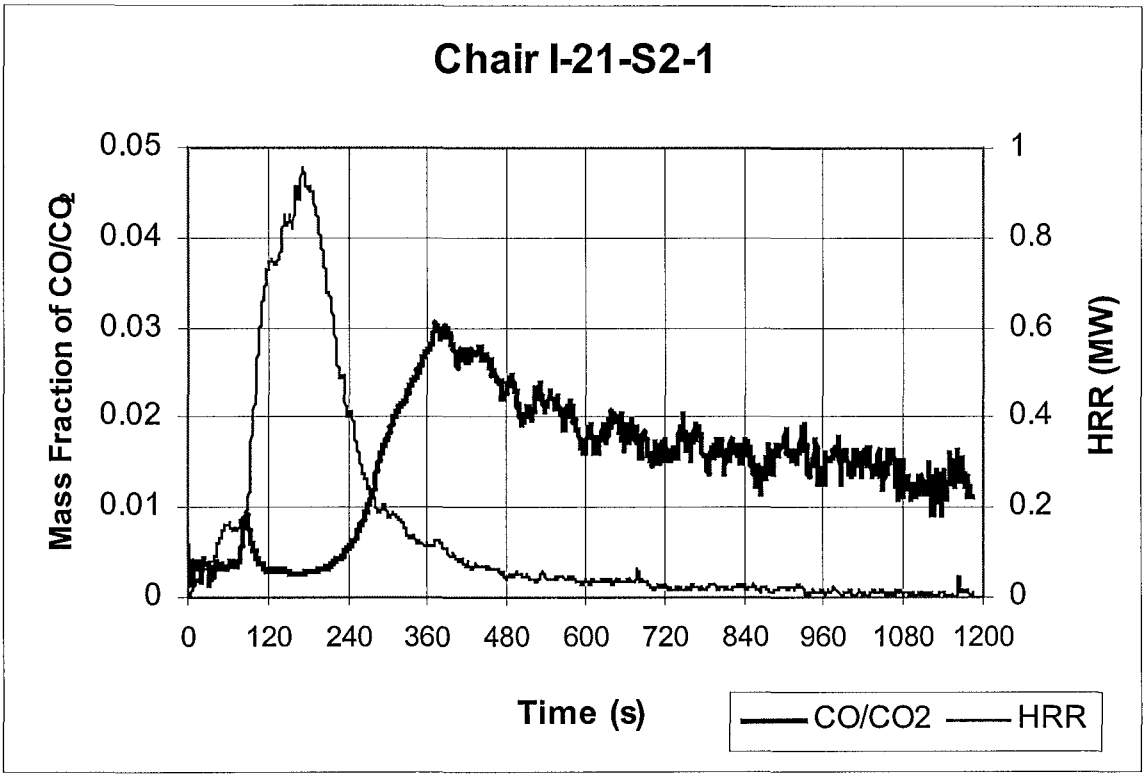
Chair I-21-S2-1
Mass Fraction of CO/CO2
HRR (MW)
0.05
0.04
0.03
0.02
0.01
0
1
0.8
0.6
0.4
0.2
0
0 120 240 360 480 600 720 840 960 1080 1200
Time (s)
CO/CO2
HRR

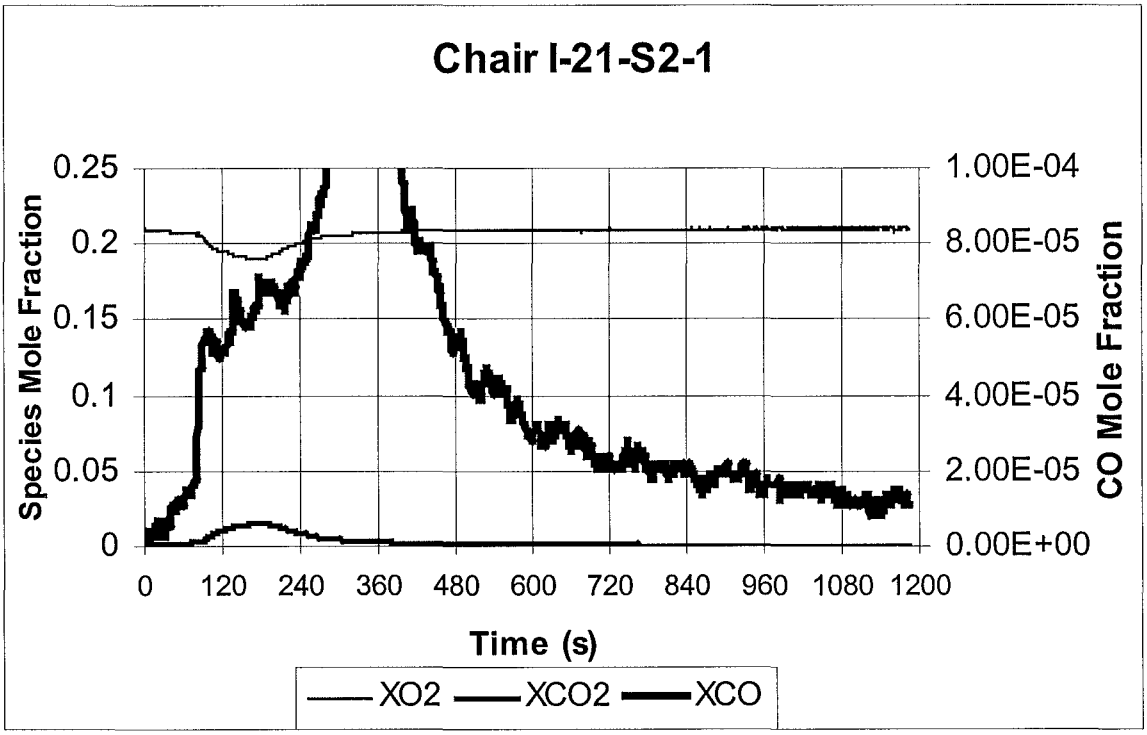
Chair I-21-S2-1
Species Mole Fraction
CO Mole Fraction
0.25
0.2
0.15
0.1
0.05
0
1.00E-04
8.00E-05
6.00E-05
4.00E-05
2.00E-05
0.00E+00
0 120 240 360 480 600 720 840 960 1080 1200
Time (s)
XO2
XCO2
XCO

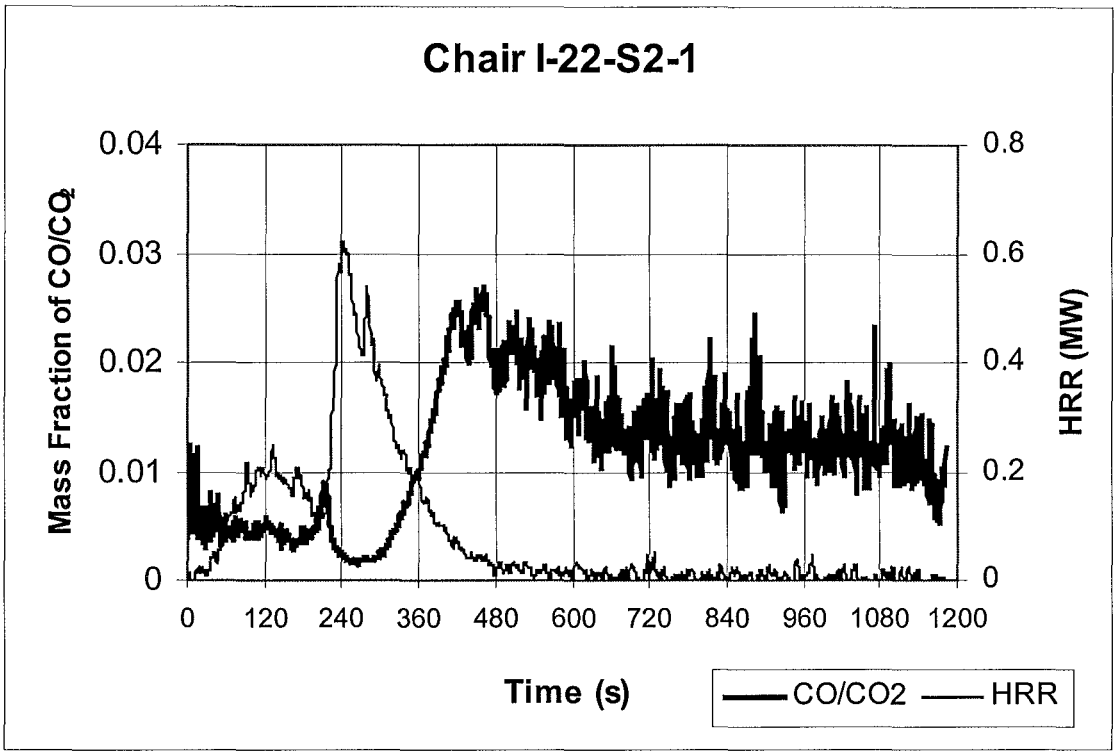
Chair I-22-S2-1
Mass Fraction of CO/CO2
HRR (MW)
0.04
0.03
0.02
0.01
0
0.8
0.6
0.4
0.2
0
0 120 240 360 480 600 720 840 960 1080 1200
Time (s)
CO/CO2
HRR

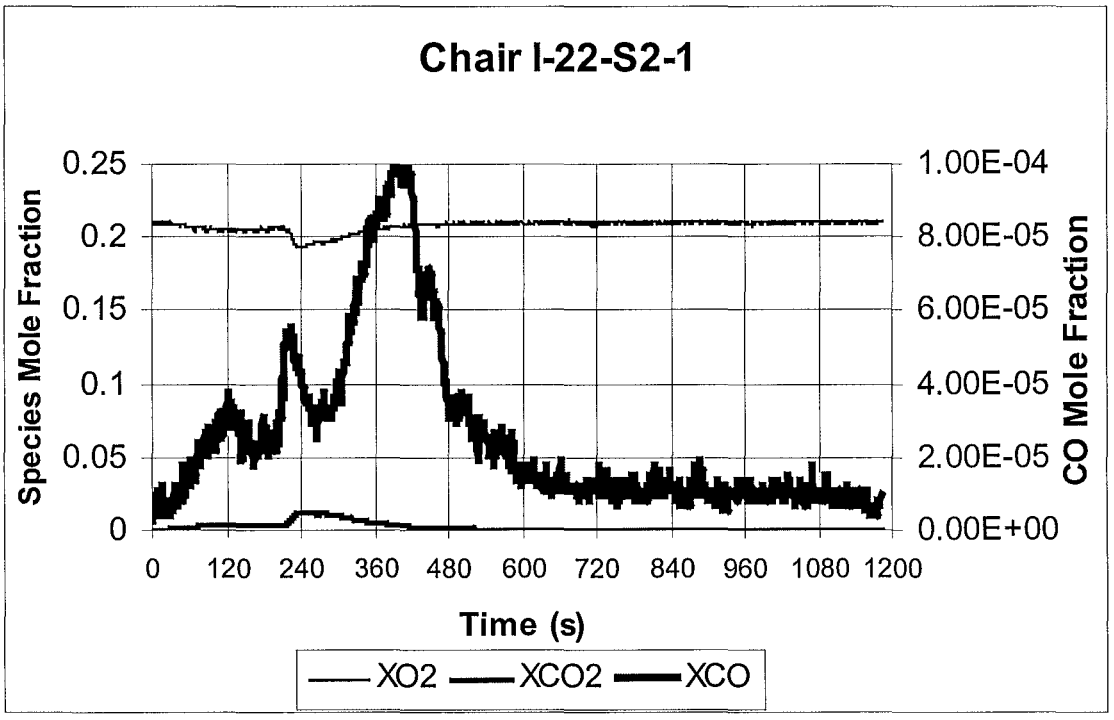
Chair I-22-S2-1
Species Mole Fraction
CO Mole Fraction
0.25
0.2
0.15
0.1
0.05
0
1.00E-04
8.00E-05
6.00E-05
4.00E-05
2.00E-05
0.00E+00
0 120 240 360 480 600 720 840 960 1080 1200
Time (s)
XO2
XCO2
XCO

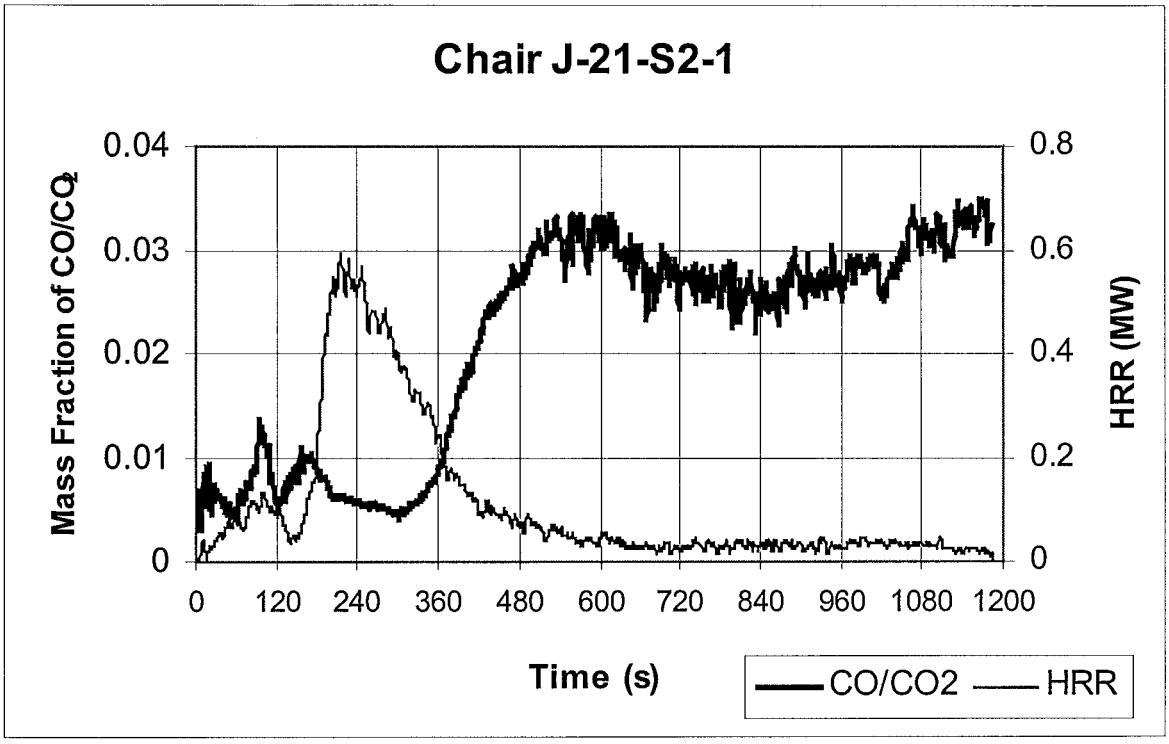
Chair J-21-S2-1
Mass Fraction of CO/CO2
HRR (MW)
0.04
0.03
0.02
0.01
0
0.8
0.6
0.4
0.2
0
0 120 240 360 480 600 720 840 960 1080 1200
Time (s)
CO/CO2
HRR

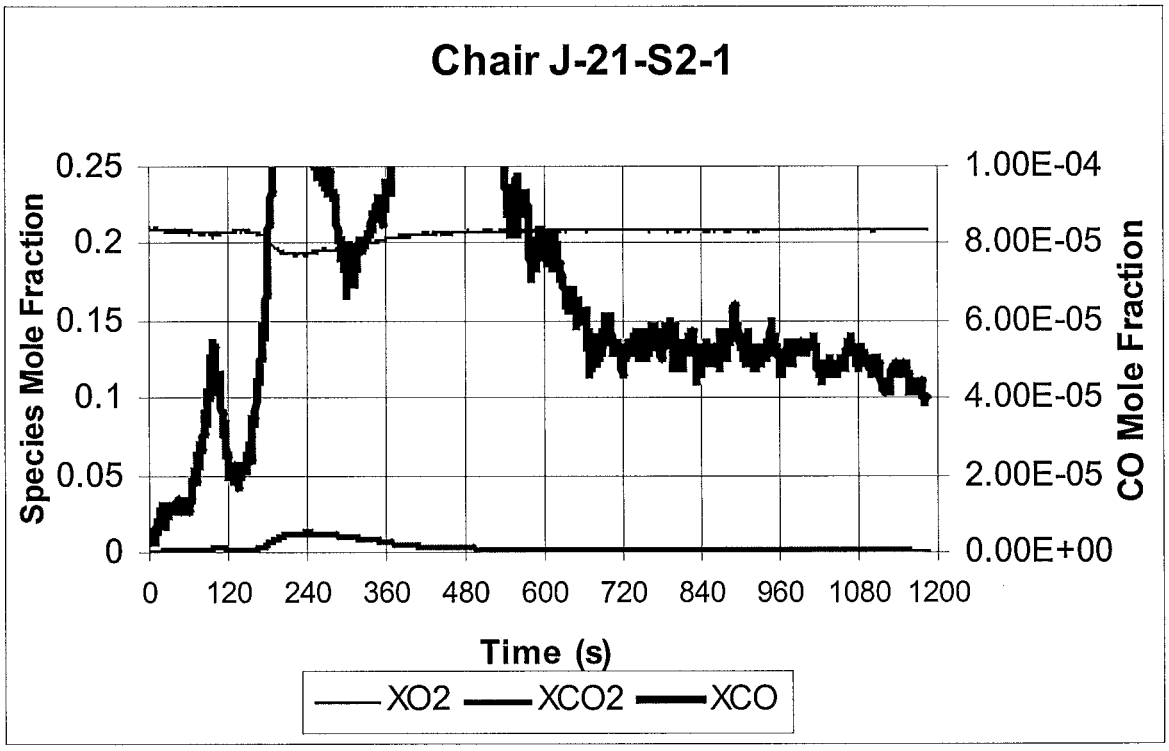
Chair J-21-S2-1
Species Mole Fraction
CO Mole Fraction
0.25
0.2
0.15
0.1
0.05
0
1.00E-04
8.00E-05
6.00E-05
4.00E-05
2.00E-05
0.00E+00
0 120 240 360 480 600 720 840 960 1080 1200
Time (s)
XO2
XCO2
XCO

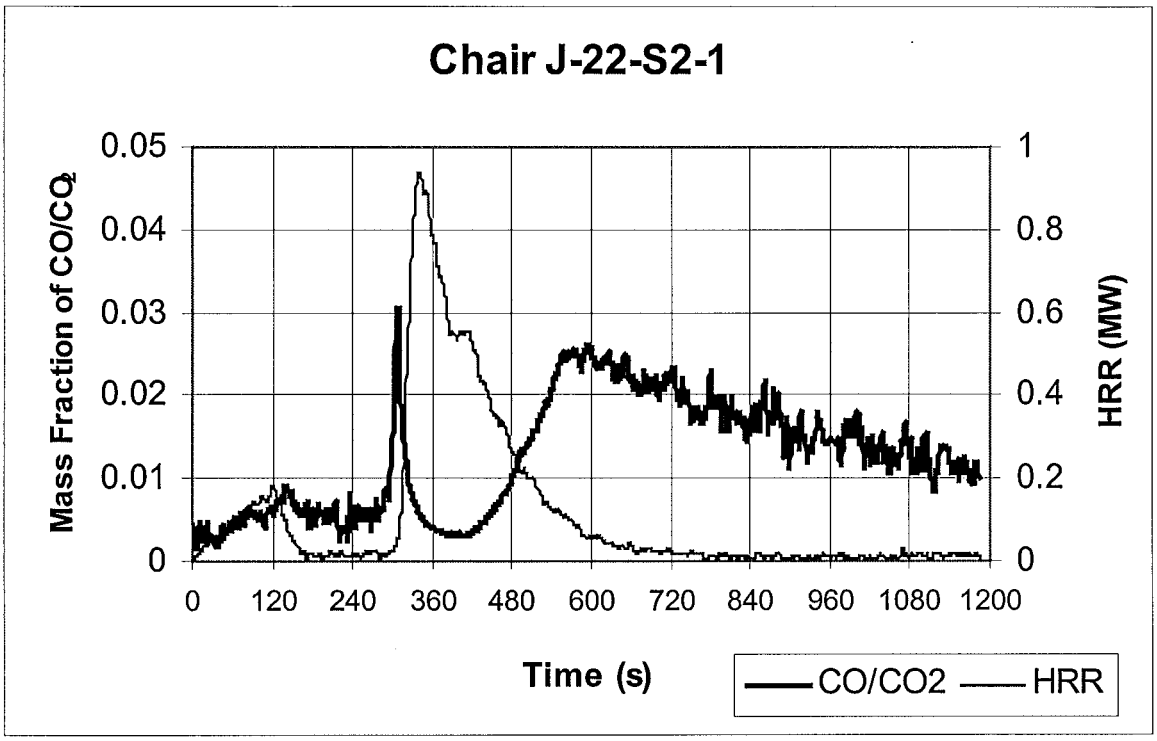
Chair J-22-S2-1
Mass Fraction of CO/CO2
0.05
0.04
0.03
0.02
0.01
0
1
0.8
0.6
0.4
0.2
0
HRR (MW)
0 120 240 360 480 600 720 840 960 1080 1200
Time (s)
CO/CO2
HRR

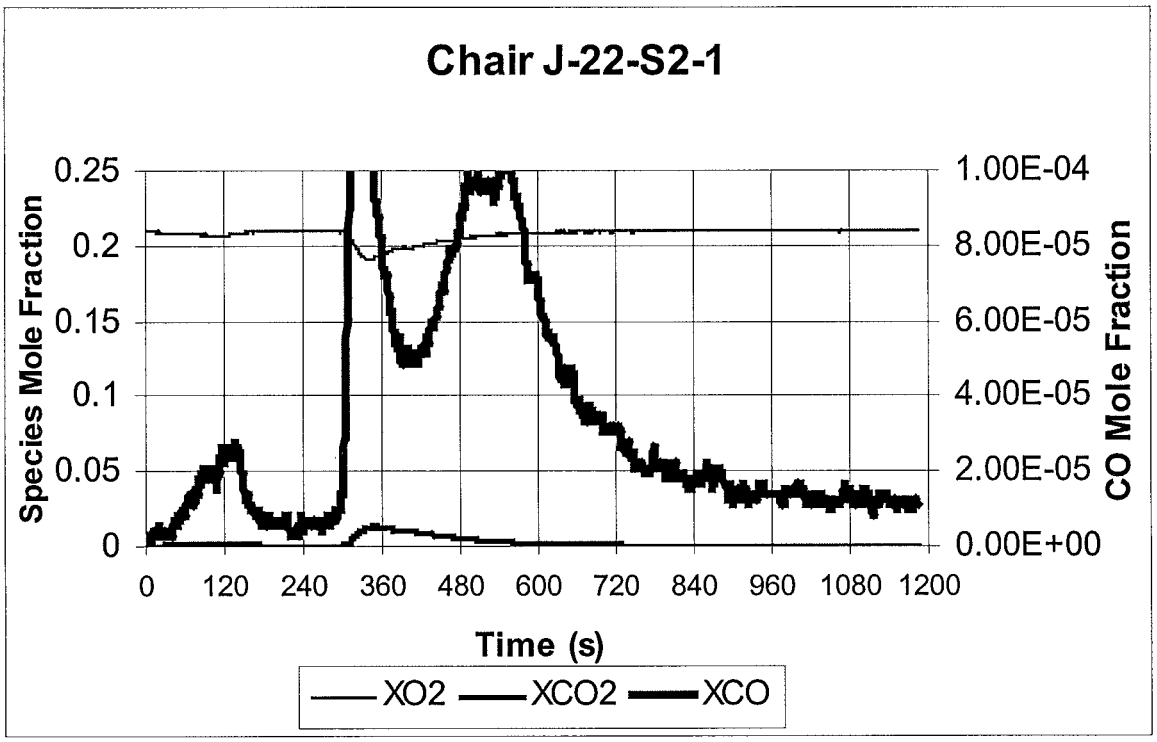
Chair J-22-S2-1
Species Mole Fraction
0.25
0.2
0.15
0.1
0.05
0
1.00E-04
8.00E-05
6.00E-05
4.00E-05
2.00E-05
0.00E+00
CO Mole Fraction
0 120 240 360 480 600 720 840 960 1080 1200
Time (s)
XO2
XCO2
XCO

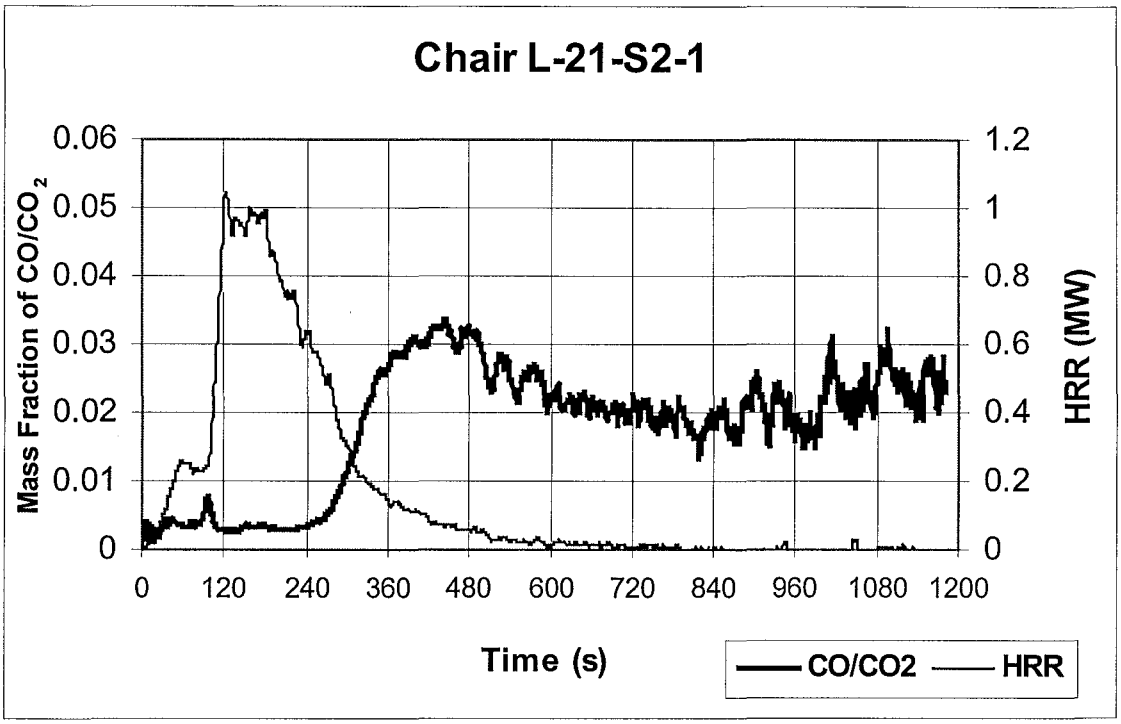
Chair L-21-S2-1
Mass Fraction of CO/CO2
0.06
0.05
0.04
0.03
0.02
0.01
0
1.2
1
0.8
0.6
0.4
0.2
0
HRR (MW)
0 120 240 360 480 600 720 840 960 1080 1200
Time (s)
CO/CO2
HRR

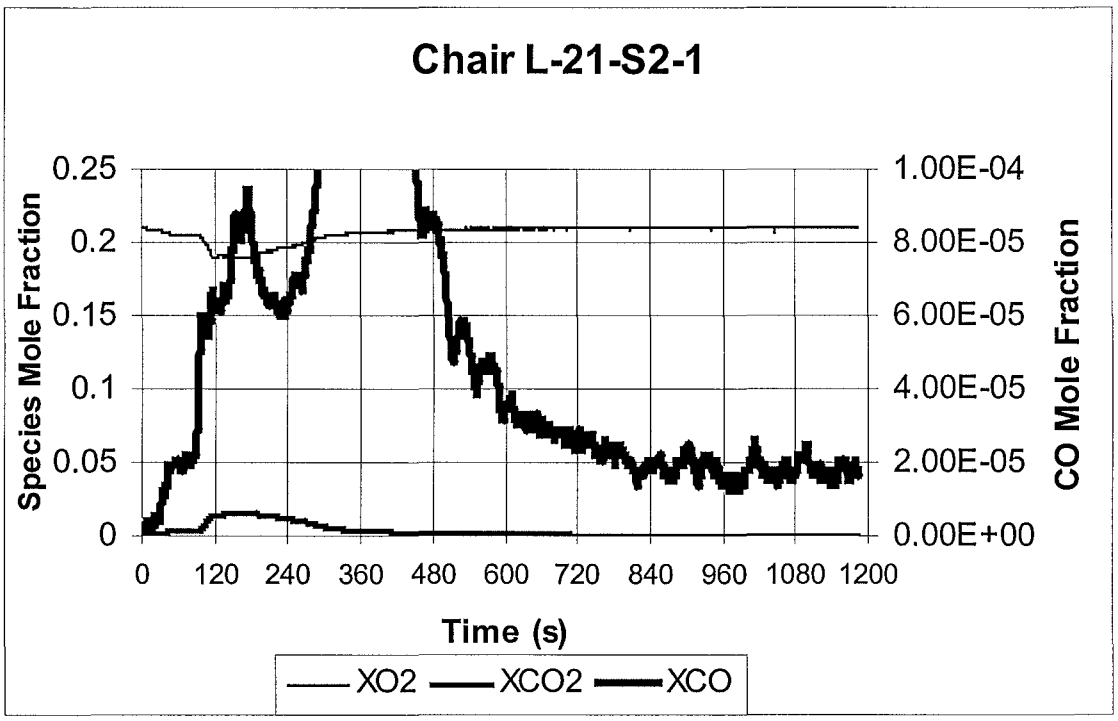
Chair L-21-S2-1
Species Mole Fraction
0.25
0.2
0.15
0.1
0.05
0
1.00E-04
8.00E-05
6.00E-05
4.00E-05
2.00E-05
0.00E+00
CO Mole Fraction
0 120 240 360 480 600 720 840 960 1080 1200
Time (s)
XO2
XCO2
XCO

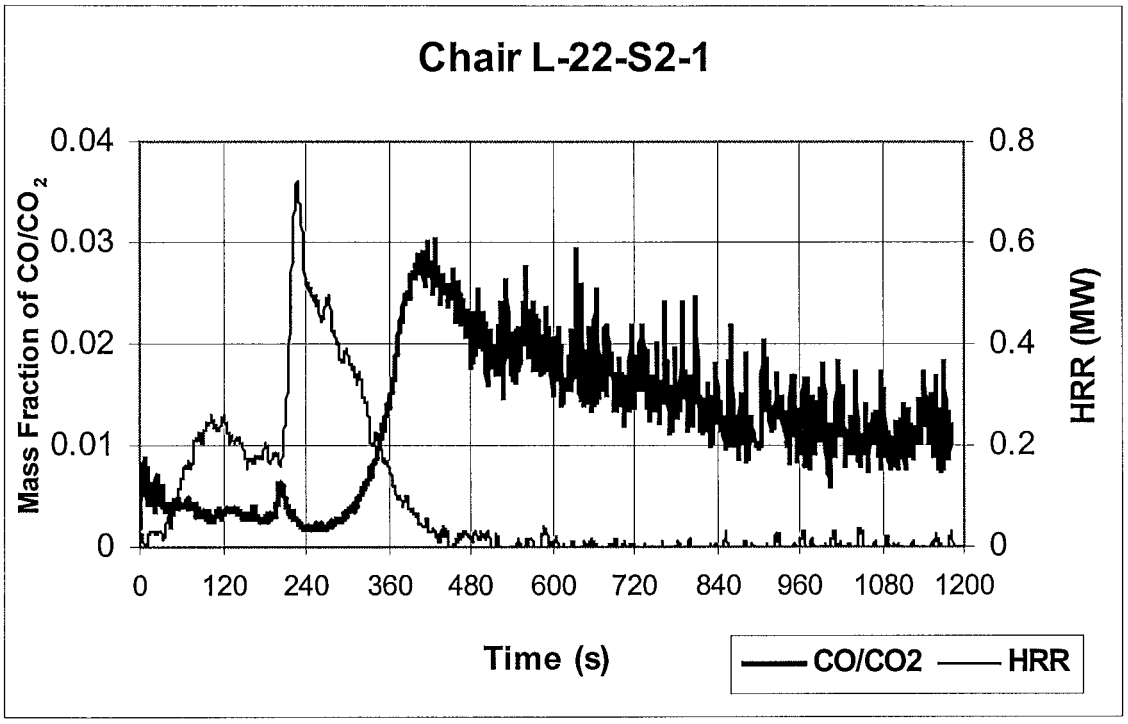
Chair L-22-S2-1
Mass Fraction of CO/CO2
HRR (MW)
0.04
0.03
0.02
0.01
0
0.8
0.6
0.4
0.2
0
0 120 240 360 480 600 720 840 960 1080 1200
Time (s)
CO/CO2
HRR

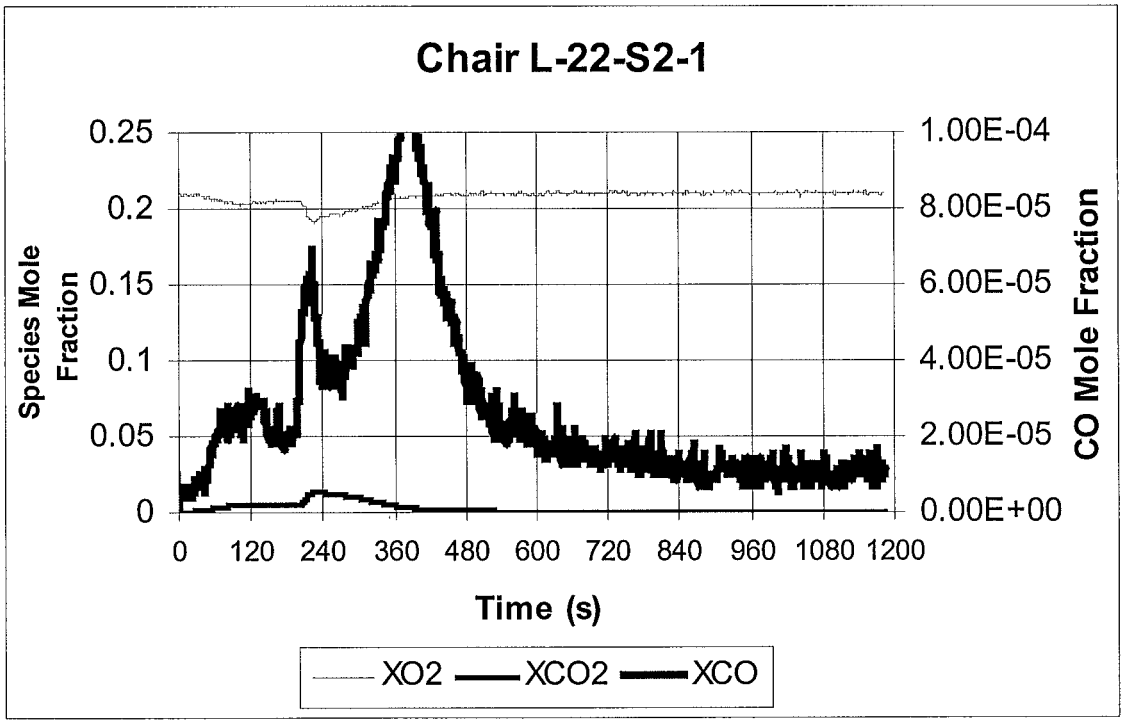
Chair L-22-S2-1
Species Mole Fraction
CO Mole Fraction
0.25
0.2
0.15
0.1
0.05
0
1.00E-04
8.00E-05
6.00E-05
4.00E-05
2.00E-05
0.00E+00
0 120 240 360 480 600 720 840 960 1080 1200
Time (s)
XO2
XCO2
XCO

# FIRE ENGINEERING RESEARCH REPORTS

| | | |
|---|---|---|
| 95/1 | Full Residential Scale Backdraft | I B Bolliger |
| 95/2 | A Study of Full Scale Room Fire Experiments | P A Enright |
| 95/3 | Design of Load-bearing Light Steel Frame Walls for Fire Resistance | J T Gerlich |
| 95/4 | Full Scale Limited Ventilation Fire Experiments | D J Millar |
| 95/5 | An Analysis of Domestic Sprinkler Systems for Use in New Zealand | F Rahmanian |
| 96/1 | The Influence of Non-Uniform Electric Fields on Combustion Processes | M A Belsham |
| 96/2 | Mixing in Fire Induced Doorway Flows | J M Clements |
| 96/3 | Fire Design of Single Storey Industrial Buildings | B W Cosgrove |
| 96/4 | Modelling Smoke Flow Using Computational Fluid Dynamics | T N Kardos |
| 96/5 | Under-Ventilated Compartment Fires - A Precursor to Smoke Explosions | A R Parkes |
| 96/6 | An Investigation of the Effects of Sprinklers on Compartment Fires | M W Radford |
| 97/1 | Sprinkler Trade Off Clauses in the Approved Documents | G J Barnes |
| 97/2 | Risk Ranking of Buildings for Life Safety | J W Boyes |
| 97/3 | Improving the Waking Effectiveness of Fire Alarms in Residential Areas | T Grace |
| 97/4 | Study of Evacuation Movement through Different Building Components | P Holmberg |
| 97/5 | Domestic Fire Hazard in New Zealand | KDJ Irwin |
| 97/6 | An Appraisal of Existing Room-Corner Fire Models | D C Robertson |
| 97/7 | Fire Resistance of Light Timber Framed Walls and Floors | G C Thomas |
| 97/8 | Uncertainty Analysis of Zone Fire Models | A M Walker |
| 97/9 | New Zealand Building Regulations Five Years Later | T M Pastore |
| 98/1 | The Impact of Post-Earthquake Fire on the Built Urban Environment | R Botting |
| 98/2 | Full Scale Testing of Fire Suppression Agents on Unshielded Fires | M J Dunn |
| 98/3 | Full Scale Testing of Fire Suppression Agents on Shielded Fires | N Gravestock |
| 98/4 | Predicting Ignition Time Under Transient Heat Flux Using Results from Constant Flux Experiments | A Henderson |
| 98/5 | Comparison Studies of Zone and CFD Fire Simulations | A Lovatt |
| 98/6 | Bench Scale Testing of Light Timber Frame Walls | P Olsson |
| 98/7 | Exploratory Salt Water Experiments of Balcony Spill Plume Using Laser Induced Fluorescence Technique | E Y Yii |
| 99/1 | Fire Safety and Security in Schools | R A Carter |
| 99/2 | A Review of the Building Separation Requirements of the New Zealand Building Code Acceptable Solutions | J M Clarke |
| 99/3 | Effect of Safety Factors in Timed Human Egress Simulations | K M Crawford |
| 99/4 | Fire Response of HVAC Systems in Multistorey Buildings: An Examination of the NZBC Acceptable Solutions | M Dixon |
| 99/5 | The Effectiveness of the Domestic Smoke Alarm Signal | C Duncan |

| | | |
|---|---|---|
| 99/6 | **Post-flashover Design Fires** | **R Feasey** |
| 99/7 | **An Analysis of Furniture Heat Release Rates by the Nordtest** | **J Firestone** |
| 99/8 | **Design for Escape from Fire** | **I J Garrett** |
| 99/9 | **Class A Foam Water Sprinkler Systems** | **D B Hipkins** |
| 99/10 | **Review of the New Zealand Standard for Concrete Structures (NZS 3101) for High Strength and Lightweight Concrete Exposed to Fire** | **M J Inwood** |
| 99/12 | **An Analytical Model for Vertical Flame Spread on Solids: An Initial Investigation** | **G A North** |
| 99/13 | **Should Bedroom Doors be Open or Closed While People are Sleeping? - A Probabilistic Risk Assessment** | **D L Palmer** |
| 99/14 | **Peoples Awareness of Fire** | **S J Rusbridge** |
| 99/15 | **Smoke Explosions** | **B J Sutherland** |
| 99/16 | **Reliability of Structural Fire Design** | **JKS Wong** |
| 00/1 | **Fire Spread on Exterior Walls** | **FNP Bong** |
| 00/2 | **Fire Resistance of Lightweight Framed Construction** | **PCR Collier** |
| 00/3 | **Fire Fighting Water: A Review of Fire Fighting Water Requirements (A New Zealand Perspective)** | **S Davis** |
| 00/4 | **The Combustion Behaviour of Upholstered Furniture Materials in New Zealand** | **H Denize** |
| 00/5 | **Full-Scale Compartment Fire Experiments on Upholstered Furniture** | **N Girgis** |
| 00/6 | **Fire Rated Seismic Joints** | **M James** |
| 00/7 | **Fire Design of Steel Members** | **K R Lewis** |
| 00/8 | **Stability of Precast Concrete Tilt Panels in Fire** | **L Lim** |
| 00/9 | **Heat Transfer Program for the Design of Structures Exposed to Fire** | **J Mason** |
| 00/10 | **An Analysis of Pre-Flashover Fire Experiments with Field Modelling Comparisons** | **C Nielsen** |
| 00/11 | **Fire Engineering Design Problems at Building Consent Stage** | **P Teo** |
| 00/12 | **A Comparison of Data Reduction Techniques for Zone Model Validation** | **S Weaver** |
| 00/13 | **Effect of Surface Area and Thickness on Fire Loads** | **H W Yii** |

School of Engineering
University of Canterbury
Private Bag 4800, Christchurch, New Zealand

Phone 643 364-2250
Fax 643 364-2758